ELECTRONIC SUPPORTING INFORMATION

Electronic Supporting Information for:

Stable cyclopropenylvinyl ligands *via* insertion into a transient cyclopropenyl-metal bond.

Lachlan J. Watson and Anthony F. Hill*

General Considerations

Unless otherwise stated, experimental work was carried out at room temperature under a dry and oxygen-free nitrogen atmosphere using standard Schlenk techniques with dried and degassed solvents.

NMR spectra were obtained on a Bruker Avance 400 (^{1}H at 400.1 MHz, ^{13}C at 100.6 MHz, ^{31}P at 162 MHz), a Bruker Avance 600 (^{1}H at 600.0 MHz, ^{13}C at 150.9 MHz), a Bruker Avance 700 (^{1}H at 700.0 MHz, ^{13}C at 176.1 MHz, ^{31}P at 283 MHz) or a Bruker Avance 800 (1H at 800.1 MHz, ^{13}C at 201.2 MHz) spectrometers at the temperatures indicated. Chemical shifts (δ) are reported in ppm with coupling constants given in Hz and are referenced to the solvent peak, or external references (85% H_3PO_4 in H_2O for ^{31}P). The multiplicities of NMR resonances are denoted by the abbreviations s (singlet), d (doublet), t (triplet), m (multiplet), br (broad) and combinations thereof for more highly coupled systems. In some cases, distinct peaks were observed in the ^{1}H and ^{13}C{^{1}H} NMR spectra, but to the level of accuracy that is reportable (*i.e.* 2 decimal places for ^{1}H NMR, 1 decimal place for ^{13}C NMR) they are reported as having the same chemical shift. The abbreviation 'napth' is used to refer to the naphthalene backbone of the dihydroperimidine based ligand, while 'i' (ipso), 'o' (ortho), 'm' (meta), and 'p' (para) refer to positions on the phenyl rings of PPh_2 groups. Extreme insolubility in many samples resulted in low quality NMR acquisitions, and as a result some resonances may not be unequivocally assigned.

Infrared spectra were obtained using a PerkinElmer Spectrum One FT-IR spectrometer. The strengths of IR absorptions are denoted by the abbreviations vs (very strong), s (strong), m (medium), w (weak), sh (shoulder) and br (broad). Elemental microanalytical data were provided by Macquarie University. High-resolution electrospray ionisation mass spectrometry (ESI-MS) was performed by the ANU Research School of Chemistry mass spectrometry service with acetonitrile or methanol as the matrix.

Data for *X*-ray crystallography were collected with an Agilent Xcalibur CCD diffractometer or an Agilent SuperNova CCD diffractometer using Mo-Kα radiation (λ = 0.71073 Å) or Cu-Kα radiation (λ = 1.54184 Å) and the CrysAlis PRO software.[1] The structures were solved by direct or Patterson methods and refined by full-matrix least-squares on F^2 using the SHELXS or SHELXT and SHELXL programs.[2] Hydrogen atoms were located geometrically and refined using a riding model. Diagrams were produced using the CCDC visualisation program Mercury.[3] Structural data for **4b** were collected at the Australian Synchrotron using the MX_2 beamline using silicon double crystal monochromated synchrotron radiation at 100 K. Raw frame data were collected using BluIce[4] and data reduction, interframe scaling, unit cell refinement and absorption corrections were processed using XDS.[5]

The synthesis of [RhCl(PhPm)] and [RhCl(CyPm)] have been reported previously.[6] The reagents [RhCl{py(NHP^{t}Bu$_2$)$_2$-2,6}],[7] triphenylcyclopropenium bromide,[8] and triphenylcyclopropenium hexafluorophosphate[9] were prepared according to literature procedures. The remaining reagents were purchased from commercial sources.

Computational Details

Computational studies were performed by using the *SPARTAN20*® suite of programs.[10] Geometry optimisation (gas phase) for diatomics and metal complexes was performed at the DFT level of theory using the exchange functionals ωB97X-D of Head-Gordon.[11,12] The Los Alamos effective core potential type basis set (LANL2Dζ) of Hay and Wadt [13-15] was used for I, Mo and W while Pople 6-31G* basis sets[16] were used for all other atoms. For the full molecule of **3a**, the def2-SV(P) basis set of Weigend and Ahlrichs[17] was used in combination with the ωB97X-D functional. Frequency calculations were performed for all compounds to confirm that each optimized structure was a local minimum and also to identify vibrational modes of interest. Cartesian atomic coordinates are provided below. Percentage buried volume[18] and NEST occupied volume[19] calculations and plots were generated using the relevant web-based application.

Synthetic Procedures

Synthesis of [RhCl{py(NHP^{t}Bu$_2$)$_2$-2,6}(C$_3$Ph$_3$)}] (1). A suspension of [RhCl{py(NHP^{t}Bu$_2$)$_2$-2,6}][7] (109 mg, 0.204 mmol) and [C$_3$Ph$_3$]PF$_6$ (250 mg, 0.607 mmol) was heated to reflux in toluene (35 mL) for 21 hours. After reducing the solvent volume to *ca.* 5 mL and addition of *n*-hexane, the suspension was filtered to collect the filtrate. After removal of the solvent under reduced pressure, the residue was ultrasonically triturated in *n*-pentane (10 mL) and collected by filtration as a yellow-brown solid. Yield: 146 mg (0.136 mmol, 67%).

IR (ATR, cm^{-1}) 3070 ν_{NH}, 1579, 1445, 1260 $\nu_{CCAromatic}$. **^{1}H NMR** (700 MHz, CDCl$_3$, 298 K): δ_H = 7.60 (d, 8 H, $^3J_{HH}$ = 7 Hz, *o*-Ph), 7.36 (s, 1 H, py-*H*), 7.30 (d, 4 H, $^3J_{HH}$ = 8 Hz, *o*-Ph), 7.27-7.23 (m, 12 H, *m*-Ph), 7.21 (t, 4 H, $^3J_{HH}$ = 8 Hz, *p*-Ph), 7.11 (t, 2 H, $^3J_{HH}$ = 7 Hz, *p*-Ph), 5.40 (br s, 2 H, N*H*), 1.26 (br s, 36 H, P^{t}Bu$_2$). **^{31}P{^{1}H} NMR** (298 MHz, CDCl$_3$, 298 K): δ_P = 111.06 (br s). **^{31}P{^{1}H} NMR** (298 MHz, CDCl$_3$, 227 K): δ_P = 111.14 (br d, $^1J_{RhP}$ = 149 Hz). **^{13}C{^{1}H}** (176 MHz, CDCl$_3$, 298 K): δ_C = 160.0 (py-$C_{1,5}$), 143.9 (py-C_3), 134.6 (*i*-Ph), 129.4 (*o*-Ph), 129.3 (*o*-Ph), 129.2 (*m*-Ph), 129.0 (*m*-Ph), 127.9 (*i*-Ph), 127.6 (*p*-Ph), 126.9 (*p*-Ph), 119.6 (β-C_3Ph$_3$), 113.1 (py-$C_{2,4}$), 35.2 (α-C_3Ph$_3$), 28.6 (P^{t}Bu$_2$). **MS** (ESI, +ve ion, m/z): Found: 1073.4281. Calcd. For $C_{65}H_{72}N_4P_2{}^{103}Rh$ [M + CH$_3$CN]: 1073.4287.

Crystals suitable for structural determination were grown from the slow evaporation of a chloroform solution of the sample. ***Crystal Data*** *for* $C_{63}H_{69}ClN_3P_2Rh$ (M_w =1068.51 gmol^{-1}): monoclinic, space group *Cc* (no. 9), *a* = 12.8504(8) Å, *b* = 24.0502(9) Å, *c* = 18.6155(10) Å, β = 106.840(6)°, *V* = 5506.5(5) Å^3, *Z* = 4, *T* = 150.0(1) K, μ(Mo Kα) = 0.459 mm^{-1}, D_{calc} = 1.289 Mgm^{-3}, 13907 reflections measured (6.598° ≤ 2Θ ≤ 59.148°), 10307 unique (R_{int} = 0.0276, R_{sigma} = 0.0637) which were used in all calculations. The final R_1 was 0.0501 ($I > 2\sigma(I)$) and wR_2 was 0.1178 (all data) for 643 refined parameters with 2 restraints. CCDC 2249870.

Synthesis of [RhBr$_3$(PhPm)] (2):. *Method A:* A solution of [RhCl(PhPm)] (50 mg, 0.078 mmol) and C$_3$Ph$_3$Br (100 mg, 0.289 mmol) were stirred in CH$_2$Cl$_2$ (10 mL) for two hours. Solvent was removed from the yellow solution under reduced pressure and the residue recrystallised from THF/Et$_2$O as a yellow powder which was isolated by filtration and dried. Yield: 54 mg (0.060 mmol, 76 %). *Method B:* A solution of [RhCl(PhPm)] (20 mg, 0.031 mmol) and pyridinium tribromide (C$_5$H$_5$NH.Br$_3$, 20 mg, 0.063 mmol) were stirred in CH$_2$Cl$_2$ for two hours. ^{31}P{^{1}H} spectroscopy indicates ~30% product conversion with ~10% of a similar species attributed to [RhClBr$_2$(PhPm)] alongside other unidentified peaks.

IR (CH$_2$Cl$_2$, cm^{-1}): 1638, 1608, 1588 ν_{CC}. IR (ATR, cm^{-1}): 1634, 1605, 1582 ν_{CC}. **^{1}H NMR** (700 MHz, CDCl$_3$, 298 K): δ_H = 7.94 (m, 8 H, *o*-PPh$_2$), 7.58 (d, 2 H, $^3J_{HH}$ = 8 Hz, napth*CH*), 7.51 (t, 2 H, $^3J_{HH}$ = 8 Hz, napth*CH*), 7.42-7.38 (2 x m, 12 H, *m*-PPh$_2$ and *p*-PPh$_2$), 7.02 (d, 2 H, $^3J_{HH}$ = 8 Hz, napth*CH*), 5.24 (s, 4 H, NC*H*$_2$P). **^{31}P{^{1}H} NMR** (283 MHz, CDCl$_3$, 298 K): δ_P = 17.30 (d, $^1J_{RhP}$ = 92 Hz). **^{13}C{^{1}H} NMR** (176 MHz, CDCl$_3$, 298 K): δ_C = 201.7 (d.t., $^1J_{RhC}$ = 39 Hz, $^2J_{PC}$ = 4 Hz, N*C*N), 134.6 (napth*C*), 134.1 (vt, $^{2,4}J_{PC}$ = 5 Hz, *o*-PPh$_2$), 133.9 (napth*C*), 131.2 (*p*-PPh$_2$), 130.0 (vt, $^{1,3}J_{PC}$ = 27 Hz, *i*-PPh$_2$), 128.5 (vt, $^{3,5}J_{PC}$ = 5 Hz, *m*-PPh$_2$), 128.5 (overlapping napth*C*H peak observed by HSQC), 123.3 (napth*C*H), 119.7 (napth*C*), 108.0 (napth*C*H), 58.3 (vt, $^{1,3}J_{PC}$ = 17 Hz, NC*H*$_2$P). **MS** (ESI, +ve ion, m/z): Found: 826.9289. Calcd. for $C_{37}H_{30}N_2P_2{}^{103}RhBr_2$ [M – Br]$^+$: 826.9284. **Anal.** Found C 48.87, H 3.36, N 3.21 %. Calcd. For $C_{37}H_{30}N_2P_2RhBr_3$: C 48.98, H 3.33, N 3.09 %. Crystals suitable for structural determination were grown from slow evaporation of a saturated benzene solution of the sample at 25 °C. ***Crystal Data*** *for* $C_{49}H_{42}Br_3N_2P_2Rh$ (M_w = 1063.42 g.mol^{-1}): triclinic, space group *P*-1 (no. 2), *a* = 10.3024(2) Å, *b* = 14.2061(4) Å, *c* = 15.4757(5) Å, α = 87.154(2)°, β = 73.829(2)°, γ = 81.829(2)°, *V* = 2153.16(10) Å^3, *Z* = 2, *T* = 150.0(1) K, μ(Cu Kα) = 7.453 mm^{-1}, D_{calc} = 1.640 Mgm^{-3}, 16278 reflections measured (8.612° ≤ 2Θ ≤ 147.642°), 8530 unique (R_{int} = 0.0214, R_{sigma} = 0.0315) which were used in all calculations. The final R_1 was 0.0247 ($I > 2\sigma(I)$) and wR_2 was 0.0623 (all data) for 514 refined parameters without restraints. CCDC 2249869.

Generation of [RhCl(κ^2-C$_3$Ph$_3$)(PhPm)]PF$_6$ (3a): In each experiment, [RhCl(PhPm)] and 1.5 equivalents or more of [C$_3$Ph$_3$]PF$_6$ were stirred in dichloromethane or acetone, causing an immediate colour change from bright orange to very deep blue. After 15 minutes, the reaction was deemed complete by ^{31}P{^{1}H} NMR spectroscopy but suffers from extremely rapid decomposition which precluded its purification. Subsequent reactions were conducted with these solutions, and characterization was performed without further purification. Conversion: *ca.* 74–93% by ^{31}P{^{1}H} NMR, tending to improve with more equivalents of [C$_3$Ph$_3$]PF$_6$. The following (Figure S1) displays the variation in conversion with1 and 2 equivalents of [C$_3$Ph$_3$]PF$_6$ over 48 hours.

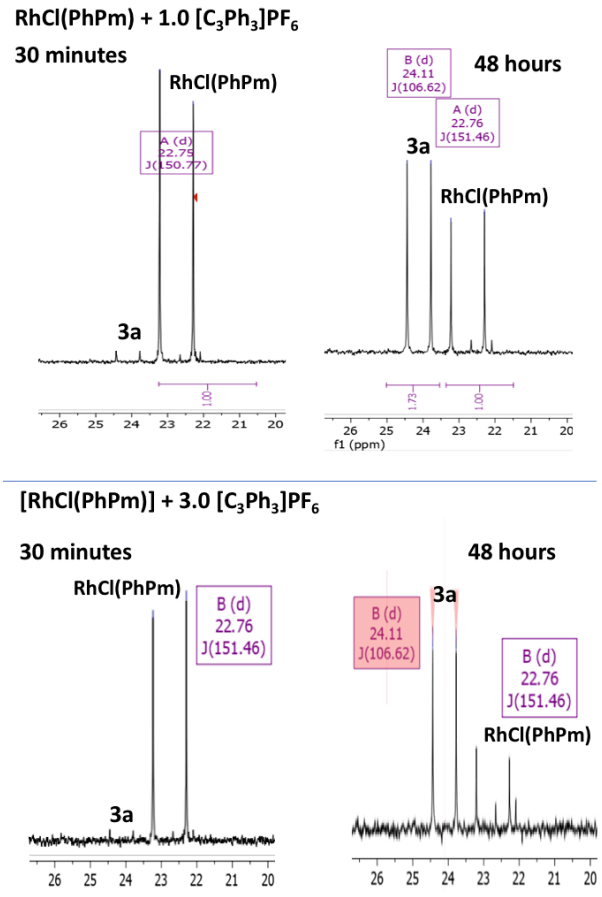

Figure S1. Stoichiometry dependence of rate of reaction of [RhCl(PhPm)] with [C$_3$Ph$_3$]PF$_6$.

^{1}H NMR (400 MHz, CD_2Cl_2, 298 K): δ_H = 8.55-6.71 (~60 H, PPh_2, RhC_3Ph_3, naphthCH and excess $C_3Ph_3PF_6$), 6.25 (d, 2 H, $^3J_{HH}$ = 8 Hz, naphthC*H*), 5.25 (d.t., 2 H, $^2J_{PH}$ = 14 Hz, $^2J_{HH}$ = 3 Hz, NCH_2P), 4.85 (d.t., 2 H, $^2J_{PH}$ = 14, $^2J_{HH}$ = 3 Hz, NCH_2P). **^{31}P{^{1}H}** NMR (162 Hz, CD_2Cl_2, 298 K): δ_P = 28.24 (d, $^1J_{RhP}$ = 104 Hz), –142 (hept, $^1J_{FP}$ = 714 Hz, PF_6). **^{1}H NMR** (400 MHz, $(CD_3)_2CO$, 298 K): δ_H = 7.91–6.80 (42 H, PPh_2, RhC_3Ph_3 and naphthCH), 6.53 (d, 2 H, $^3J_{HH}$ = 7 Hz, naphthC*H*), 5.54 (d.t., 2 H, $^2J_{PH}$ = 14 Hz, $^2J_{HH}$ = 3 Hz, NCH_2P), 5.34 (dt, 2 H, $^2J_{PH}$ = 14 Hz, $^2J_{HH}$ = 3 Hz, NCH_2P). **^{31}P{^{1}H}** NMR (162 Hz, $(CD_3)_2CO$, 298 K): δ_P = 28.7 (d, $^1J_{RhP}$ = 104 Hz), –144 (hept, $^1J_{FP}$ = 709 Hz, PF_6). **^{13}C{^{1}H}** NMR (176 MHz, CD_2Cl_2, 298 K): δ_C = 248.1 (m, C_3Ph_3), 214.8 (d.t., $^1J_{RhC}$ = 33 Hz, $^2J_{PC}$ = 6 Hz, N*C*N), 212.8 (d.t., $^1J_{RhC}$ = 22 Hz, $^2J_{PC}$ unresolved, C_3Ph_3), 165.4 (m, C_3Ph_3), 144.3, 140.7, 136.1 (3 x s, *i*-Ph), 135.1 (naphth*C*), 134.2–133.9 (PPh_2), 134.0 (vt, J_{PC} = 6 Hz, PPh_2), 133.1 (vt, $^{3,5}J_{PC}$ = 4 Hz, naphth*C*), 132.5–132.2 (PPh_2), 130.2 (*o*-Ph), 130.0 (vt, J_{PC} = 5 Hz, PPh_2), 129.3 (*m*-Ph), 129.1 (naphth*C*H), 129.0 (PPh_2), 128.7 (*m*-Ph), 128.0 (*o*-Ph), 124.0 (naphth*C*H), 120.5 (naphth*C*), 108.9 (naphth*C*H), 59.2 (vt, $^{1,3}J_{PC}$ = 19 Hz, N*C*H_2P). The remaining peaks could not be unambiguously assigned. The sensitivity of the sample prevented mass spectrometric analysis and purification for elemental analysis. In the absence of crystallographic data, the geometry of the model complex $[RhCl(C_3Ph_3)(PhPm)]^+$ was computationally optimised (ωB97X-D/6-31G*/def2-SV(P)/gas phase) as shown in Figure 10 of the manuscript.

Reaction of [RhCl(PhPm)] with $[C_3Ph_3]PF_6$ in CD_3CN – Performing the reaction of [RhCl(PhPm)] with $[C_3Ph_3]PF_6$ in CD_3CN resulted in the formation of four octahedral rhodium complexes (see 31P{1H} spectrum below). While none of the chemical shifts or associated $^1J_{PRh}$ coupling constants corresponded exactly to those measured for **3a** in CD_2Cl_2 (δ_P = 28.24, $^1J_{RhP}$ = 104 Hz), some solvent dependence of the former is to be expected. It seems plausible that one of these may well be **3a** and that the other three doublets correspond to the three isomers of $[RhCl(\sigma\text{-}C_3Ph_3)(NCMe)(PhPm)]^+$ (Figure S2). The mixture was not however amenable to chromatographic purification.

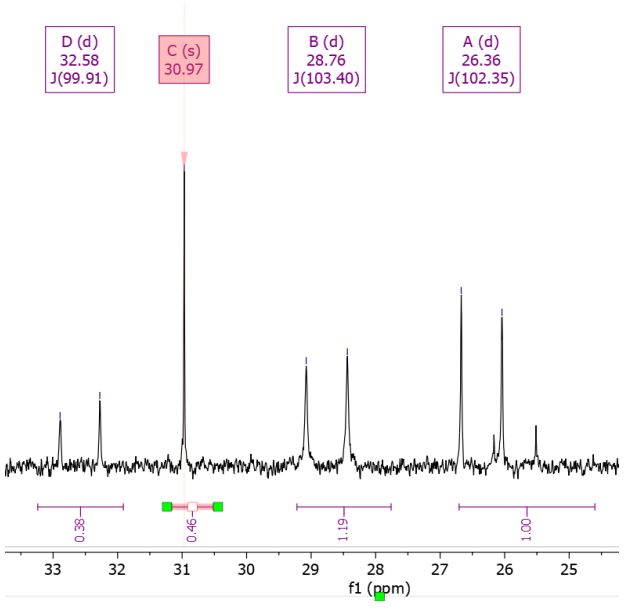

Figure S2. Crude ^{31}P{^{1}H} NMR spectrum of the reaction of [RhCl(PhPm)] with $[C_3Ph_3]PF_6$ in d_3-acetonitrile.

Generation of $[RhCl(\kappa^2\text{-}C_3Ph_3)(CyPm)]PF_6$ (3b): As for **3a** above, in each experiment, [RhCl(CyPm)] and 1.5 equivalents or more of $[C_3Ph_3]PF_6$ were stirred in dichloromethane, causing an immediate colour change from bright orange to green. No length of reaction time allowed for complete conversion, usually stabilising at ~56 % by ^{31}P{^{1}H} NMR spectroscopy after 15 mins. Efforts to isolate this species led to rapid decomposition, and subsequent reactions were conducted from these solutions without further purification. Conversion: *ca* 56% by ^{31}P{^{1}H} NMR.

^{1}H NMR (800 MHz, CD_2Cl_2, 298 K): δ_H = 8.02 (br. m, 2 H, *o*-Ph), 7.66 (t, 1 H, $^3J_{HH}$ = 7 Hz, *p*-Ph), 7.57 (d, 2 H, $^3J_{HH}$ = 8 Hz, naphth*CH*), 7.54 (t, 1 H, $^3J_{HH}$ = 7 Hz, *p*-Ph), 7.48 (t, 2 H, $^3J_{HH}$ = 8 Hz, naphth*CH*), 7.45 (t, 1 H, $^3J_{HH}$ = 7 Hz, *p*-Ph), 7.42 (t, 2 H, $^3J_{HH}$ = 8 Hz, *m*-Ph), 7.39 (t, 2 H, $^3J_{HH}$ = 8 Hz, *m*-Ph), 7.33 (br. m, 2 H, *o*-Ph), 7.18 (2 H, $^3J_{HH}$ = 8 Hz, *m*-Ph), 6.98 (d, 2 H, $^3J_{HH}$ = 7 Hz, *o*-Ph), 6.82 (d, 2 H, $^3J_{HH}$ = 8 Hz, naphth*CH*), 4.66 (d, 2 H, $^2J_{HH}$ = 13 Hz, NCH_2P), 3.89 (d, 2 H, $^2J_{HH}$ = 13 Hz, NCH_2P), 2.86–1.00 (multiplets, PCy_2). **^{13}C{^{1}H}** NMR (201 MHz, CD_2Cl_2, 298 K): δ_C = 255.3 (m, C_3Ph_3), 214.8 (d.t., $^1J_{RhC}$ = 33 Hz, $^2J_{PC}$ = 6 Hz, N*C*N), 207.7 (d.t., $^1J_{RhC}$ = 24 Hz, $^2J_{PC}$ = 7 Hz, C_3Ph_3), 165.2 (m, C_3Ph_3), 145.2 (*i*-Ph), 141.1 (*i*-Ph), 136.0 (*p*-Ph), 135.0 (*p*-Ph), 129.9 (naphth*C*H), 129.9 (*m*-Ph), 128.5 (*o*-Ph), 128.4 (*o*-Ph), 123.5 (naphth*C*H), 120.4 (naphth*C*), 119.4 (*o*-Ph), 108.2 (naphth*C*H), 53.9 (N*C*H_2P, overlapping with solvent signal), 37.8 (vt, $^{1,3}J_{PC}$ = 9 Hz, *i*-PCy_2), 34.0–26.4 (multiplets, PCy_2). Remaining signals could not be unambiguously assigned due to the presence of overlapping signals from other compounds including unreacted [RhCl(CyPm)], excess $C_3Ph_3PF_6$ and $[RhCl_2(CD_2Cl)(CyPm)]$ from reaction with the NMR solvent. **^{31}P{^{1}H}** NMR (162 MHz, CD_2Cl_2, 298 K): δ_P = 31.52 (d, $^1J_{RhP}$ = 97 Hz), -147 (sept, $^1J_{FP}$ = 712 Hz, PF_6). The sensitivity of this species precluded mass spectrometric analysis. The sensitivity of this species precluded acquisition of useful mass spectrometric or elemental microanalytical data.

Synthesis of $[Rh\{\kappa^2\text{-}CHC\{CO_2Me\}C_3Ph_3\}Cl(PhPm)]PF_6$ (4a): To the solids [RhCl(PhPm)] (120 mg, 0.171 mmol) and $[C_3Ph_3]PF_6$ (105 mg, 0.255 mmol) was added CH_2Cl_2 (20 mL) and stirred for 10 minutes, turning rapidly from orange though deep green to dark blue. Methyl propiolate (0.30 mL, 3.4 mmol) was added, causing immediate formation of a yellow solution. After one hour of stirring, the solution was condensed to *ca* 3 mL and loaded onto a silica gel column (2 x 10 cm), washing with CH_2Cl_2 (50 mL) before eluting with 4% MeCN in CH_2Cl_2 to collect a yellow band of the product. Yield: 125 mg (0.112 mmol, 65%). Crystals suitable for structural determination were grown by liquid diffusion of benzene into a chloroform solution of the sample.

IR (ATR, cm^{-1}): 1639, 1579 $\nu_{CCnapth}$, 1435, 1351. **^{1}H NMR** (700 MHz, $CDCl_3$, 298 K): δ_H = 8.43 (s, 1 H, RhC*H*), 7.68 (m, 4 H, J_{HH} = 6 Hz, *o*-PPh_2), 7.45-7.30 (overlapped multiplets, 14 H, *o*-PPh_2, *o*-Ph, *p*-PPh_2, *p*-Ph and naphth*CH*), 7.24, 7.23, 7.22 (overlapped multiplets, 6 H, naphth*CH* and *m*-Ph), 7.16 (m, 4 H, *m*-PPh_2), 7.11 (overlapped multiplets, 6 H, naphth*CH* and *m*-PPh_2), 7.06 (t, 2 H, *p*-PPh_2), 6.87 (t, 1 H, $^3J_{HH}$ = 7 Hz, *p*-C_3Ph_3), 6.78 (t, 2 H, $^3J_{HH}$ = 8 Hz, *m*-C_3Ph_3), 6.18 (d, 2 H, $^3J_{HH}$ = 8 Hz, *o*-C_3Ph_3), 5.22, 4.77 (2 x d, 2 x 2 H, $^2J_{HH}$ = 13 Hz, NCH_2P), 4.12 (s, 3 H, OCH_3). **^{31}P{^{1}H}** NMR (283 MHz, $CDCl_3$, 298 K): δ_P = 25.8 (d, $^1J_{PRh}$ = 100 Hz). **^{13}C{^{1}H} NMR** (176 MHz, $CDCl_3$, 298 K): δ_C = 196.2 (dt, $^1J_{RhC}$ = 48 Hz, $^2J_{PC}$ = 6 Hz, Rh=C_{NHC}), 182.0 (dt, $^1J_{RhC}$ = 26 Hz, $^2J_{PC}$ = 8 Hz, Rh*C*H), 180.7

(s, CO_2Me), 143.1 (d, $^2J_{RhC}$ = 16 Hz, *i*-Ph), 134.1 (napth*C*), 133.6 (vt, $^{2,4}J_{PC}$ = 6 Hz, *o*-PPh_2), 132.8 (napth*C*), 132.3, 132.2 (2 x s, p-PPh_2), 130.6 (vt, $^{3,5}J_{PC}$ = 5 Hz, *m*-PPh_2), 129.8 (vt, $^{3,5}J_{PC}$ = 5 Hz, *m*-PPh_2), 129.5 (*m*-Ph), 129.2 (*p*-Ph), 129.09 (vt, $^{2,4}J_{PC}$ = 5 Hz, *o*-PPh_2), 129.0 (*o*-Ph), 128.8 (napth*C*H), 127.9 (*m*-Ph), 127.4 (Rh-CH=*C*R_2), 127.1 (vt, $^{1,3}J_{PC}$ = 25 Hz, *i*-PPh_2), 125.9 (*o*-Ph), 125.3 (vt, $^{1,3}J_{PC}$ = 25 Hz, *i*-PPh_2), 125.1 (*p*-Ph), 123.8 (napth*C*H), 119.3 (napth*C*), 116.5 (C_β of C_3Ph_3), 109.4 (napth*C*H), 57.1 (vt, $^1J_{CP}$ = 19 Hz, N*C*H_2P), 54.9 (s, O*C*H_3), 34.3 (s, *C*α of C_3Ph_3). **MS** (ESI, +ve ion, m/z): Found: 1053.2012. Calcd. for $C_{62}H_{49}ClN_2O_2P_2{}^{103}Rh$ $[M–PF_6]^+$: 1053.2013. Found: 787.0916. Calcd. for $C_{41}H_{35}ClN_2O_2P_2Rh$ $[M\text{-}C_3Ph_3\text{-}PF_6+H)]^+$: 787.0917. **Anal.** Found: C 62.01, H 4.15, N 2.43. Calcd. For $C_{62}H_{49}ClF_6N_2O_2P_3Rh$: C 62.09, H 4.12, N 2.34.

Crystal Data *for* $C_{81}H_{72}ClN_2O_3P_2Rh$ (M_w =1321.70 gmol^{-1}): triclinic, space group *P*-1 (no. 2), *a* = 13.9449(3) Å, *b* = 16.4856(4) Å, *c* = 17.4017(4) Å, α = 82.943(2)°, β = 81.746(2)°, γ = 84.942(2)°, *V* = 3918.90(16) Å^3, *Z* = 2, *T* = 150.0(1) K, μ(Mo Kα) = 0.337 mm^{-1}, D_{calc} = 1.120 Mgm^{-3}, 40382 reflections measured (6.828° ≤ 2Θ ≤ 60.2°), 18758 unique (R_{int} = 0.0260, R_{sigma} = 0.0460) which were used in all calculations. The final R_1 was 0.0386 ($I > 2\sigma(I)$) and wR_2 was 0.0864 (all data) for 812 refined parameters without restraints. CCDC 2249872.

Synthesis of [Rh{κ^2-C(CO_2Me)C(CO_2Me)C_3Ph_3}Cl(PhPm)]PF_6 (5a): To the solids [RhCl(PhPm)] (80 mg, 0.114 mmol) and $C_3Ph_3PF_6$ (70 mg, 0.170 mmol) was added CH_2Cl_2 (20 mL) and stirred for 10 minutes, turning rapidly from orange though deep green to dark blue. Dimethyl acetylenedicarboxylate (0.30 mL, 2.5 mmol) was added, causing immediate formation of a yellow solution. After one hour stirring, the solution was condensed to *ca.* 3 mL and loaded onto a silica column (2 x 10 cm), washing with CH_2Cl_2 (50 mL) before eluting with 4% MeCN in CH_2Cl_2 to collect a yellow band of the product. Yield: 91 mg (0.072 mmol, 64%). Crystals suitable for structural determination were grown from a solution of benzene and heptane left to stand at room temperature for a week.

IR (CH_2Cl_2, cm^{-1}): 1701 ν_{CO}, 1640, 1586 $\nu_{CCnapth}$, 1493, 1347. Due to the number of overlapped peaks, many ^{1}H and ^{13}C NMR resonances cannot be unequivocally assigned. **^{1}H** NMR (400 MHz, $CDCl_3$, 298 K): δ_H = 7.67 (d, 4 H, $^3J_{HH}$ = 8 Hz, *o*-PPh_2), 7.53 (d, 2 H, $^3J_{HH}$ = 8 Hz, napth*C*H or C_3Ph_3), 7.49 (m, *o*-PPh_2), 7.49-7.43 (overlapped multiplets), 7.41 (m, *m*-PPh_2), 7.33 (t, 2 H, coupling not resolved, *p*-PPh_2), 7.31-7.26 (overlapped multiplets), 7.26 (m, *m*-PPh_2), 7.21-7.16 (overlapped multiplets), 7.16 (m, *m*-Ph), 7.16-7.12 (overlapped multiplets), 7.06 (t, 1 H, $^3J_{HH}$ = 7 Hz, *p*-Ph), 6.92 (t, 1 H, $^3J_{HH}$ = 8 Hz, *p*-Ph), 6.77 (t, 2 H, $^3J_{HH}$ = 8 Hz, *m*-Ph), 6.28 (d, 2 H, $^3J_{HH}$ = 7 Hz, *o*-Ph), 5.40, 5.11 (2 x d, 2 x 2 H, $^2J_{HH}$ = 14 Hz, N*C*H_2P), 4.24, 2.40 (2 x s, 2 x 3 H, C(O)CH_3). **^{31}P{^{1}H} NMR** (283 MHz, $CDCl_3$, 298 K): δ_P = 23.7 (d, $^1J_{PRh}$ = 97 Hz), -144.0 (hept, $^1J_{FP}$ = 713 Hz, PF_6). **^{13}C{^{1}H} NMR** (176 MHz, $CDCl_3$, 298 K): 196.4 (dt, $^1J_{RhC}$ = 48 Hz, $^2J_{PC}$ = 5 Hz, N*C*N), 182.0 (*C*O_2Me), 179.1 (dt, $^1J_{RhC}$ = 30 Hz, $^2J_{PC}$ = 8 Hz, Rh*C*R{CO_2Me}), 172.5 (*C*O_2Me), 144.1, 143.2, 142.7 (3 x s, *i*-Ph), 134.2 (napth*C*), 133.2, 131.8 (2 x br s, *o*-PPh_2), 127.1 (vt, $^{1,3}J_{PC}$ = 25 Hz, *i*-PPh_2), 125.5 (napth*C*H), 123.9 (*o*-Ph), 119.1 (napth*C*), 119.0 (C_β of C_3Ph_3), 109.25 (napth*C*H), 55.7 (vt, $^1J_{CP}$ = 19 Hz, N*C*H_2P), 55.3, 51.7 (2 x s, O*C*H_3), 36.5 (s, Cα of C_3Ph_3). Remaining resonances could not be unequivocally assigned. **MS** (ESI, +ve ion, m/z): Found: 1111.2065. Calcd. For $[M–PF_6]^+$: 1111.2068.

Crystal Data *for* $C_{64}H_{51}ClN_2O_4P_2Rh$ (M_w =1112.36 gmol^{-1}): monoclinic, space group C_2/c (no. 15), *a* = 26.245(5) Å, *b* = 12.218(2) Å, *c* = 39.590(8) Å, *β* = 100.99(3)°, *V* = 12462(4) Å^3, *Z* = 8, *T* = 100.0(2) K, μ(Synchrotron) = 0.412 mm^{-1}, D_{calc} = 1.186 Mgm^{-3}, 73491 reflections measured (2.096° ≤ 2Θ ≤ 52.744°), 11824 unique (R_{int} = 0.0896, R_{sigma} = 0.0658) which were used in all calculations. The final R_1 was 0.0654 ($I > 2\sigma(I)$) and wR_2 was 0.1876 (all data) for 688 refined parameters without restraints. CCDC 2249871.

Synthesis of [Rh{κ^2-CHC(CO_2Me)C_3Ph_3}Cl(CyPm)]PF_6 (4b): Addition of CH_2Cl_2 (5 mL) to the solids [RhCl(CyPm)] (105 mg, 0.144 mmol), and $[C_3Ph_3]PF_6$ (80 mg, 0.19 mmol), resulted in immediate formation of a deep green solution. After 20 minutes stirring, methylpropiolate (0.15 mL, 1.7 mmol) was added and stirred for two hours as a yellow solution. Addition of Et_2O (20 mL) afforded a light brown precipitate which was collected by filtration, washing with Et_2O (20 mL) and *n*-pentane (20 mL) before drying *in vacuo*. This species was not amenable to silica or alumina gel chromatography. Yield: 19 mg (0.016 mmol, 11%).

IR (CH_2Cl_2, cm^{-1}): 1643 ν_{CO}, 1585 ν_{CC}. IR (ATR, cm^{-1}): 1638 ν_{CO}, 1583 ν_{CC}. **^{1}H** NMR (800 MHz, $CDCl_3$, 298 K): δ_H = 9.22 (s, Rh-C*H*R), 7.80 (d, 4 H, $^3J_{HH}$ = 8 Hz, *o*-Ph), 7.48 (t, 4 H, $^3J_{HH}$ = 8 Hz, *m*-Ph), 7.46, 7.45, 7.44 (overlapped doublets, 4 H, napth*CH*), 7.38 (t, 2 H, $^3J_{HH}$ = 7 Hz, *p*-Ph), 7.33 (d, $^3J_{HH}$ = 8 Hz, *o*-Ph), 7.25 (t, 2 H, $^3J_{HH}$ = 8 Hz, *m*-Ph) 7.15 (t, 1 H, $^3J_{HH}$ = 7 Hz, *p*-Ph), 6.94 (d, $^3J_{HH}$ = 7 Hz, napth*CH*), 4.55 (d, 2 H, $^2J_{HH}$ = 13 Hz, N*C*H_2P), 4.08 (s, 3 H, Rh-C=C(CO_2CH_3)), 3.91 (d, 2 H, $^2J_{HH}$ = 13 Hz, N*C*H_2P), 1.99-0.8 (series of multiplets, PCy_2). **^{31}P{^{1}H}** NMR (162 MHz, $CDCl_3$, 298 K): δ_P = 33.09 (d, $^1J_{RhP}$ = 94 Hz), 144, (sept, PF_6). **^{13}C{^{1}H}** NMR (201 MHz, $CDCl_3$, 298 K): δ_C = 196.5 (d.t., $^1J_{RhC}$ = 49 Hz, $^2J_{PC}$ = 5 Hz, Rh=*C*), 185.9 (br. d, $^1J_{RhC}$ = 29 Hz, Rh-*C*H=CR_2), 179.9 (Rh-C=C(*C*$O_2$$CH_3$)R), 143.7 (*i*-Ph), 142.1 (*i*-Ph), 134.2 (napth*C*), 132.7 (napth*C*), 129.9 (*p*-Ph), 129.6 (*o*-Ph), 129.5 (*m*-Ph), 128.8 (*m*-Ph), 128.7, (napth*C*H), 127.9 (Rh–C=*C*(CO_2CH_3)R), 127.0 (*o*-Ph), 126.3 (*p*-Ph), 123.6 (napth*C*H), 119.4 (napthC), 118.3 (C_β of C_3Ph_3), 108.9 (napth*C*H), 54.6 (Rh-C=C(CO_2*C*H_3)R), 52.0 (vt, $^{1,3}J_{RhC}$ = 15 Hz), 34.9 (C_α of C_3Ph_3), 28.4–25.4 (PCy_2). **MS** (ESI, +ve ion, m/z): Found: 1077.3881. Calcd. for $C_{62}H_{73}N_2O_2P_2{}^{35}Cl{}^{103}Rh$ $[M – PF_6]^+$: 1077.3891.

Successive Reaction of [RhCl(CyPm)] with HC≡CCO_2Me and $[C_3Ph_3]PF_6$ – Treating a solution of [RhCl(CyPm)] in CD_2Cl_2 with excess methypropiolate results in the formation of two products in a ratio of 5:3. These were neither identified (no Rh–H resonances were observed in the ^{1}H NMR spectrum) nor isolated. Rather, subsequent treatment with [C3Ph3]PF6 resulted in the formation of *five* new octahedral rhodium complexes ($^1J_{RhP}$ = 86 to 96 Hz), however none of these corresponded to **4b**. The 31P{1H} NMR spactra are shown below for (a) addition of excess methylpropiolate followed by (b) addition of $[C_3Ph_3]PF_6$.

(a) RhCl(CyPm) + excess methylpropiolate

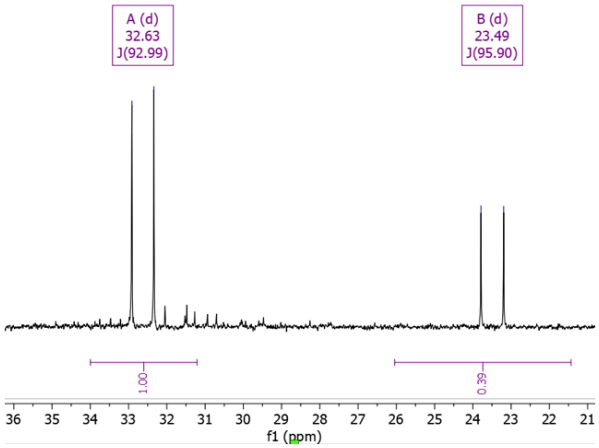

(b) RhCl(CyPm) + (i) excess methylpropiolate; (ii) $[C_3Ph_3]PF_6$

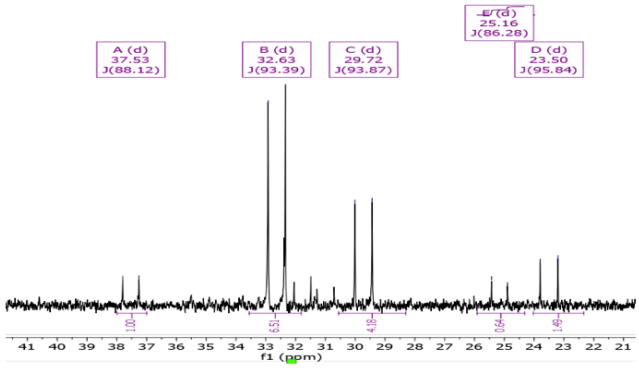

Figure S3. 31P{1H} NMR spectra for the successive addition of methyl propiolate and $[C_3Ph_3]PF_6$ to [RhCl(CyPm)].

References

1 CrysAlis PRO, Agilent Technologies Ltd, Yarnton, Oxfordshire, England, 2014.

2 (a) G. Sheldrick, *Acta Crystallogr. Sect. A: Found. Crystallogr.*, 2008, **64**, 112-122; (b) G. M. Sheldrick, *Acta Crystallogr. Sect. C: Cryst. Struct. Commun.*, 2015, **71**, 3-8.

3 (a) C. F. Macrae, P. R. Edgington, P. McCabe, E. Pidcock, G. P. Shields, R. Taylor, M. Towler and J. van de Streek, *J. Appl. Crystallogr.*, 2006, **39**, 453-457; (b) C. F. Macrae, I. J. Bruno, J. A. Chisholm, P. R. Edgington, P. McCabe, E. Pidcock, L. Rodriguez-Monge, R. Taylor, J. van de Streek and P. A. Wood, *J. Appl. Crystallogr.*, 2008, **41**, 466-470.

4 T. M. McPhillips, S. E. McPhillips, H.J. Chiu, A. E. Cohen, A. M. Deacon, P. J. Ellis, E. Garman, A. Gonzalez, N. K. Sauter, R. P. Phizackerley, S. M. Soltis, P. Kuhn, *J. Synchrotron Radiat.*, 2002, **9**, 401-406.

5 W. Kabsch, *J. Appl. Crystallogr*. 1993, **26**, 795-800.

6 A. F. Hill and C. M. A. McQueen, *Organometallics*, 2012, **31**, 8051–8054.

7 Y. Wang, B. Zheng, Y. Pan, C. Pan, L. He and K.-W. Huang, *Dalton Trans.*, 2015, **44**, 15111–15115.

8 R. Xu and R. Breslow, *Org, Synth.* 1997, **74**, 72.

9 R. P. Hughes, J. W. Reisch and A. L. Rheingold, *Organometallics*, 1985, **4**, 1754–1761.

10 *Spartan 20*® (2020) Wavefunction, Inc., 18401 Von Karman Ave., Suite 370 Irvine, CA 92612 U.S.A.

11 J. D. Chai and M. Head-Gordon, *J Chem Phys.*, 2008, **128**, 084106.

12 J. D. Chai and M. Head-Gordon, *Phys Chem Chem Phys*, 2008, **10**, 6615-6620.

13 P. J. Hay and W. R. Wadt, *J. Chem. Phys.*, 1985, **82**, 270-283.

14 P. J. Hay and W. R. Wadt, *J. Chem. Phys.*, 1985, **82**, 299-310.

15 W. R. Wadt and P. J. Hay, *J. Chem. Phys.*, 1985, **82**, 284-298.

16 W. J. Hehre, R. Ditchfeld and J. A. Pople, *J. Chem. Phys.*, 1972, **56**, 2257–2261.

17 F. Weigend and R. Ahlrichs, *Phys. Chem. Chem. Phys.* 2005, **7**, 3297-3305.

18 L. Falivene, Z. Cao, A. Petta, L. Serra, A. Poater, R. Olivia, V. Scarano and L. Cavallo, *Nat. Chem.*, 2019, **11**, 872-879.

19 G. Zuccarello, L. J. Nannini, A. Arroyo-Bondía, N. Fincias, I. Arranz, A. H. Pérez-Jimeno, M. Peeters, I. Martín-Torres, A. Sadurní, V. García, Y. Wang, M. S. Kirillova, M. Montesinos-Magraner, U. Caniparoli, G. D. Núñez, F. Maseras, M. Besora, I. Escofet, A. M. Echavarren. *JACS Au* , 2023, **3**, 1742-1754.

Computational Results

Percent Buried Volume:
(Falivene, L. et al. Nat. Chem. 2019, 11, 872)

For [RhCl(PNP^{t}Bu)]:

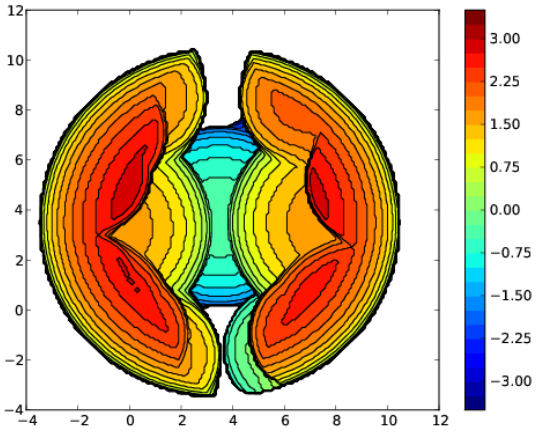

%V Free	%V Buried	% V Tot/V Ex
26.1	**73.9**	100.0

Quadrant	V f	V b	V t	%V f	%V b
SW	9.7	35.1	44.9	**21.7**	78.3
NW	11.6	33.3	44.9	**25.8**	74.2
NE	13.4	31.5	44.9	**29.8**	70.2
SE	12.1	32.8	44.9	**27.0**	73.0

Figure S4. Steric map for 'Rh(PN^{t}Bu)' based on coordinates for [RhCl(PN^{t}Bu)].

For [RhCl(PhPm)]:

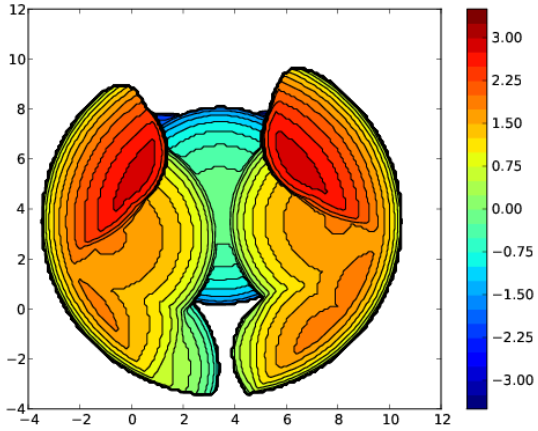

%V Free	%V Buried	% V Tot/V Ex
35.6	**64.4**	100.0

Quadrant	V f	V b	V t	%V f	%V b
SW	13.9	31.0	44.9	**31.0**	69.0
NW	18.3	26.6	44.9	**40.7**	59.3
NE	15.4	29.5	44.9	**34.3**	65.7
SE	16.3	28.6	44.9	**36.2**	63.8

Figure S5. Steric map for 'Rh(PhPm)' based on coordinates for [RhCl(PhPm)].

For [RhCl(CyPm)]:

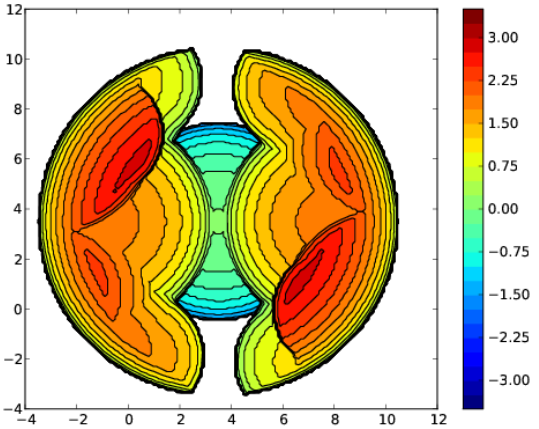

%V Free	%V Buried	% V Tot/V Ex
30.4	**69.6**	100.0

Quadrant	V f	V b	V t	%V f	%V b
SW	14.2	30.7	44.9	**31.7**	68.3
NW	13.1	31.8	44.9	**29.2**	70.8
NE	14.2	30.7	44.9	**31.5**	68.5
SE	13.1	31.8	44.9	**29.1**	70.9

Figure S6. Steric map for 'Rh(CyPm)' based on coordinates for [RhCl(CyPm)].

Additional Crystal Data

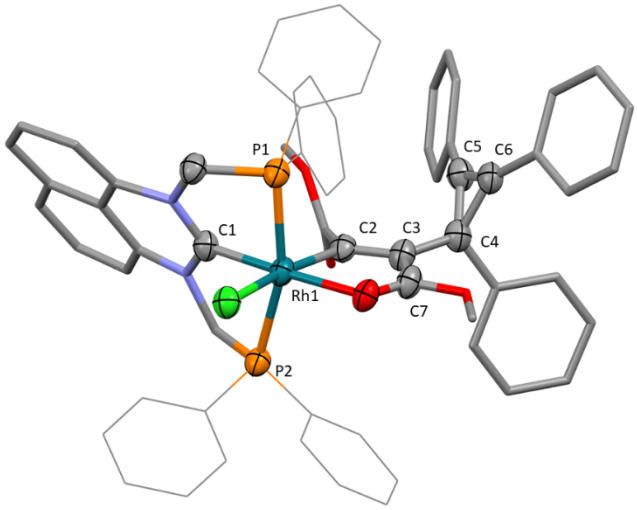

Figure S7. Molecular structure of **3b** in a crystal of **3b**.2($CHCl_3$). A solent mask was required to model disordered solvent and counter anion peaks. The naphthalene and phenyl groups are simplified, and hydrogen atoms are omitted for clarity. Selected distances [Å] and angles [°]: Rh1–C1 1.978(4), Rh1–O1 2.118(3), Rh1–Cl1 2.4267(10), Rh1–P1 2.3140(10), Rh1–P2 2.3111(11), Rh1–C2 2.050(4), C2–C3 1.353(5), C3–C4 1.515(5), C3–C7 1.458(5), P1–Rh1–P2 162.06(4), C1–Rh1–O1 177.18(12), Cl1–Rh1–C2 169.15(11).

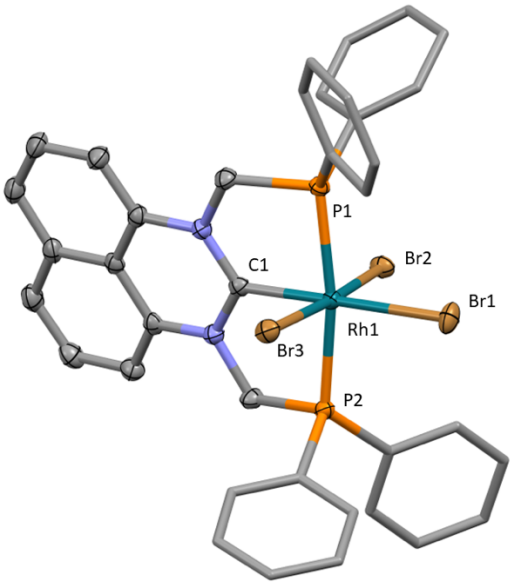

Figure S8. Molecular structure of **2** in a crystal of **2**.2(C_6H_6) showing 50% thermal probability ellipsoids. Phenyl rings simplified for clarity and hydrogen atoms omitted. Selected distances [Å] and angles [°]: Rh1–C1 1.994(2), Rh1–Br1 2.5463(3), Rh1–Br2 2.4964(3), Rh1–Br3 2.4796(3), P1–Rh1–P2 169.500(19), Br2–Rh1–Br3 173.695(10).

Table S1: Cartesian coordinates for [RhCl(HPm)]

Atom	x	y	z
Rh	-0.000560	0.001681	-2.058813
N	-0.000300	-0.000529	0.021996
C	0.000054	0.002005	2.793279
C	1.165944	0.000374	0.709804
C	-1.166332	-0.001603	0.710249
C	-1.203614	-0.000077	2.106033
C	1.203417	0.001955	2.105759
H	-2.153816	0.000359	2.627289
H	2.153811	0.002927	2.626679
H	0.000185	0.003628	3.878701
N	2.318285	-0.000006	-0.043442
H	3.190866	-0.000010	0.463876
N	-2.318872	-0.004251	-0.043077
H	-3.191320	-0.002096	0.464427
P	2.228736	-0.002179	-1.765208
H	3.099551	-1.061643	-2.099399
H	3.100085	1.055716	-2.103200
P	-2.229159	-0.003087	-1.764565
H	-3.101151	1.055042	-2.100172
H	-3.098306	-1.062973	-2.101525
Cl	0.002497	0.014768	-4.428689

Computationally Optimised Geometries.

1. **[RhCl{py(NHPH$_2$)$_2$-2,6] [DFT:ωB97X-D/6-31G*/LANL2Dζ]**

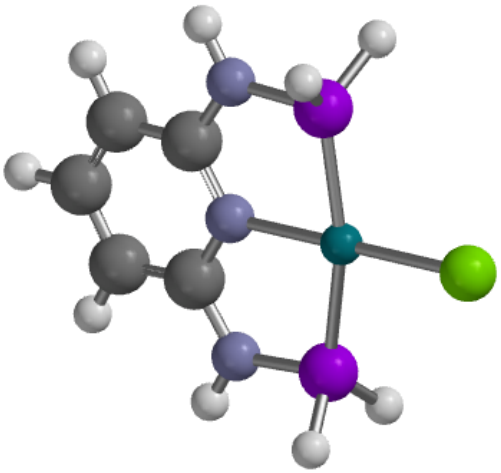

Figure S9: Optimised structure of [RhCl(HPm)] in the gas phase.

2. **[RhCl(CH$_3$){C(NHCH)$_2$}(PH$_3$)$_2$]$^+$ [DFT:ωB97X-D/6-31G*/LANL2Dζ]**

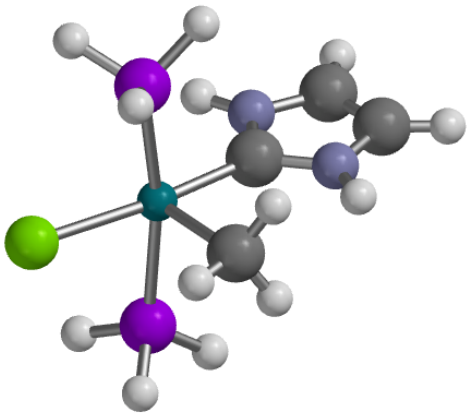

Figure S10: Optimised structure of [RhCl(CH$_3$){C(NHCH)$_2$}(PH$_3$)$_2$]$^+$ in the gas phase.

Table S2: Cartesian coordinates for $[RhCl(CH_3)\{C(NHCH)_2\}(PH_3)_2]^+$

Atom	x	y	z
Rh	-0.966859	-0.322854	-0.630553
P	-0.821316	-2.613620	-0.109070
H	-0.871348	-3.478712	-1.211192
H	-1.895163	-3.081310	0.659166
H	0.271687	-3.142223	0.599520
P	-1.556339	1.857019	-1.296869
H	-1.812530	2.009439	-2.666543
H	-0.721643	2.961550	-1.052940
H	-2.761770	2.299543	-0.737089
Cl	-3.082778	-0.910049	-1.543199
C	0.938095	0.125296	-0.104168
N	2.010611	0.082119	-0.925376
H	1.958021	-0.182256	-1.898320
N	1.459549	0.519491	1.074079
H	0.905915	0.649339	1.907566
C	3.179828	0.442646	-0.274872
H	4.136598	0.467328	-0.770587
C	2.828014	0.720949	0.999377
H	3.415293	1.037279	1.845996
C	-1.560986	0.090670	1.292954
H	-2.639082	-0.078209	1.291625
H	-1.340787	1.130760	1.549033
H	-1.073010	-0.584194	2.001462

3. $[RhCl(\sigma\text{-}C_3H_3)\{C(NHCH)_2\}(PH_3)_2]^+$ [DFT:ωB97X-D/6-31G*/LANL2DZ]

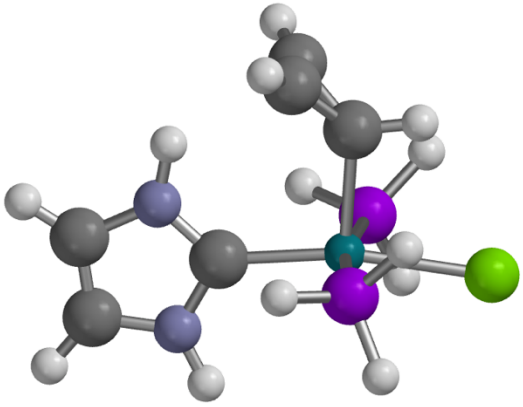

Figure S11: Optimised structure of $[RhCl(\sigma\text{-}C_3H_3)\{C(NHCH)_2\}(PH_3)_2]^+$ in the gas phase.

Table S3: Cartesian coordinates for $[RhCl(\sigma\text{-}C_3H_3)\{C(NHCH)_2\}(PH_3)_2]^+$

Atom	x	y	z
Rh	-0.876099	-0.363757	-0.836240
P	-0.711480	-2.655649	-0.349233
H	-0.680362	-3.503976	-1.465638
H	-1.813327	-3.173081	0.345933
H	0.350643	-3.185140	0.405945
P	-1.437126	1.805232	-1.537930
H	-1.581711	1.966106	-2.923732
H	-0.641491	2.924541	-1.233878
H	-2.690149	2.244179	-1.089613
Cl	-2.949226	-0.974819	-1.874992
C	1.042788	0.082484	-0.331366
N	2.073496	0.027313	-1.207521
H	1.967363	-0.240709	-2.175178
N	1.631963	0.474791	0.815163
H	1.111509	0.609235	1.670851
C	3.278582	0.377957	-0.620756
H	4.208427	0.392164	-1.165701
C	2.996321	0.663083	0.669202
H	3.631401	0.975803	1.482662
C	-1.736860	-0.010723	1.020140
H	-2.783155	-0.232823	0.803401
C	-1.096539	-0.257354	2.314347
H	-0.760448	-0.982709	3.040784
C	-1.293675	0.996489	1.987323
H	-1.240846	2.041364	2.256025

4. $[RhCl(\kappa^2\text{-}C_3H_3)(CO)(PH_3)_2]^+$ [DFT:ωB97X-D/6-31G*/LANL2DZ]

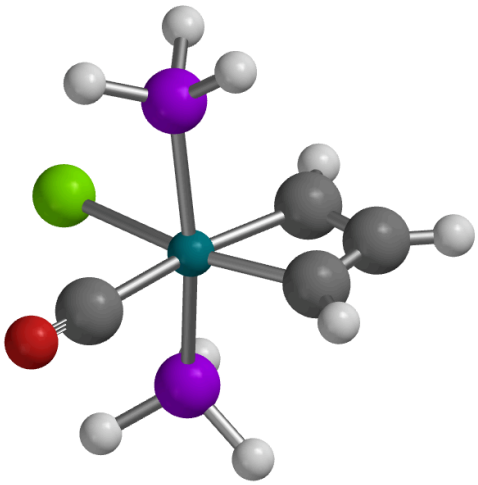

Figure S12: Optimised structure of $[RhCl(\kappa^2\text{-}C_3H_3)(CO)(PH_3)_2]^+$ in the gas phase.

Table S4: Cartesian coordinates for $[RhCl(\kappa^2\text{-}C_3H_3)(CO)(PH_3)_2]^+$

Atom	x	y	z
Rh	-0.312750	0.001160	-0.213876
P	-0.185125	2.355285	-0.515590
H	-1.255265	2.911046	-1.225229
H	0.915555	2.741901	-1.287687
H	-0.083409	3.211079	0.592843
P	-0.213899	-2.356976	-0.494205
H	-1.287091	-2.902967	-1.206540
H	-0.131919	-3.205670	0.621398
H	0.886462	-2.765435	-1.255254
Cl	-0.247057	-0.013103	-2.647682
C	-2.354319	0.012106	-0.335220
O	-3.480799	0.018325	-0.433929
C	1.650878	-0.007545	0.265421
H	2.562002	-0.015327	-0.333929
C	0.142064	0.006425	1.738960
H	-0.438450	0.010700	2.662839
C	1.536006	-0.000134	1.645718
H	2.297119	-0.000871	2.421962

Table S5: Cartesian coordinates for $[RhCl_2(\kappa^2\text{-}C_3H_4)(PH_3)_2]$

Atom	x	y	z
Rh	-0.272456	0.002390	-0.284996
P	-0.459900	2.323722	-0.526783
H	0.676974	3.120678	-0.758691
H	-1.069647	3.055425	0.504588
H	-1.258969	2.650087	-1.625944
P	-0.537572	-2.313093	-0.500299
H	-1.620121	-2.620114	-1.329368
H	-0.804450	-3.117177	0.623862
H	0.501262	-3.050793	-1.089781
Cl	-0.115856	-0.115854	-2.743527
C	1.650221	-0.049307	0.187371
H	2.572056	-0.088774	-0.394871
C	0.135315	0.030054	1.651525
H	-0.475735	0.065402	2.554745
C	1.527110	-0.015454	1.576100
H	2.284069	-0.022698	2.358223
Cl	-2.732299	0.145504	-0.202154

5. $[RhCl_2(\kappa^2\text{-}C_3H_4)(PH_3)_2]$ [DFT:ωB97X-D/6-31G*/LANL2Dζ]

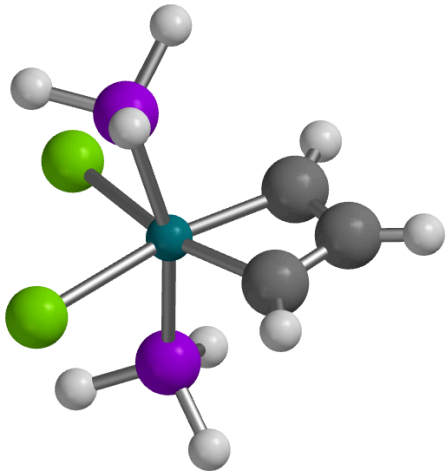

Figure S13: Optimised structure of $[RhCl_2(\kappa^2\text{-}C_3H_4)(PH_3)_2]$ in the gas phase.

6. $[RhCl(\kappa^2\text{-}C_3Me_3)\{C(NHCH)_2\}(PH_3)_2]^+$ [DFT:ωB97X-D/6-31G*/LANL2Dζ]

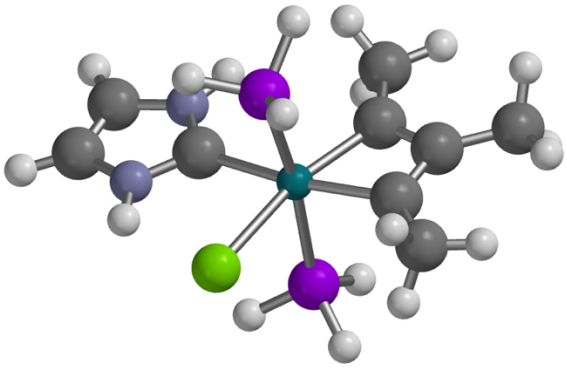

Figure S14: Optimised structure of $[RhCl(\kappa^2\text{-}C_3Me_3)\{C(NHCH)_2\}(PH_3)_2]^+$ in the gas phase.

Table S6: Cartesian coordinates for $[RhCl(\kappa^2\text{-}C_3Me_3)\{C(NHCH)_2\}(PH_3)_2]^+$

Atom	x	y	z
Rh	-0.082152	0.005313	-0.608053
P	-0.101515	-2.326093	-0.829929
H	0.965486	-2.864915	-1.560820
H	-1.195217	-2.849371	-1.534384
H	-0.100708	-3.167981	0.297326
P	-0.106800	2.339298	-0.801109
H	0.976708	2.893731	-1.495596
H	-0.137758	3.164997	0.337673
H	-1.184109	2.868625	-1.525592
Cl	-0.124058	0.015693	-3.095733
C	-2.081571	-0.000824	-0.174200
C	-0.587177	-0.006600	1.335487
C	-1.976078	-0.010670	1.222833
C	2.033609	0.006278	-0.711260
N	2.728484	0.008445	-1.862170
H	2.236988	0.010942	-2.753826
N	2.994873	0.003027	0.238798
H	2.795350	-0.000684	1.226656
C	4.092444	0.004714	-1.651762
H	4.807127	0.005373	-2.458676
C	4.267722	0.002683	-0.309348
H	5.162402	0.000123	0.291763
C	0.215810	-0.012502	2.580603
H	0.871664	0.868009	2.598863
H	0.868349	-0.895748	2.591468
H	-0.391576	-0.016291	3.491427
C	-3.026900	-0.024799	2.298217
H	-2.878285	0.794092	3.009472
H	-3.005129	-0.962908	2.862773
H	-4.027260	0.083801	1.872221
C	-3.285208	0.008648	-1.020248
H	-3.281218	0.920915	-1.632084
H	-4.230224	-0.063946	-0.473519
H	-3.214073	-0.801374	-1.757271

7. $[RhCl(\sigma\text{-}\pi\text{-}C_3Ph_3)(MePm)]^+$ [DFT:ωB97X-D/6-31G*/LANL2Dζ]

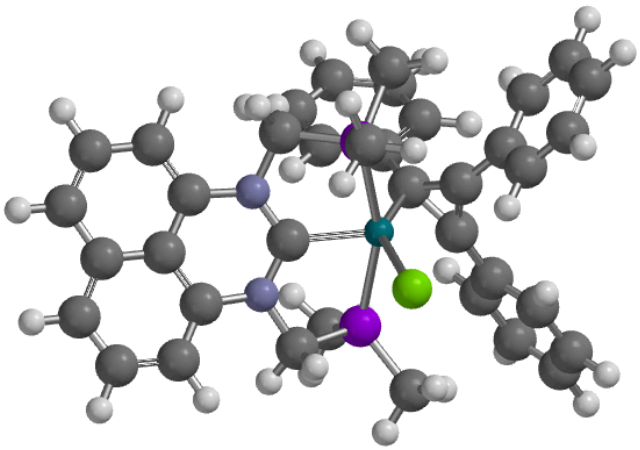

Figure S15: Optimised structure of $[RhCl(\sigma\text{-}\pi\text{-}C_3Ph_3)(MePm)]^+$ in the gas phase.

Table S7: Cartesian coordinates for $RhCl(\sigma\text{-}\pi\text{-}C_3Ph_3)(MePm)]^+$

Atom	x	y	z
Rh	0.568649	-0.235924	-0.455769
Cl	2.560909	-1.488179	-1.370768
P	-0.607165	-2.192244	-0.874781
P	1.835297	1.331072	0.710545
N	0.487506	-2.458100	1.556121
N	0.879325	-0.408477	2.532917
C	0.631515	-1.122323	1.407138
C	-0.880477	1.161686	-0.917833
C	0.197243	-3.265636	0.377222
H	-0.469842	-4.085106	0.658208
H	1.125320	-3.665580	-0.045022
C	0.809416	-0.950160	3.843120
C	0.790933	-2.359595	3.946944
C	1.222382	1.000836	2.415100
H	1.994430	1.239226	3.153099
H	0.346352	1.633234	2.606309
C	0.864722	-2.977806	5.219252
C	0.205667	1.465185	-1.872120
C	0.710781	-3.149239	2.776689
C	-0.754965	0.571630	-2.229979
C	0.926370	-4.393159	5.278286
H	0.988615	-4.878533	6.247003
C	0.804269	-4.519652	2.858108
H	0.797285	-5.145293	1.974773
C	0.827043	-0.788469	6.245317
H	0.823916	-0.160389	7.130012
C	0.878775	-2.151059	6.371681
H	0.929890	-2.614141	7.351876
C	0.920789	-5.132578	4.125455
H	0.991808	-6.214063	4.173511
C	3.629472	1.039198	0.763082
H	3.816685	-0.010341	1.000599
H	4.117725	1.694647	1.490718
H	4.035879	1.222651	-0.235053
C	1.645132	3.145593	0.629617
H	2.010970	3.593603	1.559377
H	0.592546	3.407458	0.491152
H	2.221163	3.547265	-0.205760
C	-0.480457	-3.176606	-2.401592
H	0.543495	-3.100746	-2.775958
H	-1.175047	-2.796298	-3.153319
H	-0.724362	-4.223290	-2.192372
C	-2.371398	-2.229903	-0.401690
H	-2.482577	-1.802899	0.598227
H	-2.762627	-3.251796	-0.412899
H	-2.951897	-1.624653	-1.100100
C	0.801814	-0.168887	4.975820
H	0.780664	0.912479	4.921839
C	-1.936110	1.894511	-0.201320
C	-3.935241	3.285396	1.169992
C	-2.247412	1.563449	1.118370
C	-2.641465	2.924609	-0.834696
C	-3.633640	3.616226	-0.149754
C	-3.244075	2.255197	1.801080
H	-1.708543	0.749047	1.596092
H	-2.416891	3.176186	-1.868319
H	-4.174109	4.415155	-0.647847
H	-3.482242	1.986981	2.825763
H	-4.710653	3.827130	1.701803
C	-1.378122	-0.054879	-3.376750

C	-2.546793	-1.258176	-5.590312
C	-0.582990	-0.424947	-4.467884
C	-2.760066	-0.268607	-3.403307
C	-3.342013	-0.868867	-4.513858
C	-1.170551	-1.031647	-5.569562
H	0.488915	-0.256142	-4.428440
H	-3.370894	0.061008	-2.567365
H	-4.414599	-1.029856	-4.542890
H	-0.557738	-1.328942	-6.413933
H	-3.002693	-1.732536	-6.453542
C	1.146030	2.423526	-2.453077
C	2.947321	4.242844	-3.545162
C	0.792820	3.770915	-2.567798
C	2.400483	1.984310	-2.887290
C	3.297412	2.899386	-3.429739
C	1.694130	4.675614	-3.117318
H	-0.177440	4.109592	-2.216619
H	2.669774	0.936145	-2.771053
H	4.273857	2.559172	-3.762866
H	1.419011	5.720639	-3.207952
H	3.650588	4.952917	-3.968545

8. [RhCl(κ²-C_3Ph_3)(PhPm)]⁺

[DFT:ωB97X-D/6-31G*/def2-SV(P)]

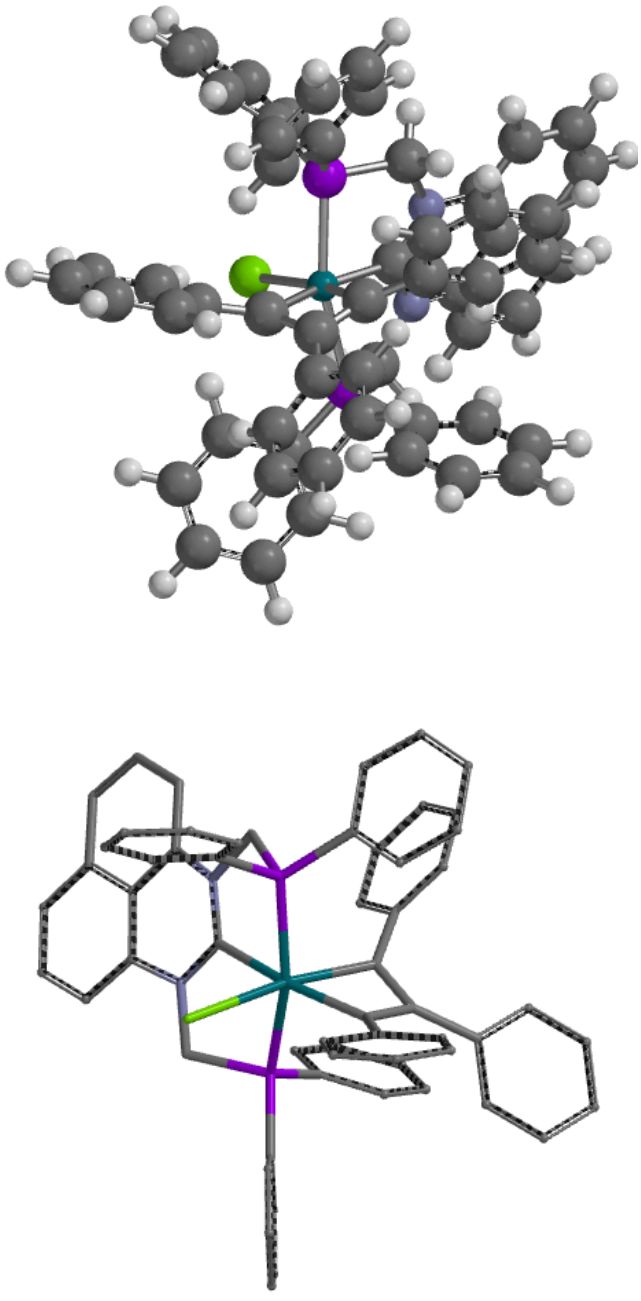

Figure S16: Optimised structure of [RhCl(κ²-C_3Ph_3)(PhPm)]⁺ in the gas phase.

Table S8: Cartesian coordinates for $[RhCl(\kappa^2\text{-}C_3Ph_3)(PhPm)]^+$

Atom	x	y	z
Rh	-0.031271	0.144035	-0.802327
Cl	0.463329	0.441235	-3.212527
P	-0.044571	-2.149265	-1.206927
P	0.682429	2.282235	-0.271527
N	2.535930	-1.372165	-1.140827
N	2.806230	0.586835	0.064973
C	1.995530	-0.255565	-0.609327
C	-0.832871	-0.072165	1.025173
C	1.664129	-2.287665	-1.880727
H	2.033029	-3.315865	-1.785127
H	1.625129	-2.005865	-2.943727
C	4.148630	0.277435	0.393473
C	4.720130	-0.847465	-0.256127
C	2.263030	1.832935	0.591273
H	3.002330	2.634335	0.451373
H	2.055130	1.724335	1.668674
C	6.093030	-1.154965	-0.062227
C	-2.070871	0.383035	-0.596827
C	3.922930	-1.660165	-1.104727
C	-2.183071	-0.176165	0.699473
C	6.653030	-2.243765	-0.782327
H	7.708830	-2.483665	-0.644727
C	4.501030	-2.692065	-1.815027
H	3.924130	-3.297265	-2.511527
C	6.254430	0.689035	1.499774
H	6.835430	1.291835	2.200074
C	6.847030	-0.356965	0.839573
H	7.901530	-0.589565	0.998273
C	5.876730	-2.971765	-1.647627
H	6.316230	-3.792965	-2.216627
C	4.898630	1.024035	1.278473
H	4.473430	1.872735	1.810274
C	1.181329	3.417835	-1.600227
C	1.914930	5.091335	-3.710627
C	2.312030	3.122235	-2.372127
C	0.412729	4.547435	-1.899227
C	0.781029	5.379935	-2.954227
C	2.680730	3.963335	-3.416827
H	2.903830	2.226135	-2.173227
H	-0.470971	4.791435	-1.306127
H	0.180029	6.262635	-3.180827
H	3.564430	3.729035	-4.012827
H	2.203329	5.746935	-4.534727
C	-0.191771	3.318635	0.943873
C	-1.619171	4.856435	2.796074
C	0.481629	3.999735	1.965174
C	-1.582371	3.439235	0.842173
C	-2.292971	4.204935	1.764174
C	-0.230871	4.758735	2.890074
H	1.568229	3.945735	2.055874
H	-2.118871	2.934535	0.038773
H	-3.377571	4.289235	1.673474
H	0.302529	5.280535	3.686874
H	-2.175071	5.451635	3.523274
C	-0.041871	-3.208865	0.275673
C	-0.130371	-4.578865	2.716974
C	-1.261471	-3.408665	0.935673
C	1.132129	-3.723065	0.841273
C	1.083829	-4.408265	2.054574
C	-1.305071	-4.082765	2.152174
H	-2.191271	-3.038965	0.500073
H	2.101929	-3.585765	0.358173
H	2.004330	-4.806965	2.485274
H	-2.263671	-4.216465	2.657374
H	-0.162071	-5.106766	3.671974
C	-1.159671	-2.961265	-2.382927
C	-2.908971	-4.170865	-4.186027
C	-1.906671	-2.173965	-3.267627
C	-1.292271	-4.356965	-2.402727
C	-2.163871	-4.957666	-3.306527
C	-2.780071	-2.783065	-4.166127
H	-1.783271	-1.090165	-3.265227
H	-0.725571	-4.976266	-1.702927
H	-2.265971	-6.044466	-3.321327
H	-3.360771	-2.167065	-4.855227
H	-3.595371	-4.644865	-4.890827
C	-0.161371	0.051035	2.318874
C	1.265129	0.462535	4.700874
C	1.015129	-0.669865	2.582974
C	-0.605171	0.990235	3.264974
C	0.110529	1.199635	4.440874
C	1.710230	-0.479865	3.771474
H	1.373229	-1.394765	1.853074
H	-1.490471	1.593435	3.052274
H	-0.236971	1.947635	5.156074
H	2.611830	-1.063065	3.969174
H	1.820329	0.623135	5.627174
C	-3.076171	1.111735	-1.349227
C	-4.909071	2.645235	-2.819127
C	-4.332071	1.460235	-0.798127
C	-2.755371	1.573635	-2.642327
C	-3.671971	2.321435	-3.374327
C	-5.233471	2.222635	-1.525627
H	-4.589671	1.146935	0.213873
H	-1.770071	1.342635	-3.056727
H	-3.412771	2.664535	-4.377527
H	-6.196671	2.491835	-1.087827
H	-5.624971	3.240435	-3.390527
C	-3.336571	-0.763965	1.416973
C	-5.468271	-2.122765	2.653474
C	-3.455371	-0.788565	2.813074
C	-4.298771	-1.448165	0.653073
C	-5.354371	-2.117565	1.262773
C	-4.515171	-1.458765	3.422674
H	-2.716571	-0.288665	3.437074
H	-4.206371	-1.466465	-0.436127
H	-6.088471	-2.643765	0.649273
H	-4.593771	-1.460465	4.511674
H	-6.296271	-2.646565	3.135174

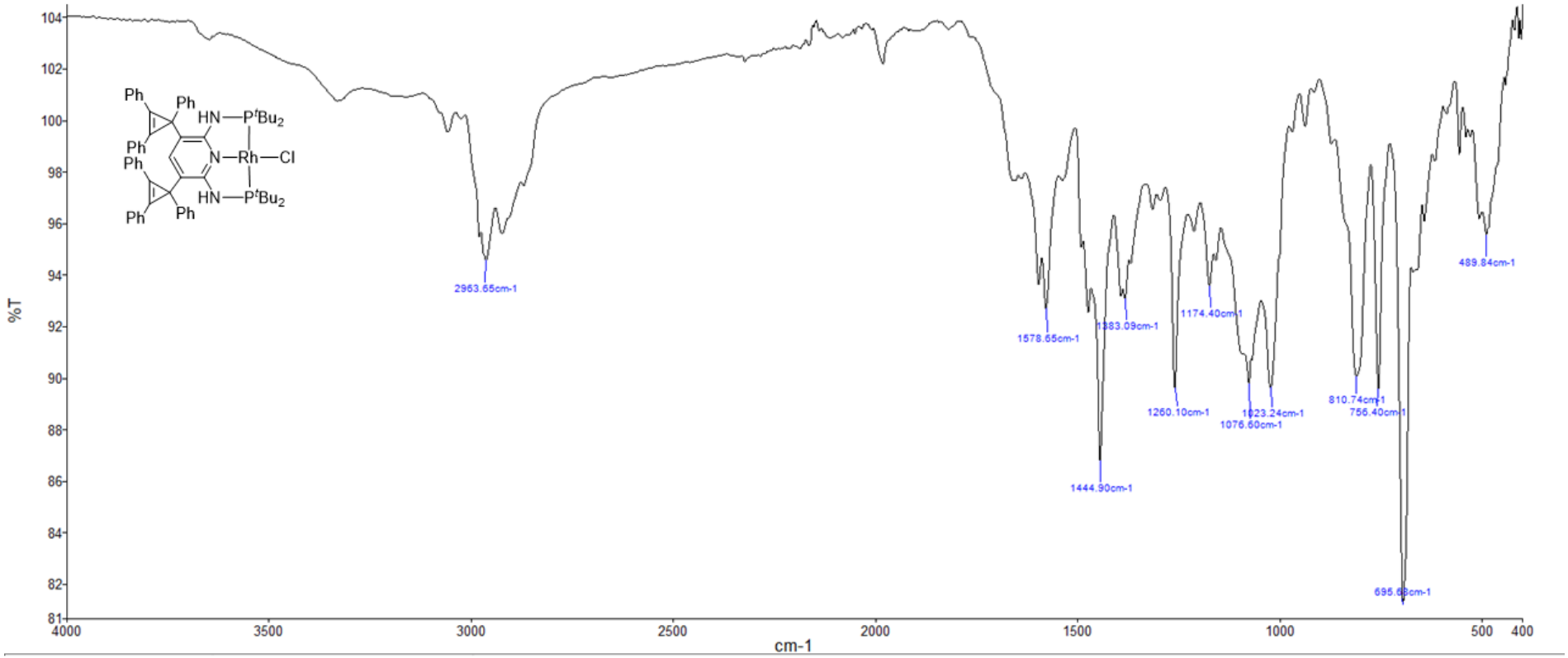

Figure S17. IR (ATR, cm^{-1}) for [RhCl{PNP^{t}Bu.2(C$_3$Ph$_3$)}]. (**1**)

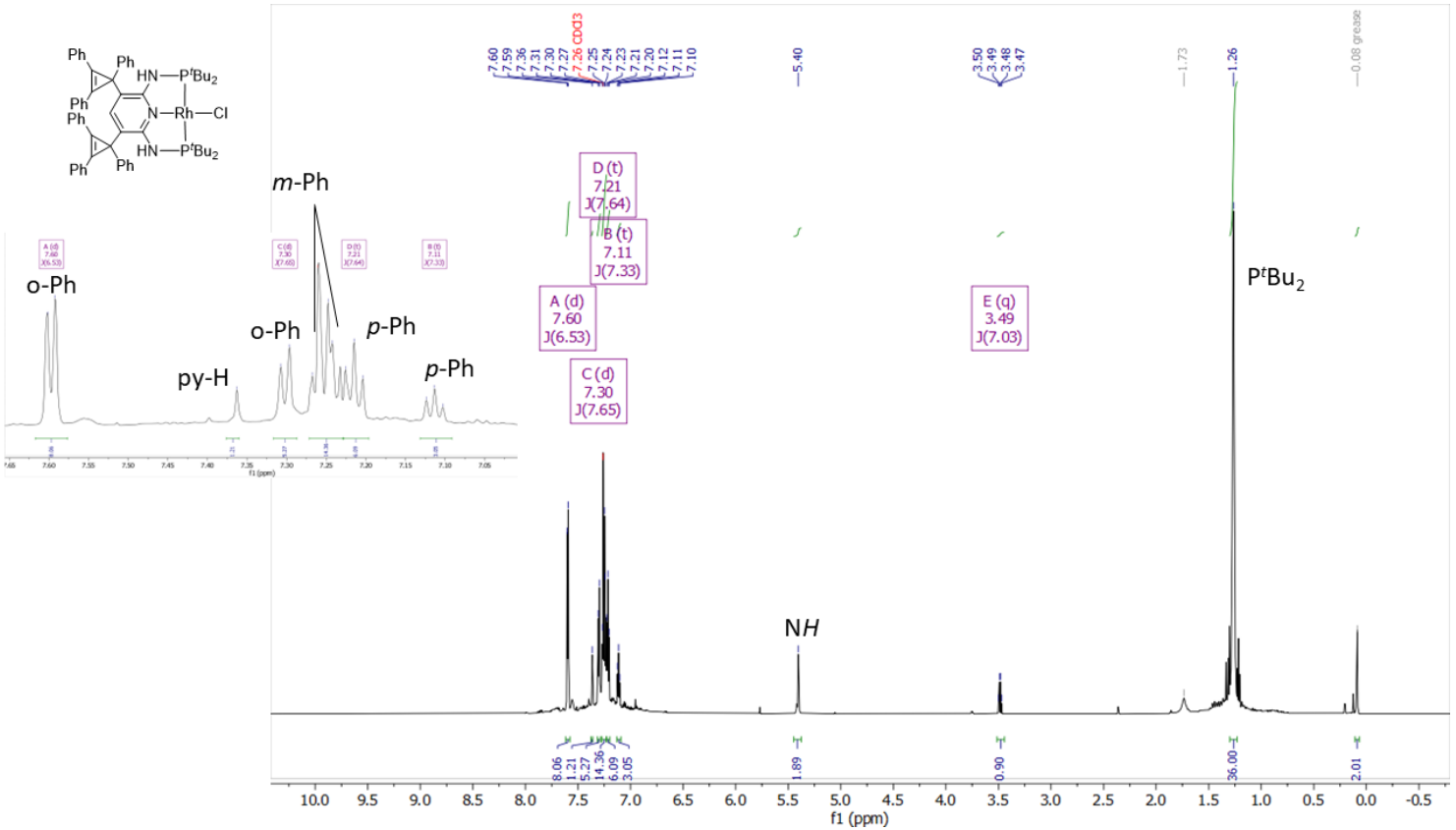

Figure S18. ^{1}H NMR (700 MHz, $CDCl_3$, 298 K) for [RhCl{PNP^{t}Bu$_2$(C_3Ph$_3$)]. (**1**)

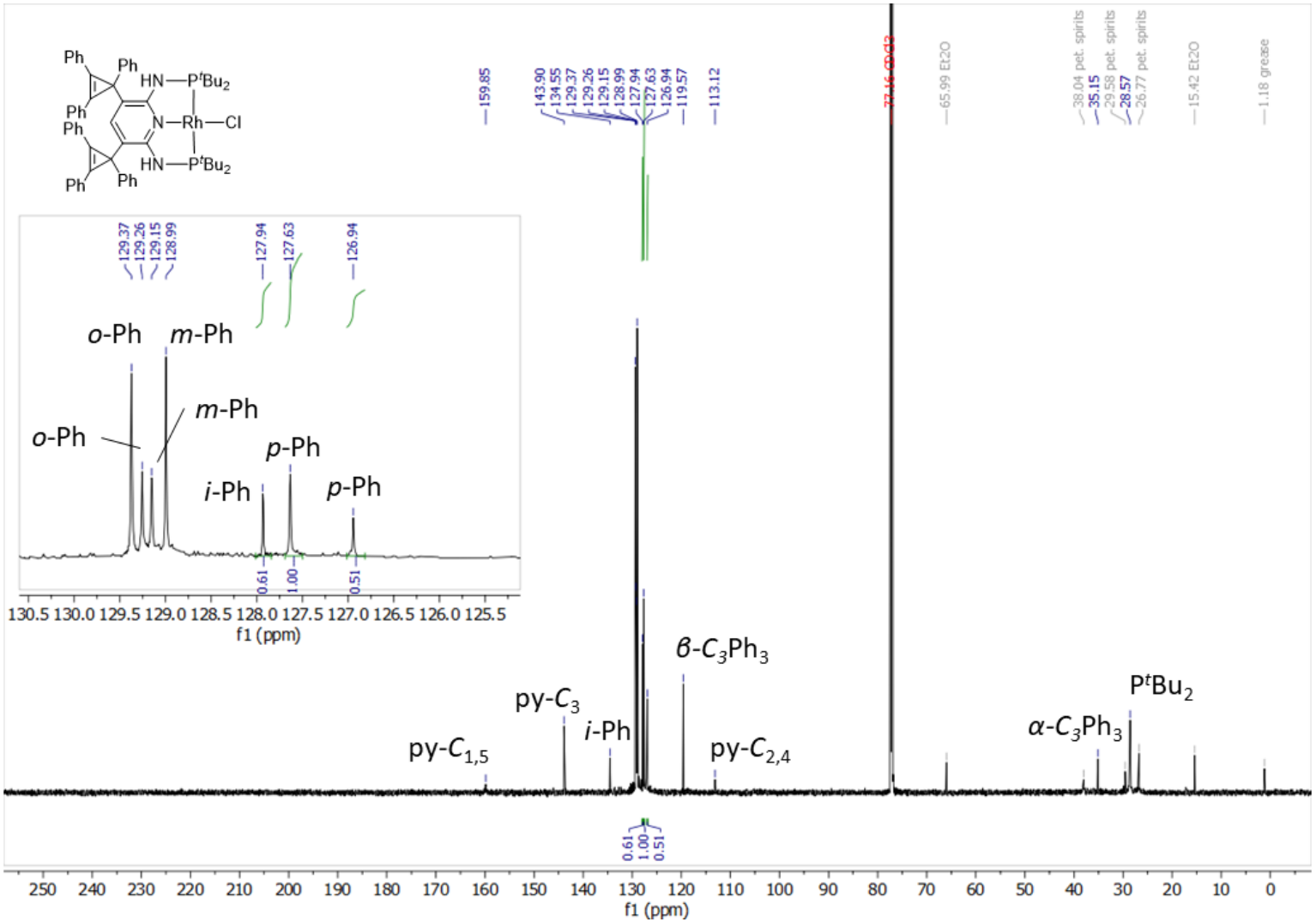

Figure S19. ^{13}C NMR (176 MHz, $CDCl_3$, 298 K) for [RhCl{PNP^{t}Bu.2(C_3Ph_3)}]. (**1**)

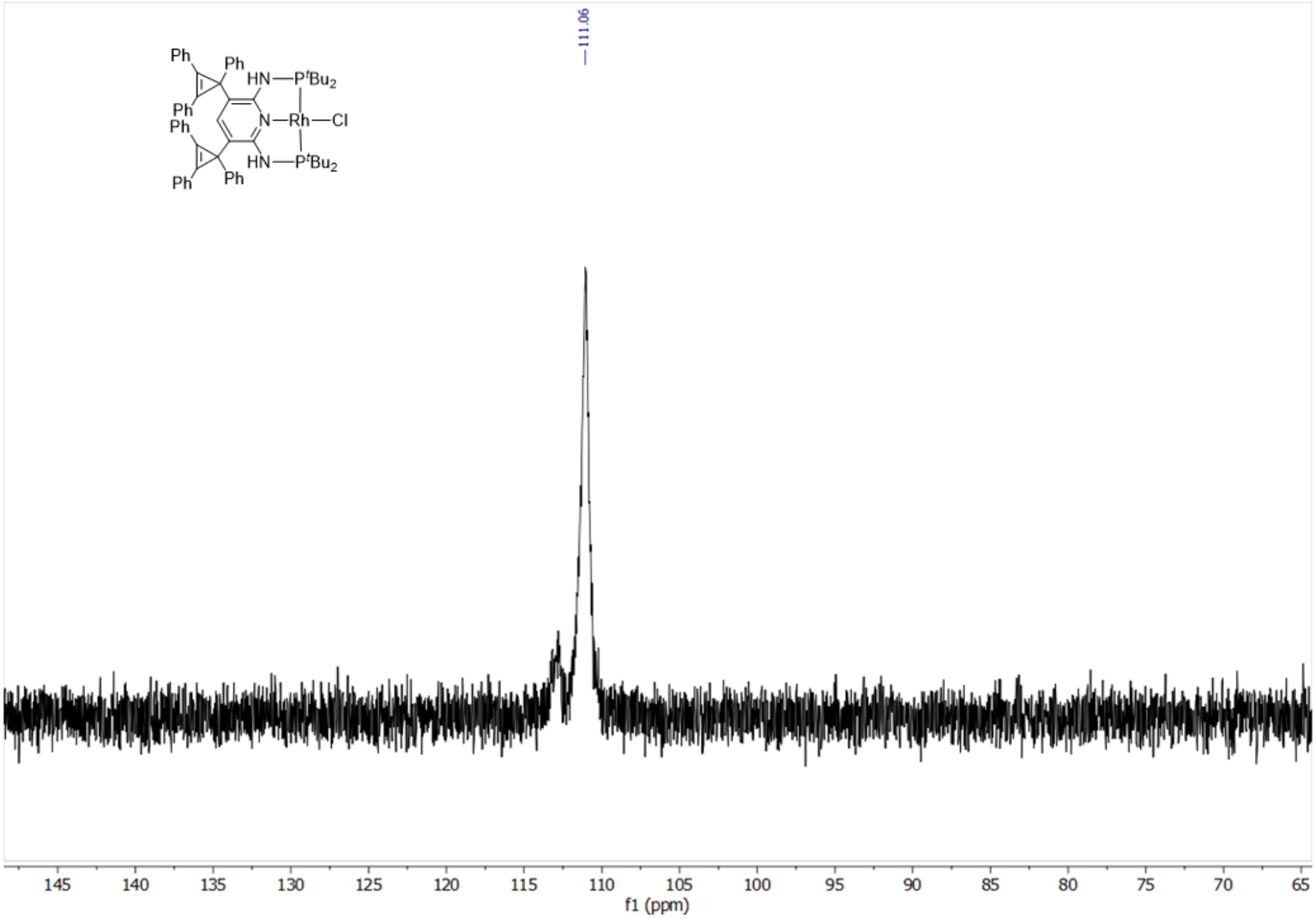

Figure S20. $^{31}P\{^1H\}$ NMR (700 MHz, $CDCl_3$, 298 K) for [RhCl{PNP^{t}Bu.2(C_3Ph_3)}]. (**1**)

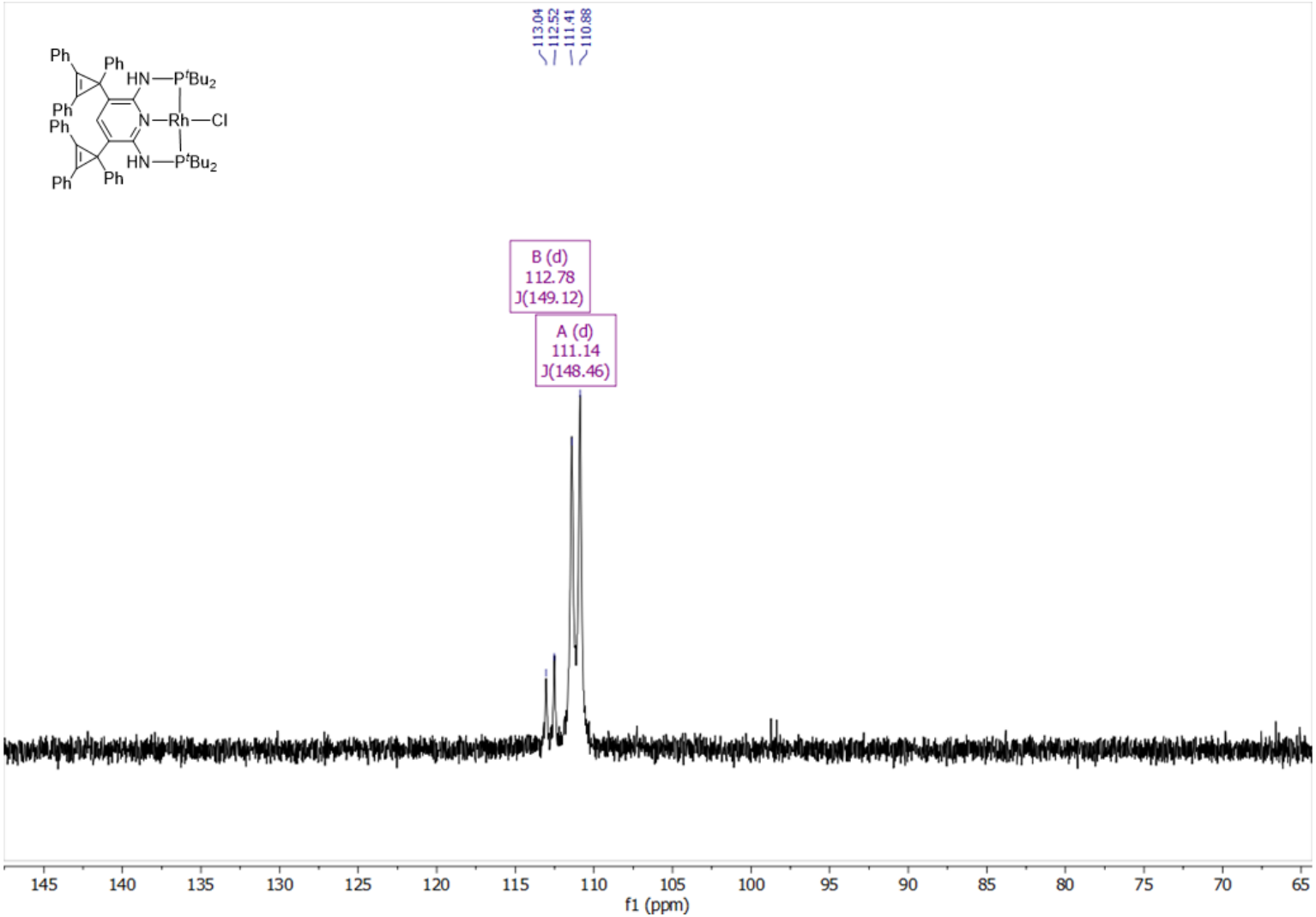

Figure S21. $^{31}P\{^{1}H\}$ NMR (700 MHz, $CDCl_3$, 227 K) for $[RhCl\{PNP^tBu_2(C_3Ph_3)_2\]$ (**1**)

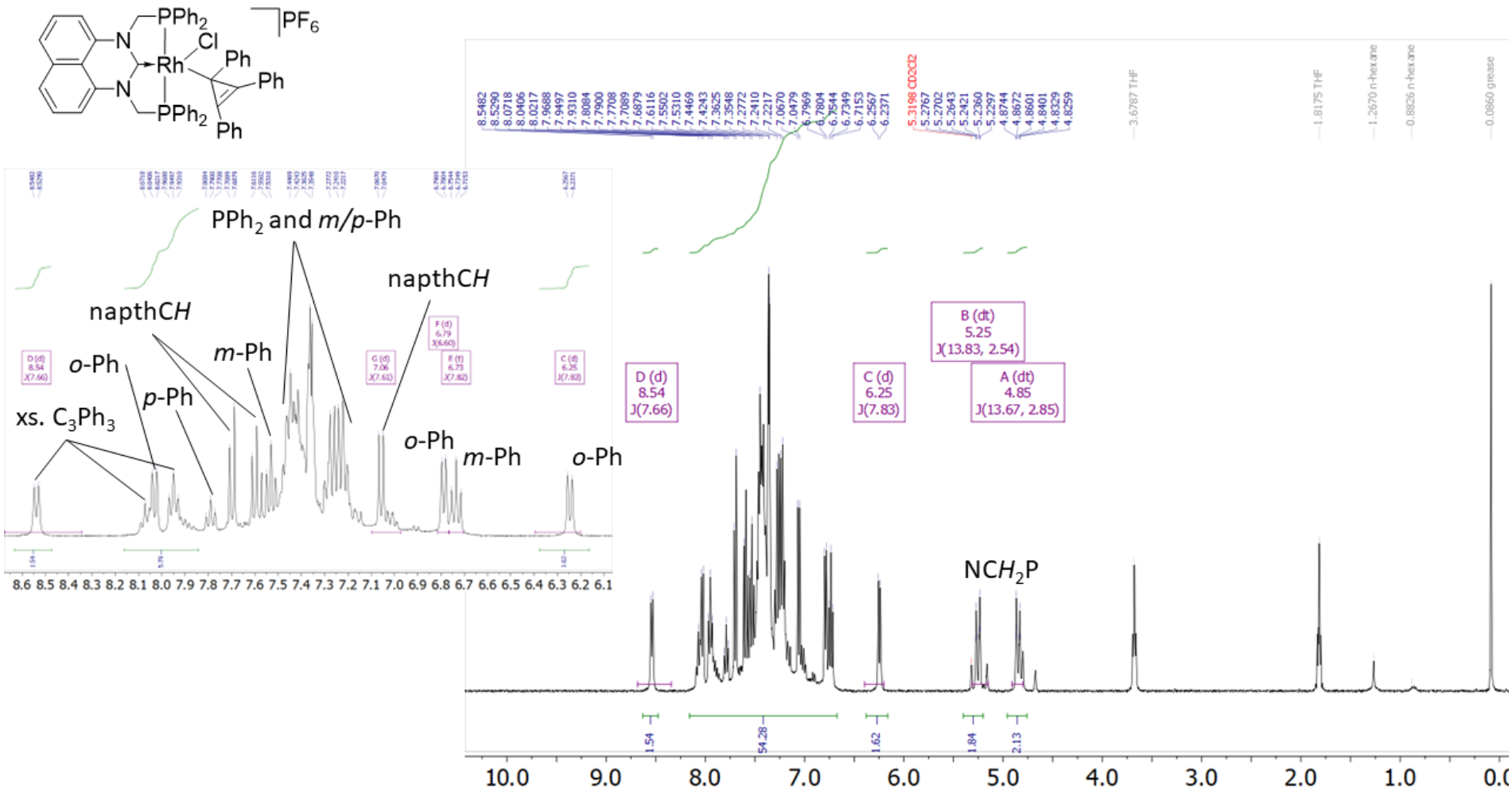

Figure S22. ^{1}H NMR (400 MHz, CD_2Cl_2, 298 K) for [RhCl(κ^2-C_3Ph_3)(PhPm)]PF_6 (**3a**)

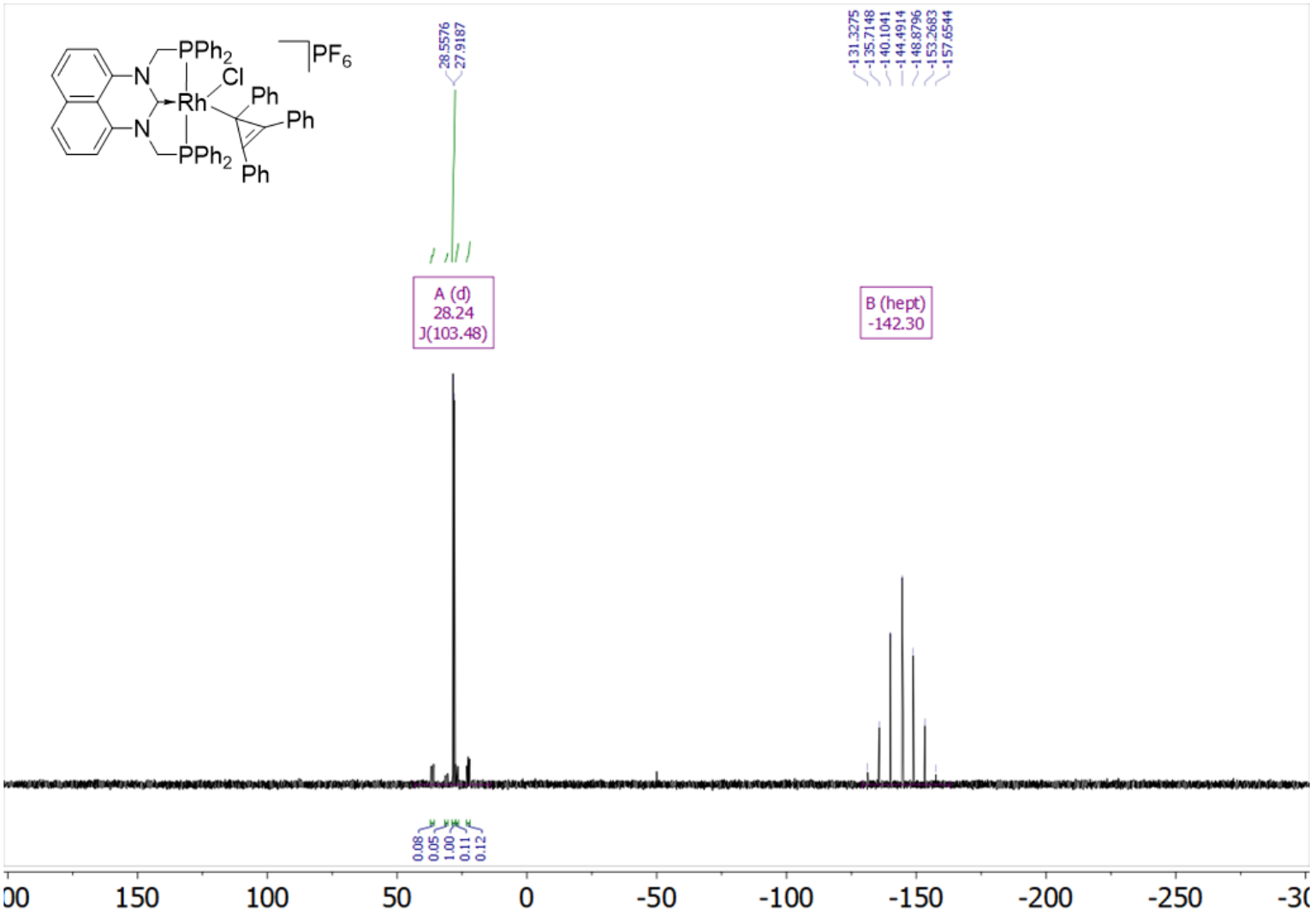

Figure S23. $^{31}P\{^{1}H\}$ NMR (162 MHz, CD_2Cl_2, 298 K) for $[RhCl(\kappa^2\text{-}C_3Ph_3)(PhPm)]PF_6$. (**3a**)

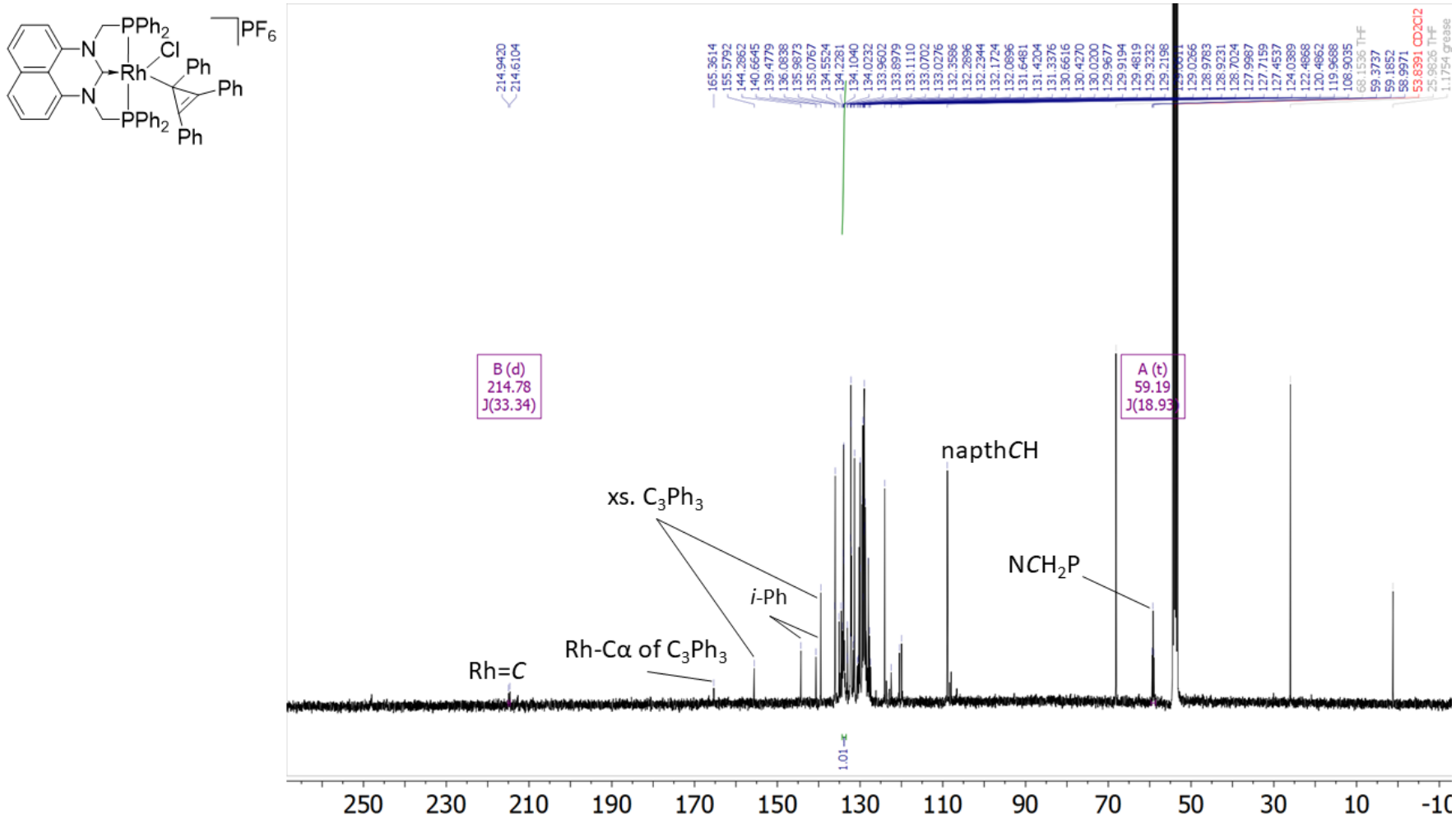

Figure S24. $^{13}C\{^{1}H\}$ NMR (100 MHz, CD_2Cl_2, 298 K) for $[RhCl(\kappa^2\text{-}C_3Ph_3)(PhPm)]PF_6$ (more detail on next page). (**3a**)

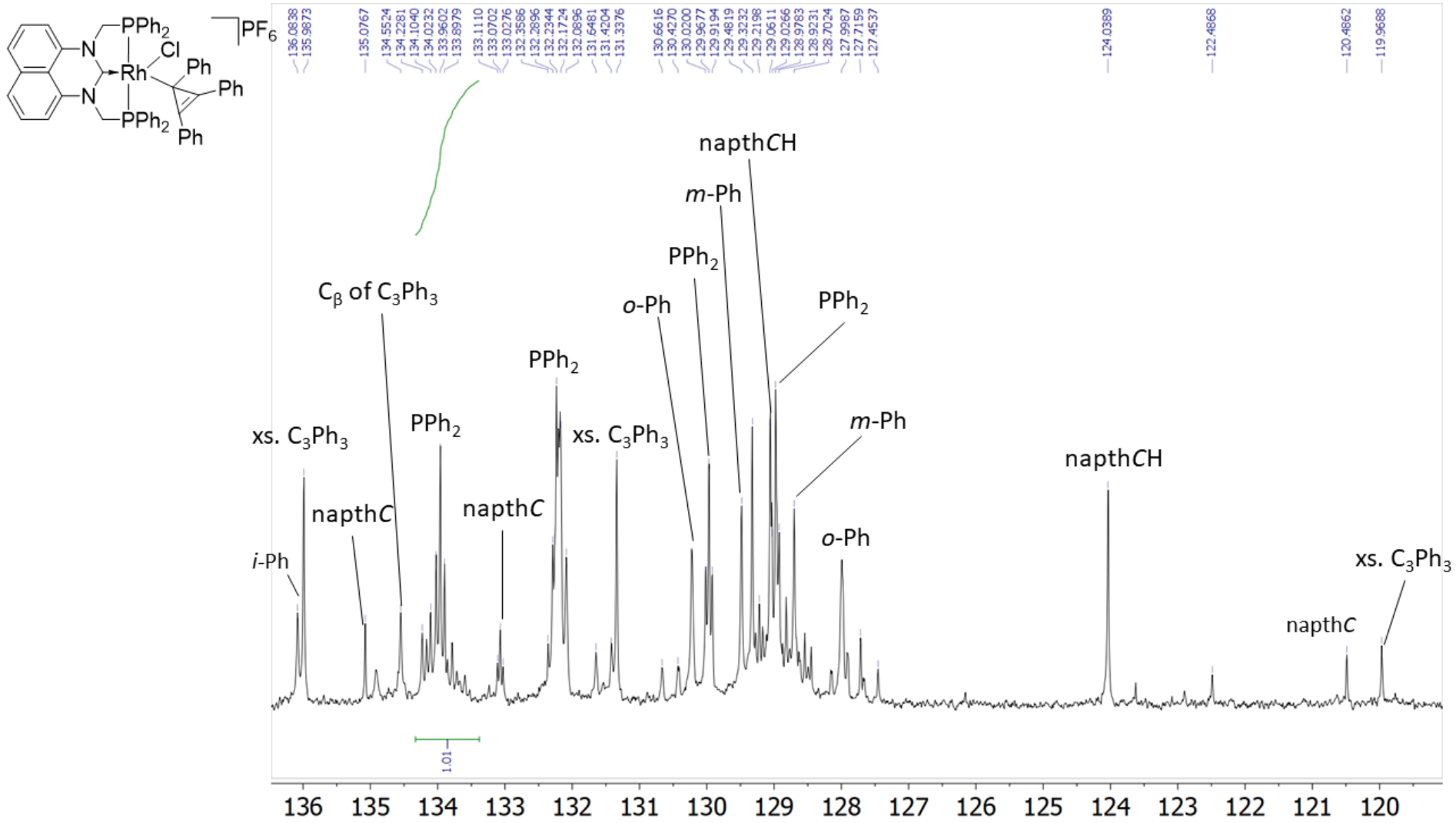

Figure S25 (continued). $^{13}C\{^{1}H\}$ NMR (100 MHz, CD_2Cl_2, 298 K) for $[RhCl(\kappa^2\text{-}C_3Ph_3)(PhPm)]PF_6$ (**3a**)

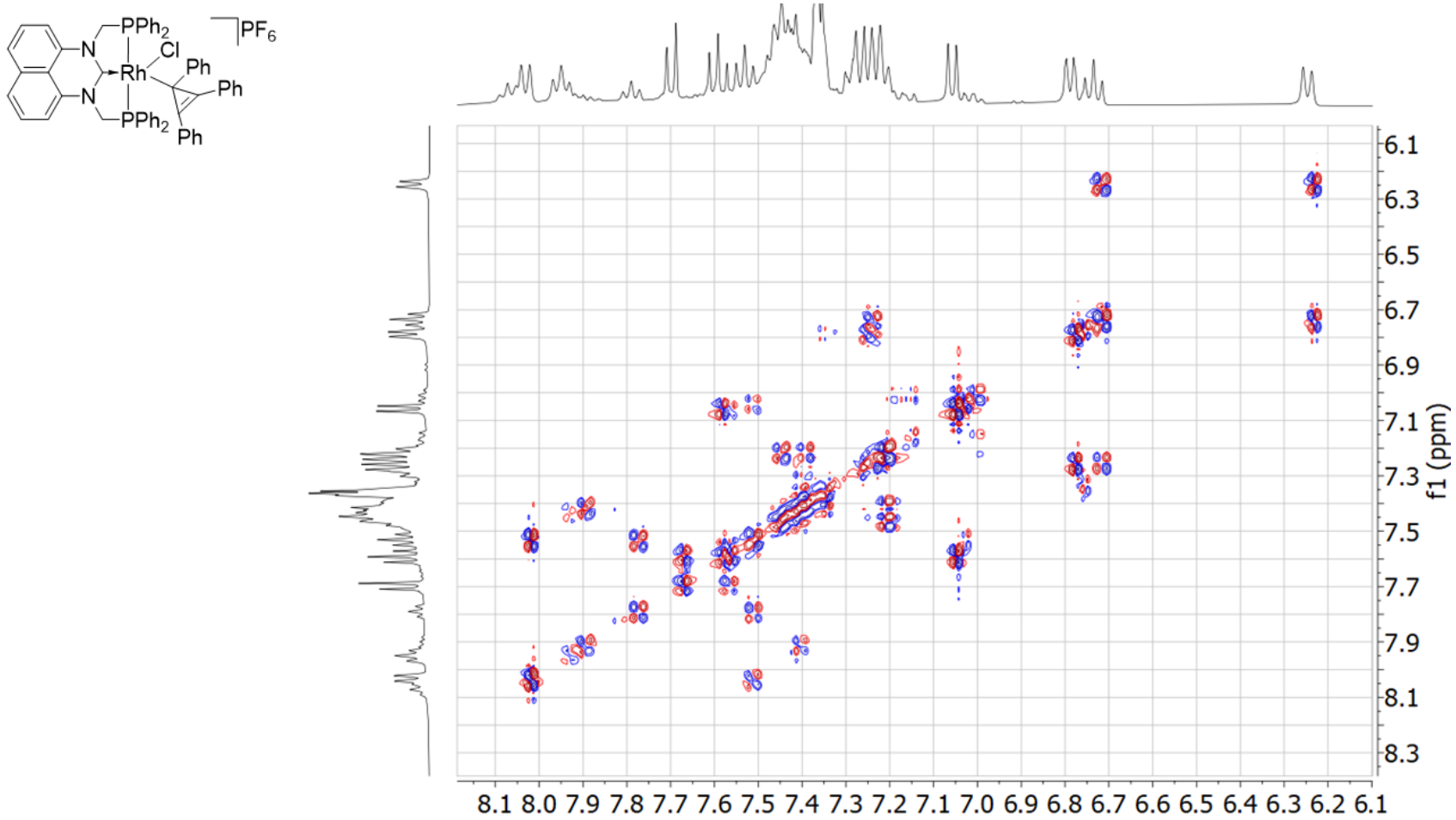

Figure S26. COSY NMR (400 MHz, CD_2Cl_2, 298 K) for $[RhCl(\kappa^2\text{-}C_3Ph_3)(PhPm)]PF_6$ (**3a**)

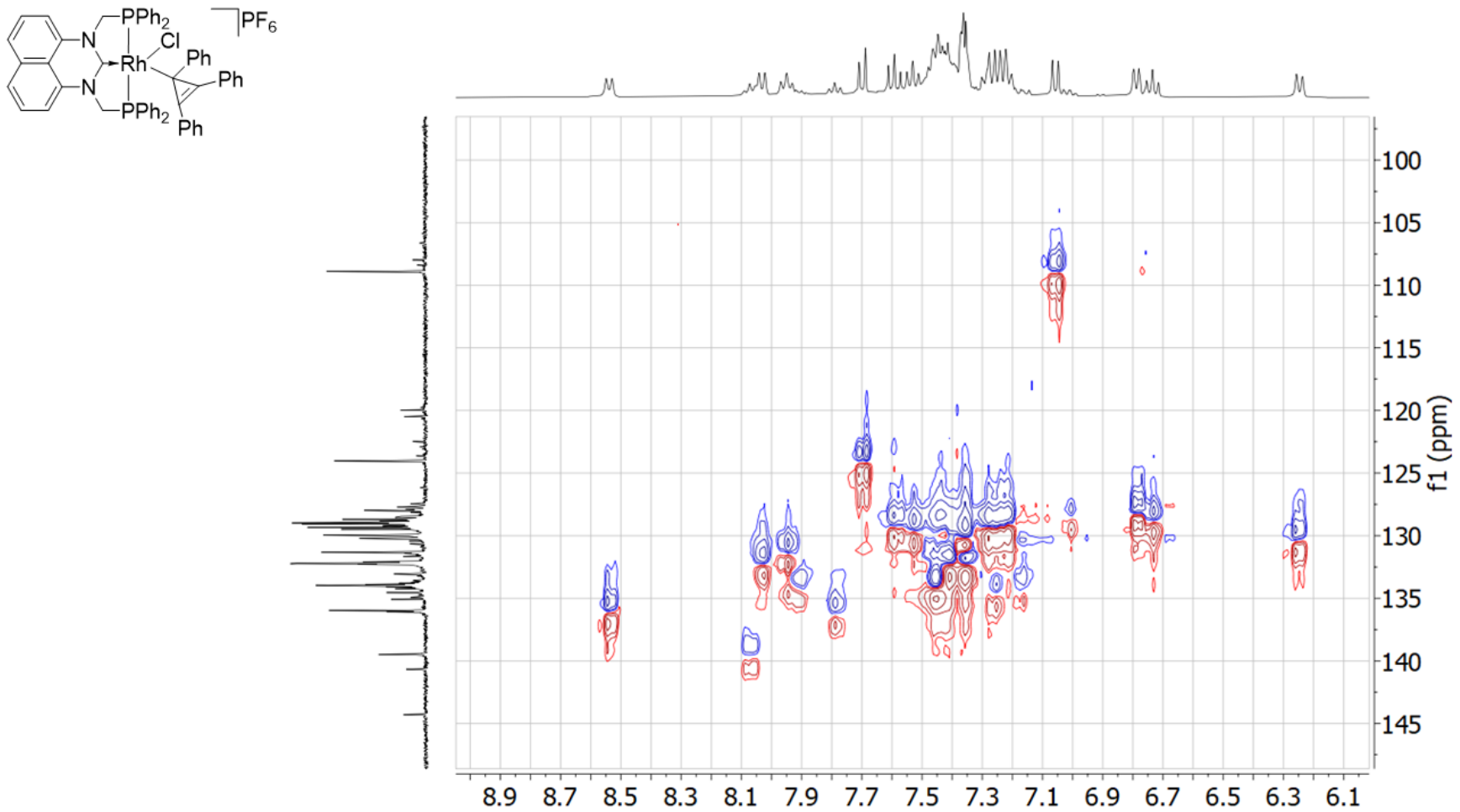

Figure S27. ^{13}C-^{1}H HSQC NMR (100/400 MHz, CD_2Cl_2, 298 K) for $[RhCl(\kappa^2\text{-}C_3Ph_3)(PhPm)]PF_6$ (**3a**)

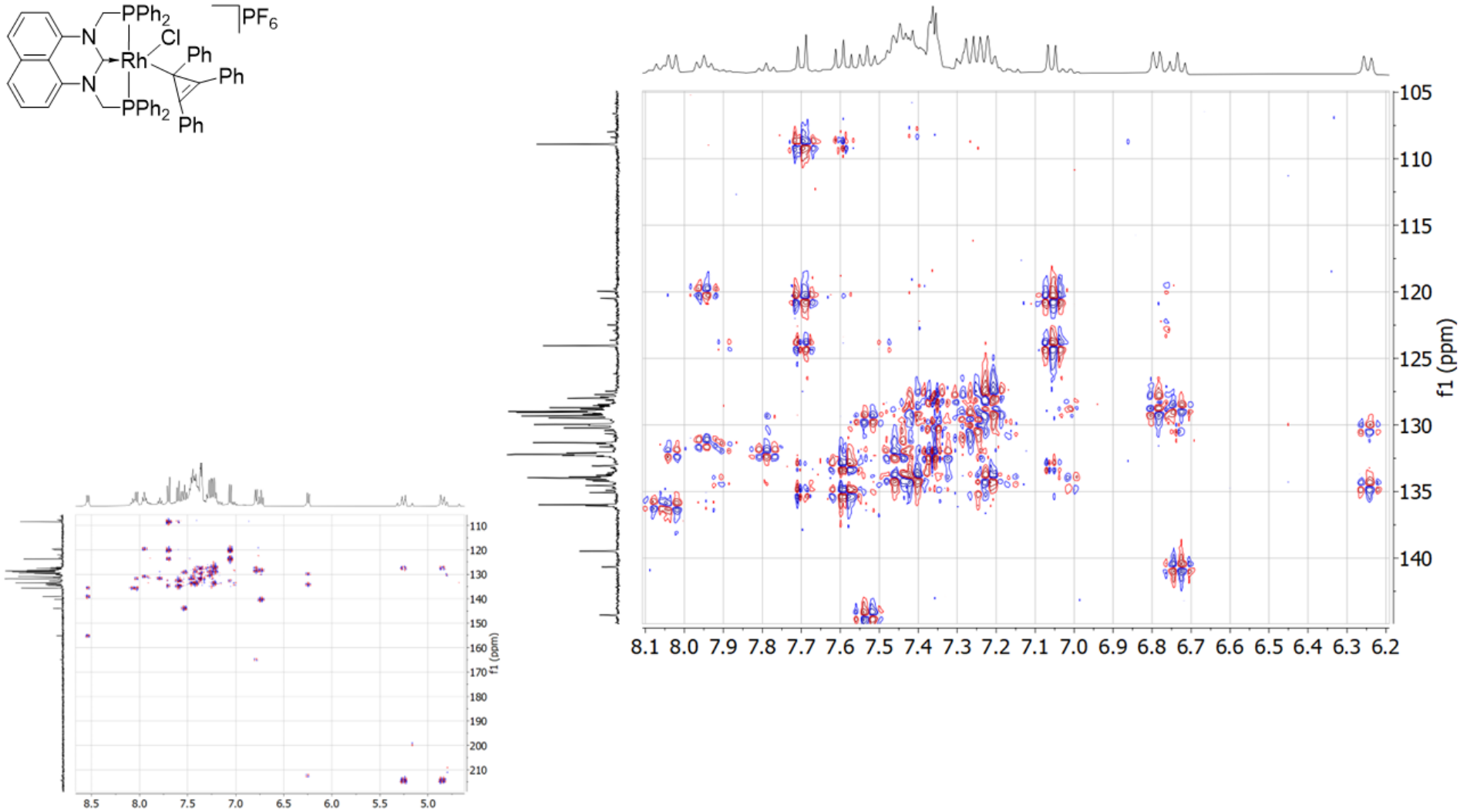

Figure S28. ^{13}C-^{1}H HMBC NMR (100/400 MHz, CD_2Cl_2, 298 K) for [RhCl(κ²-C_3Ph_3)(PhPm)]PF_6 (**3a**)

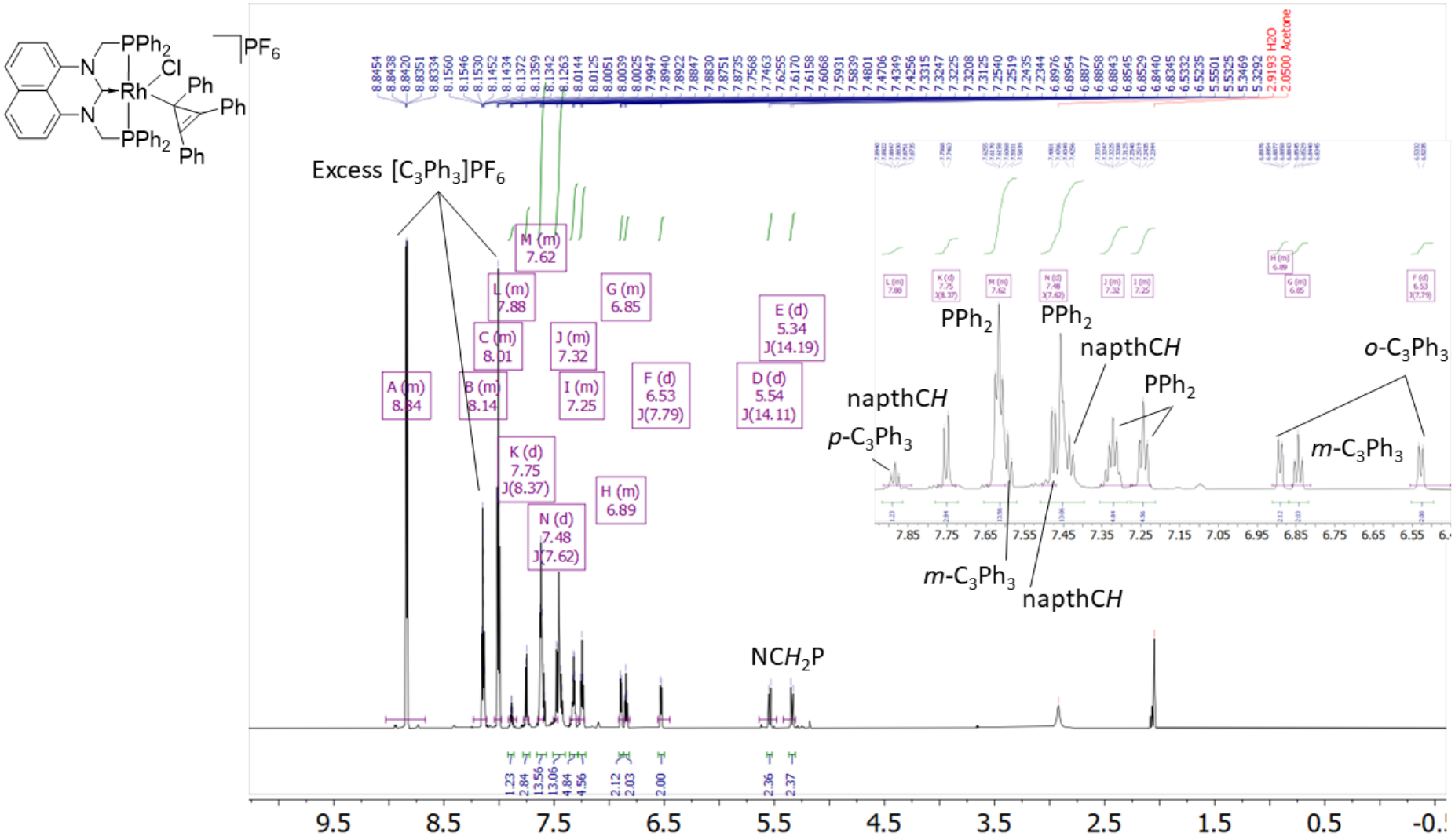

Figure S29. ^{1}H NMR (400 MHz, $(CD_3)_2CO$, 298 K) for $[RhCl(\kappa^2\text{-}C_3Ph_3)(PhPm)]PF_6$ (**3a**)

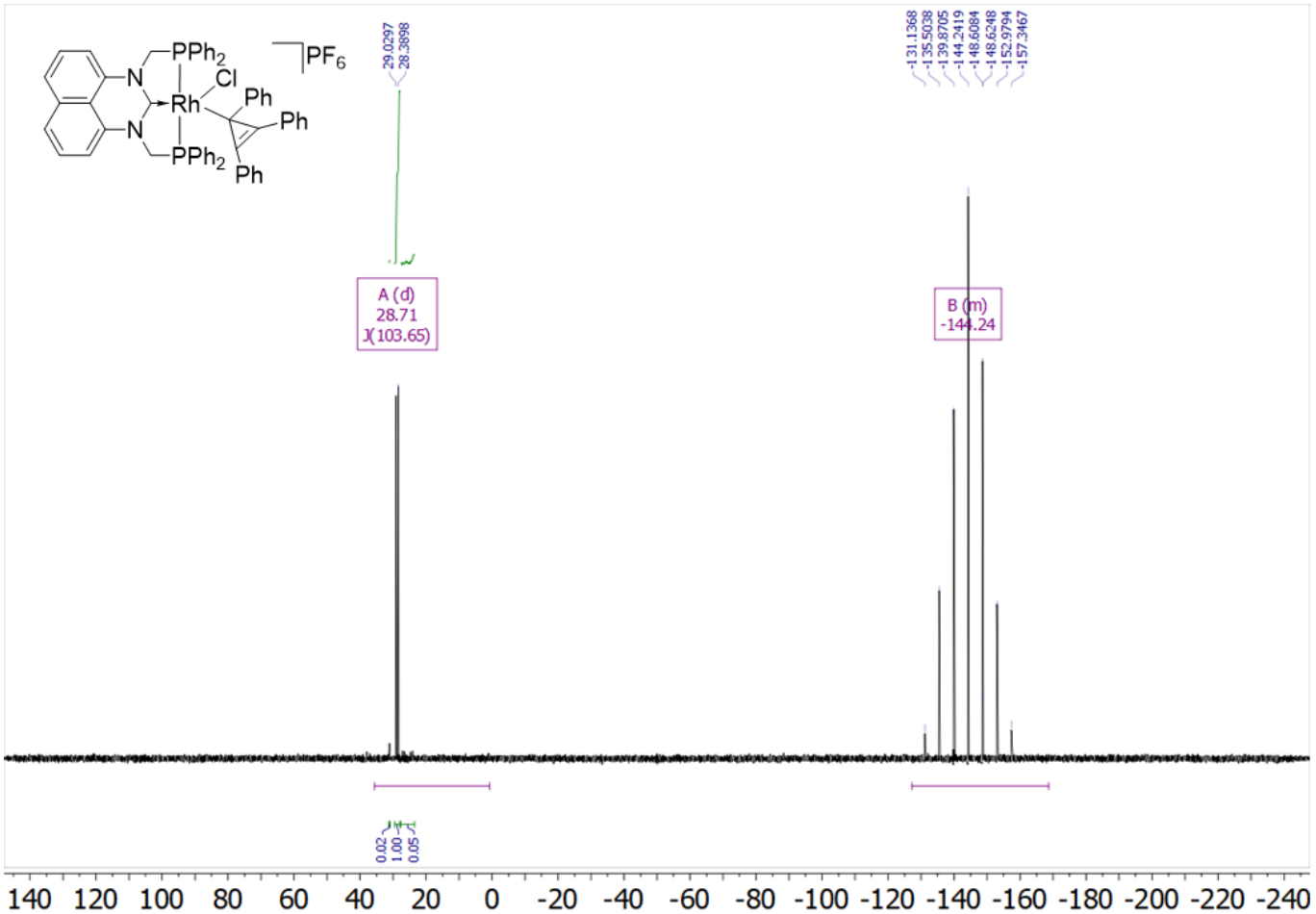

Figure S30. $^{31}P\{^{1}H\}$ NMR (162 MHz, $(CD_3)_2CO$, 298 K) for $[RhCl(\kappa^2\text{-}C_3Ph_3)(PhPm)]PF_6$ (**3a**)

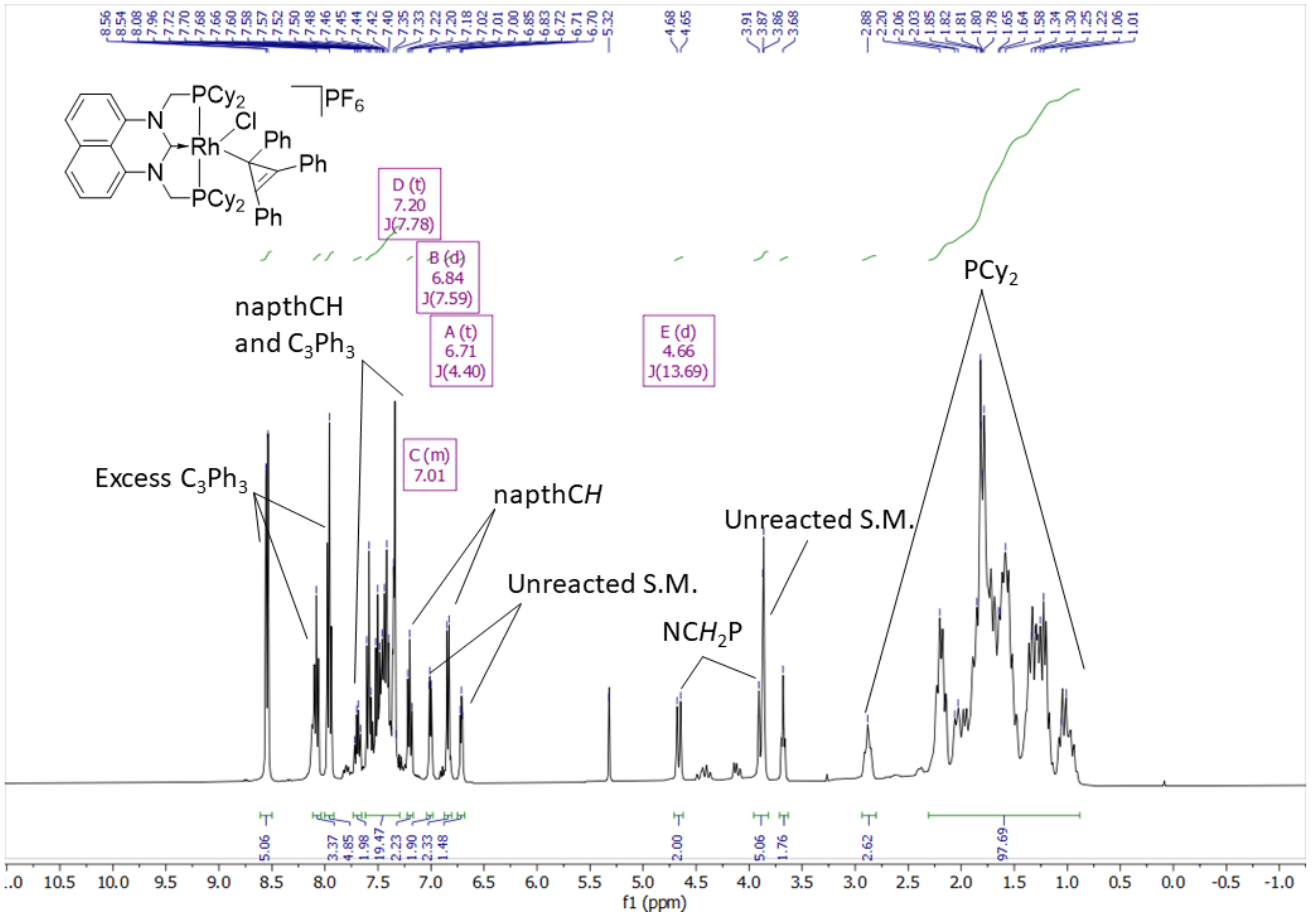

Figure S31. ^{1}H NMR (400 MHz, CD_2Cl_2, 298 K) for $[RhCl(\kappa^2\text{-}C_3Ph_3)(CyPm)]PF_6$ (**3b**)

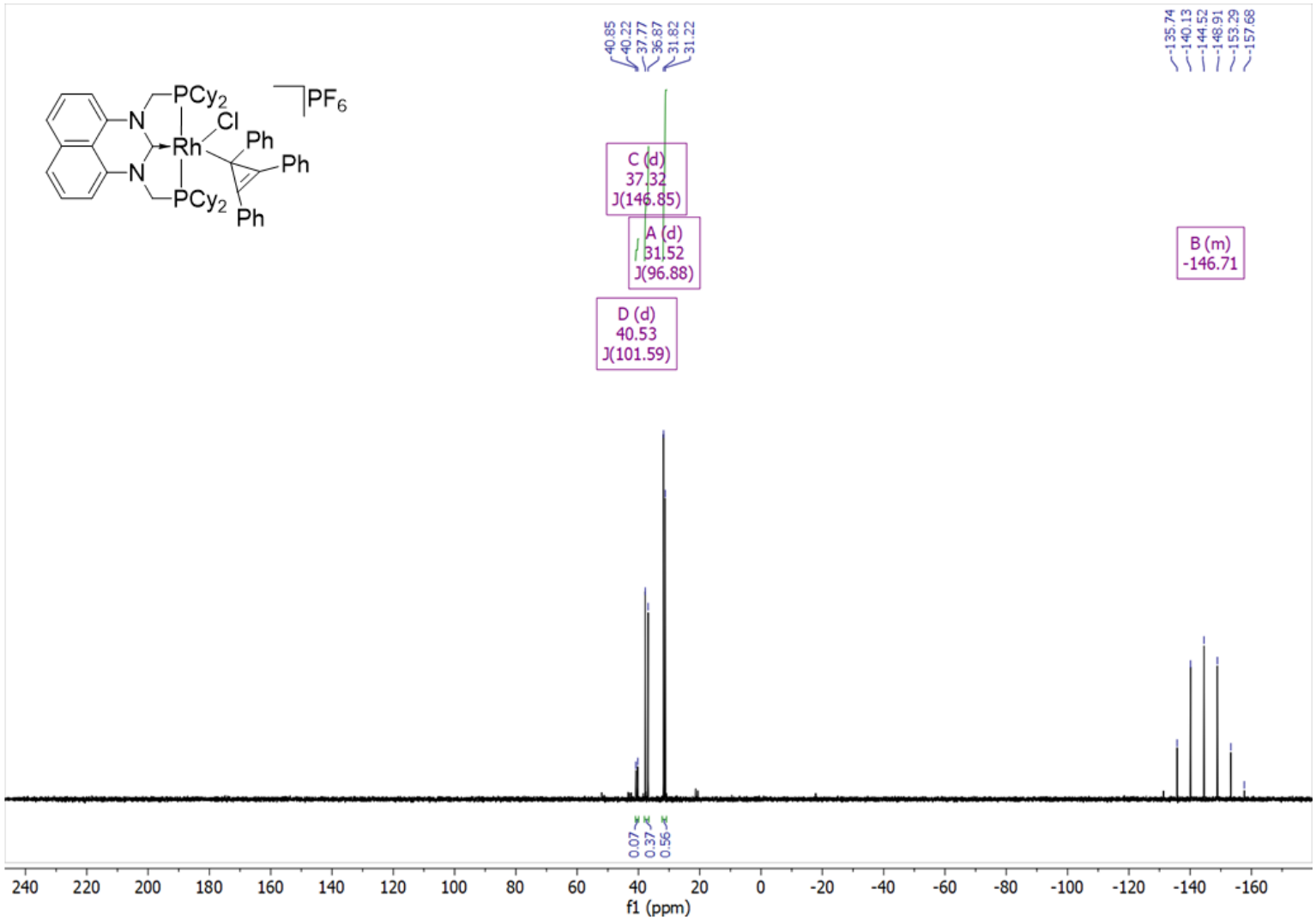

Figure S32. $^{31}P\{^{1}H\}$ NMR (400 MHz, CD_2Cl_2, 298 K) for $[RhCl(\kappa^2\text{-}C_3Ph_3)(PhPm)]PF_6$ (**3b**)

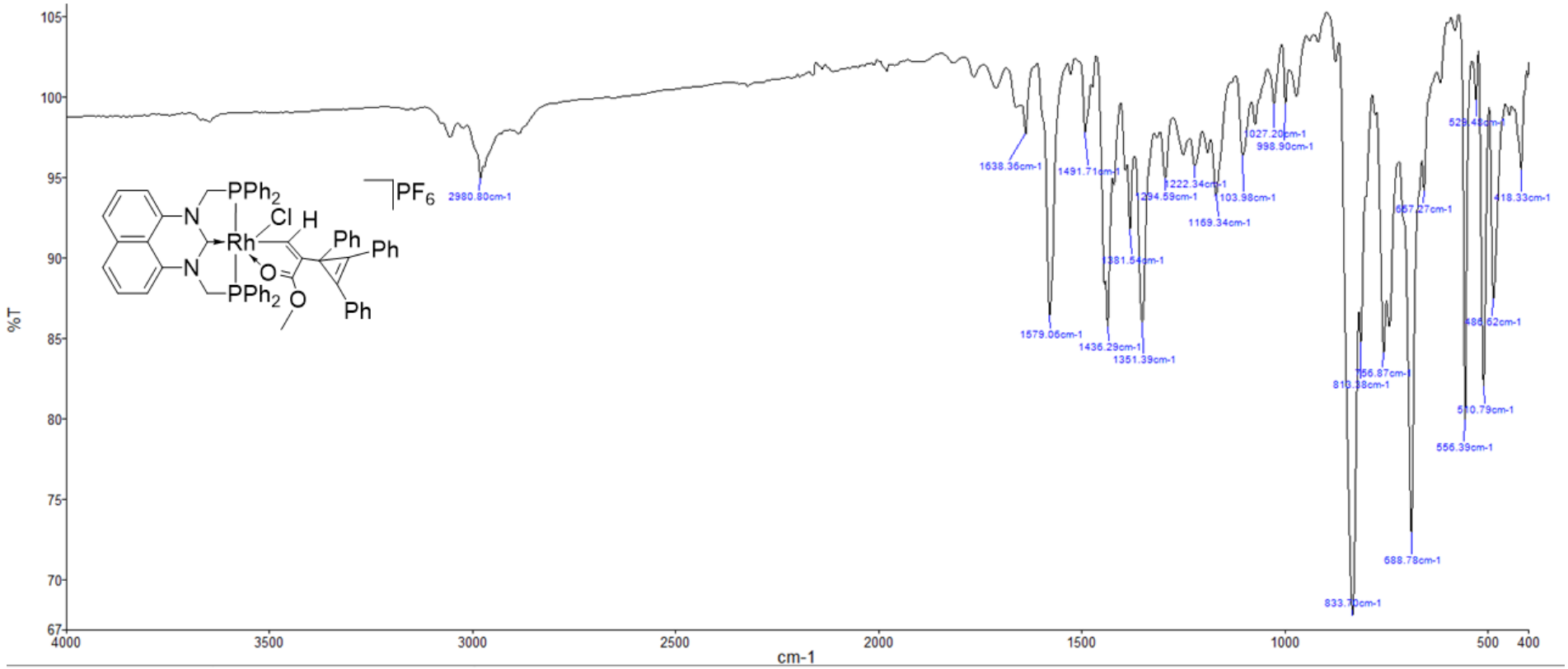

Figure S33. IR Spectrum (ATR, cm^{-1}) for $[RhCl\{\kappa^2\text{-}CHC(CO_2Me)(C_3Ph_3)\}(PhPm)]PF_6$ (**4a**)

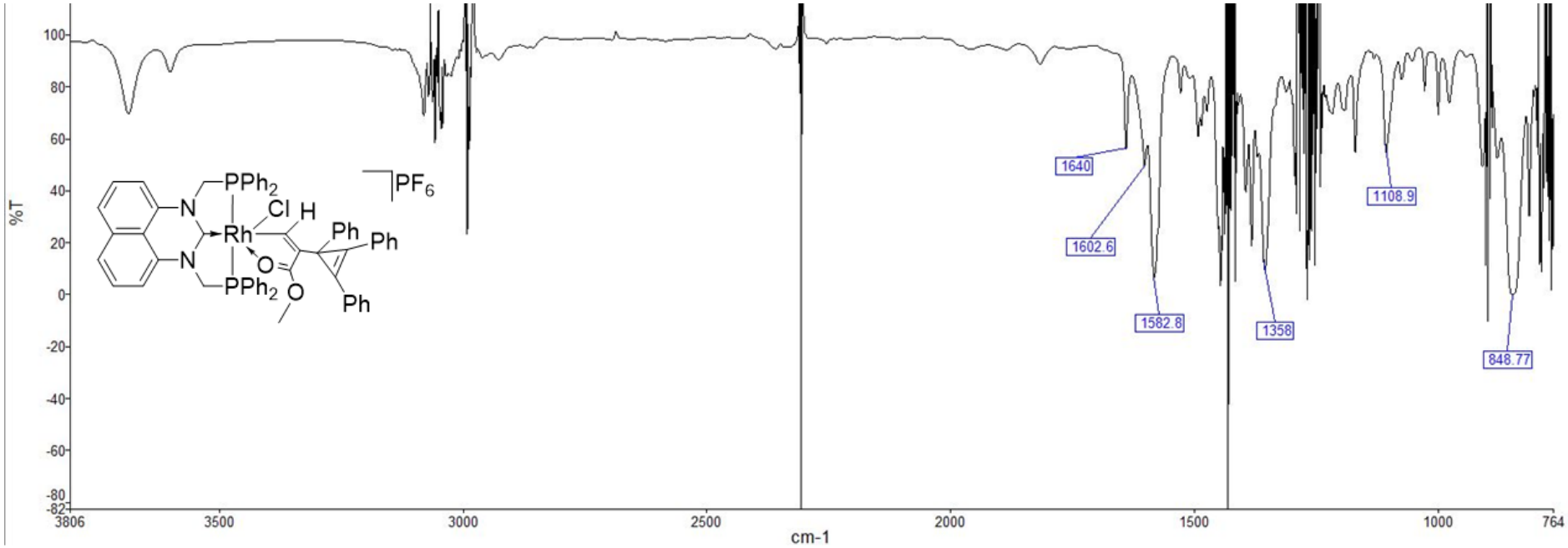

Figure S34. IR Spectrum (CH_2Cl_2, cm^{-1}) for [RhCl{κ²-CHC(CO_2Me)(C_3Ph_3)}(PhPm)]PF_6 (**4a**)

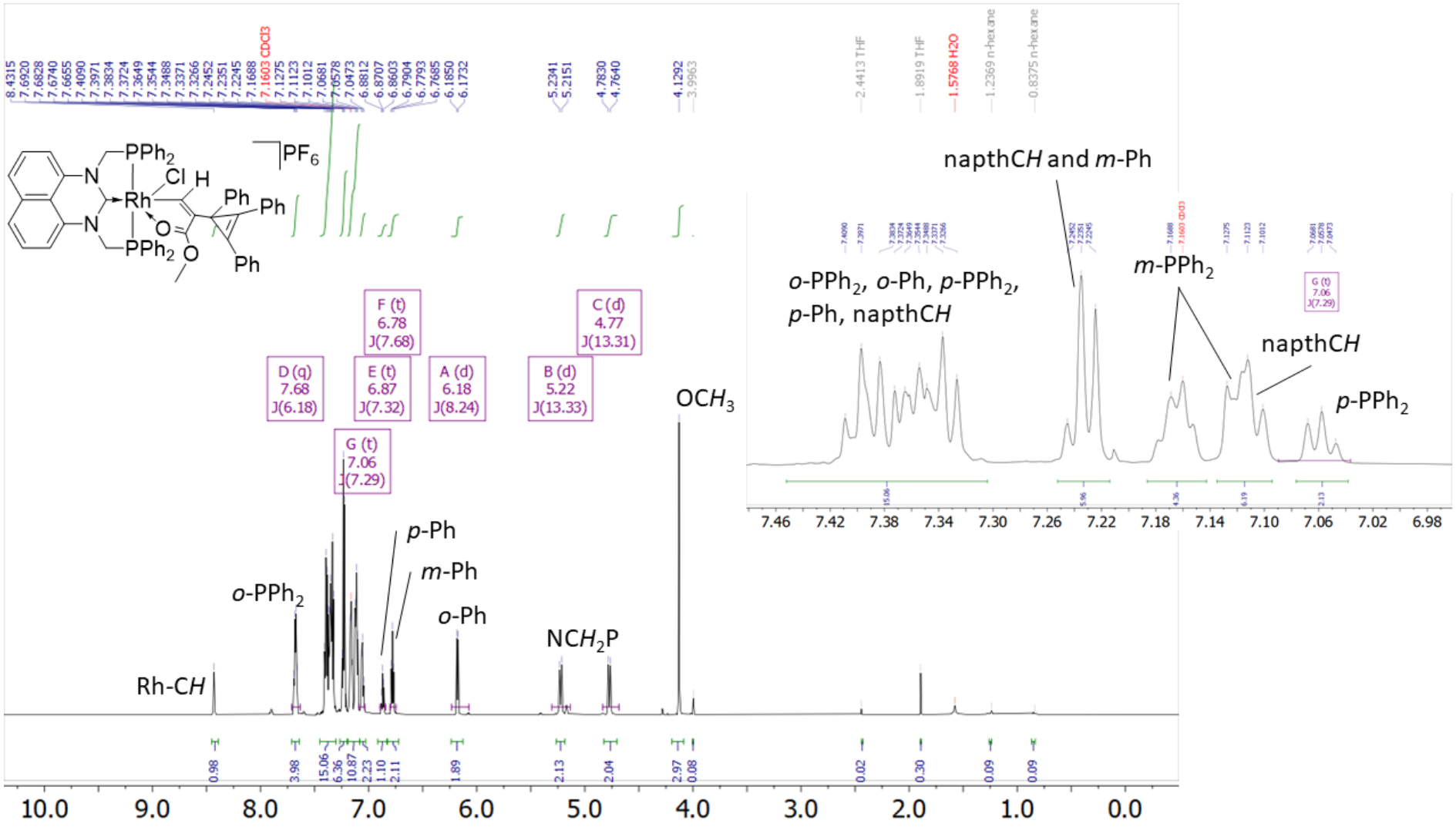

Figure S35. ^{1}H NMR Spectrum (700 MHz, $CDCl_3$, 298 K) for $[RhCl\{\kappa^2\text{-}CHC(CO_2Me)(C_3Ph_3)\}(PhPm)]PF_6$ (**4a**)

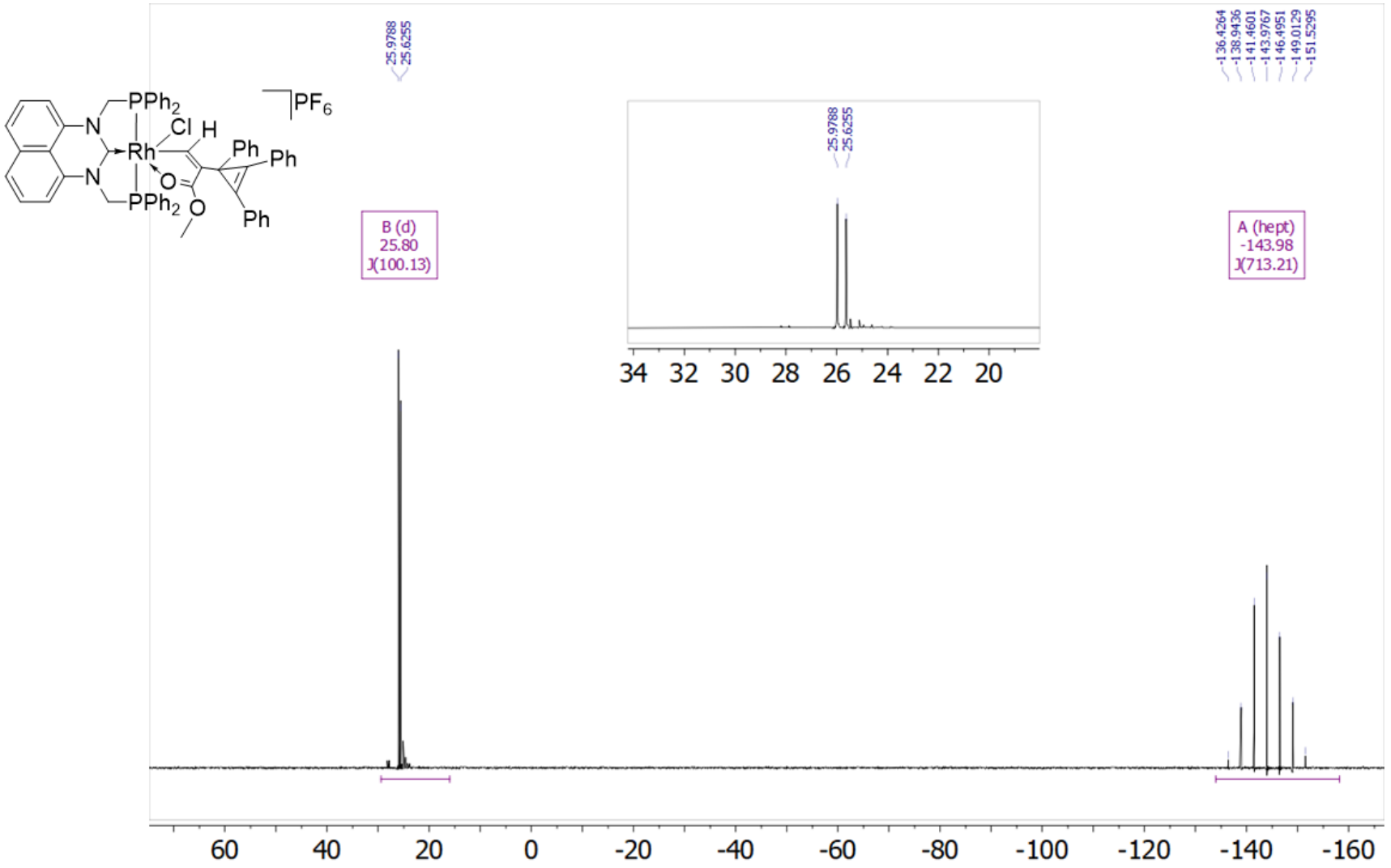

Figure S36. $^{31}P\{^{1}H\}$ NMR Spectrum (283 MHz, $CDCl_3$, 298 K) for $[RhCl\{\kappa^2\text{-}CHC(CO_2Me)(C_3Ph_3)\}(PhPm)]PF_6$ (**4a**)

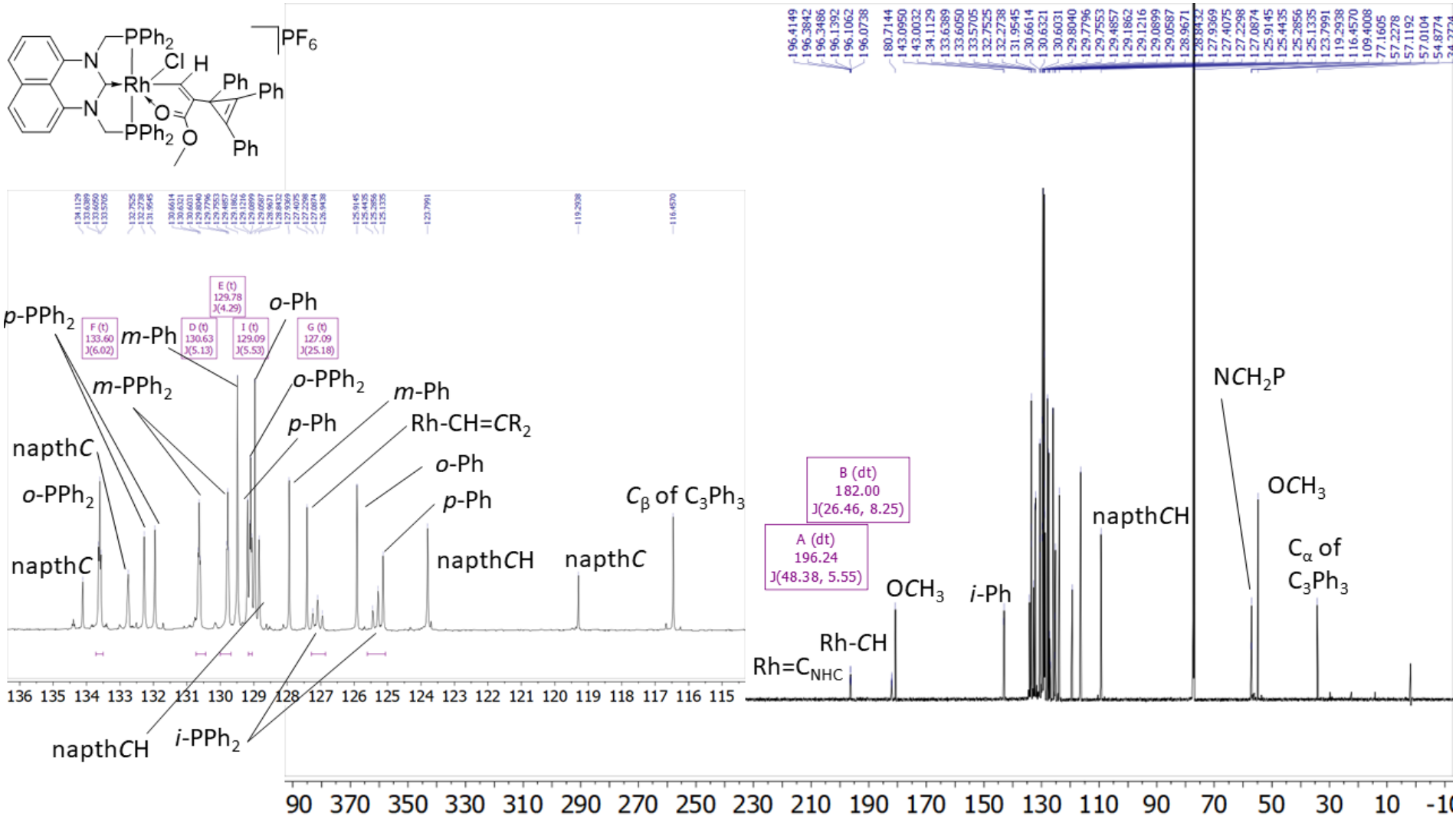

Figure S37. $^{13}C\{^{1}H\}$ NMR Spectrum (176 MHz, $CDCl_3$, 298 K) for $[RhCl\{\kappa^2\text{-}CHC(CO_2Me)(C_3Ph_3)\}(PhPm)]PF_6$ (**4a**)

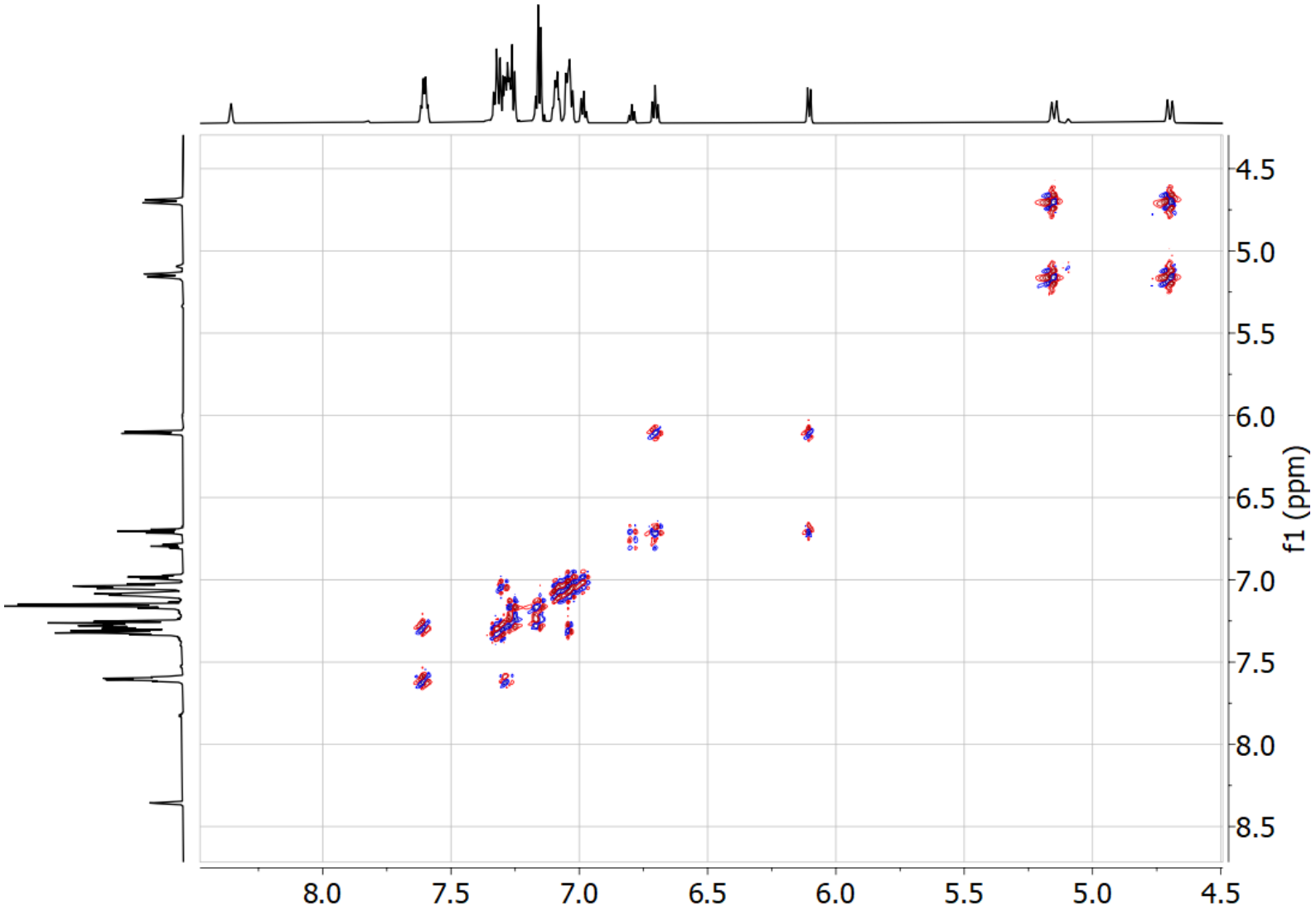

Figure S38. COSY NMR Spectrum (700 MHz, $CDCl_3$, 298 K) for [RhCl{κ²-CHC(CO_2Me)(C_3Ph_3)}(PhPm)]PF_6 (**4a**)

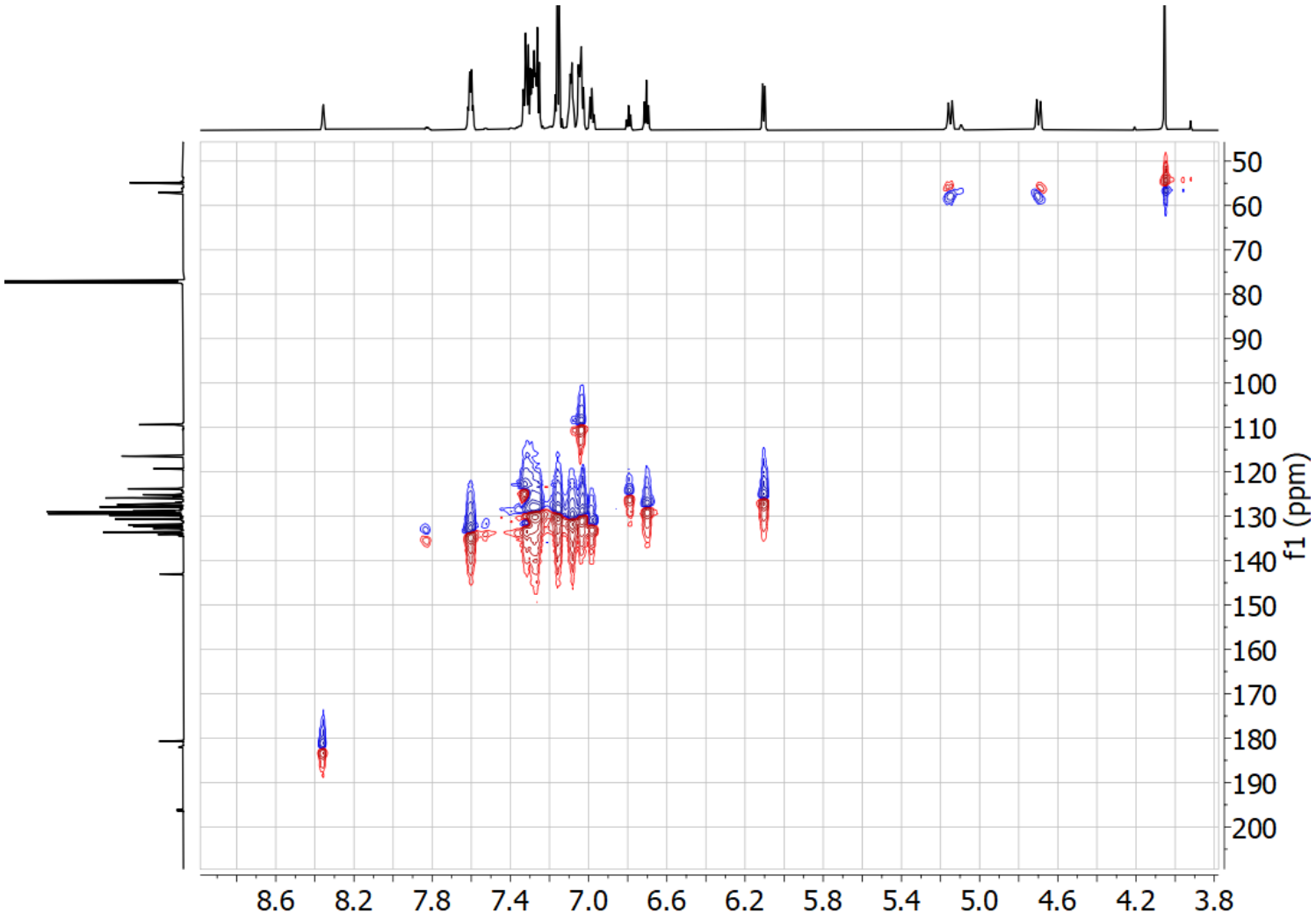

Figure S39. ^{13}C-^{1}H HSQC NMR Spectrum ($CDCl_3$, 298 K) for [RhCl{κ²-CHC(CO_2Me)(C_3Ph_3)}(PhPm)]PF_6 (**4a**)

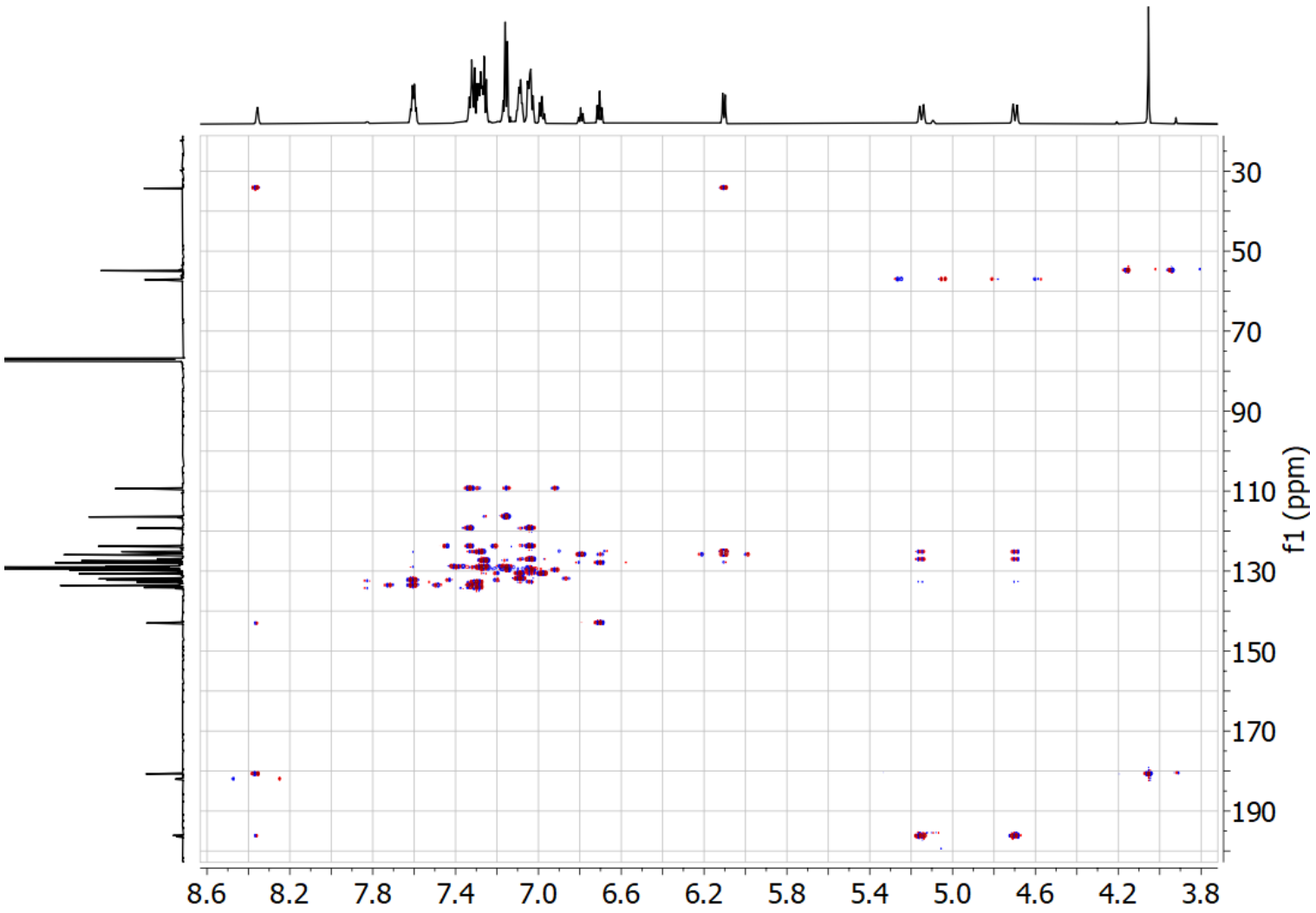

Figure S40. ^{13}C-^{1}H HMBC NMR Spectrum ($CDCl_3$, 298 K) for $[RhCl\{\kappa^2\text{-}CHC(CO_2Me)(C_3Ph_3)\}(PhPm)]PF_6$ (**4a**)

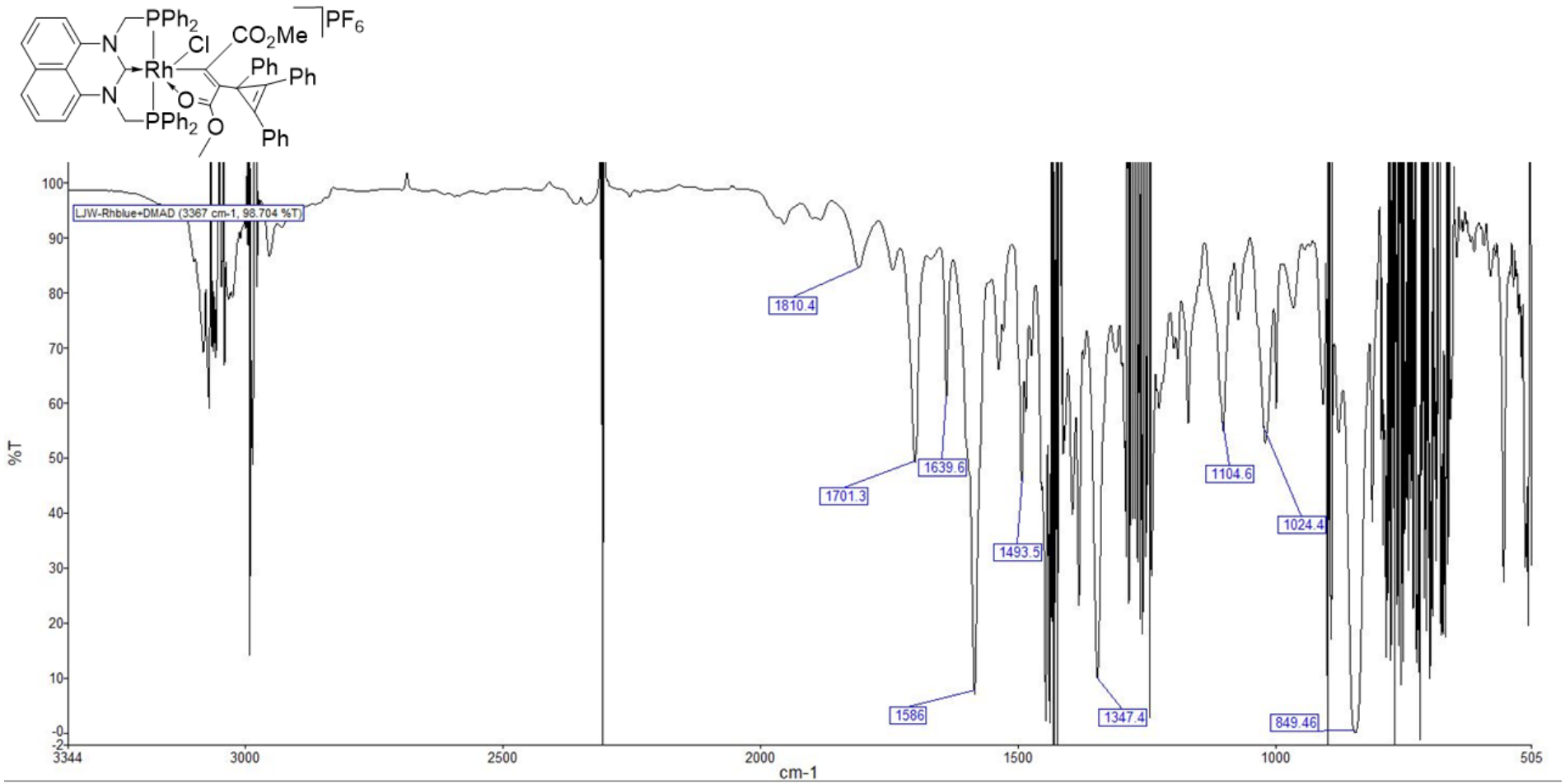

Figure S41. IR NMR Spectrum (CH_2Cl_2, cm^{-1}) for [RhCl{κ²-C(CO_2Me)C(CO_2Me)(C_3Ph_3)}(PhPm)]PF_6 (**5a**)

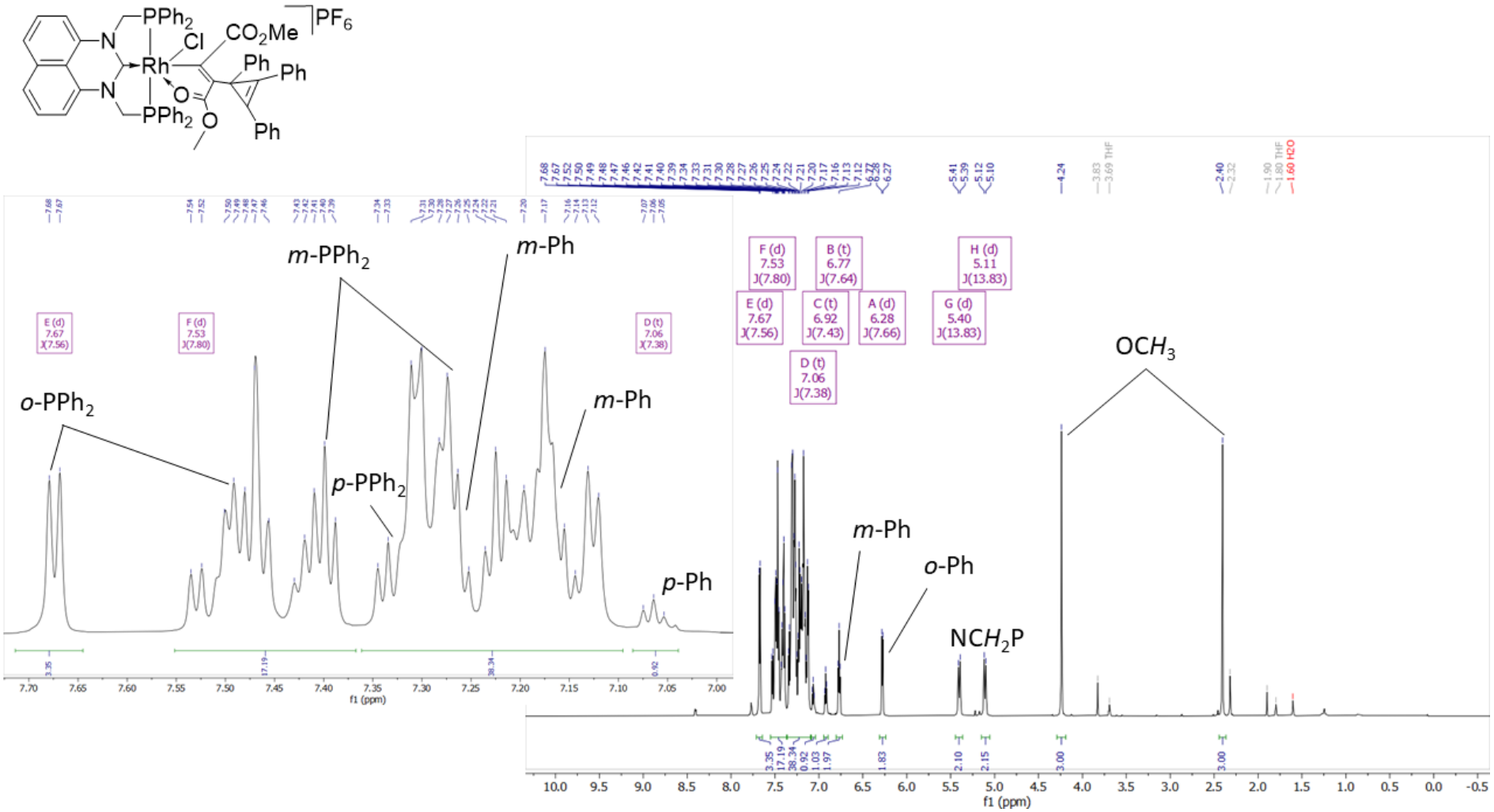

Figure S42. ^{1}H NMR Spectrum (400 MHz, $CDCl_3$, 298 K) for $[RhCl\{\kappa^2\text{-}C(CO_2Me)C(CO_2Me)(C_3Ph_3)\}(PhPm)]PF_6$ (**5a**)

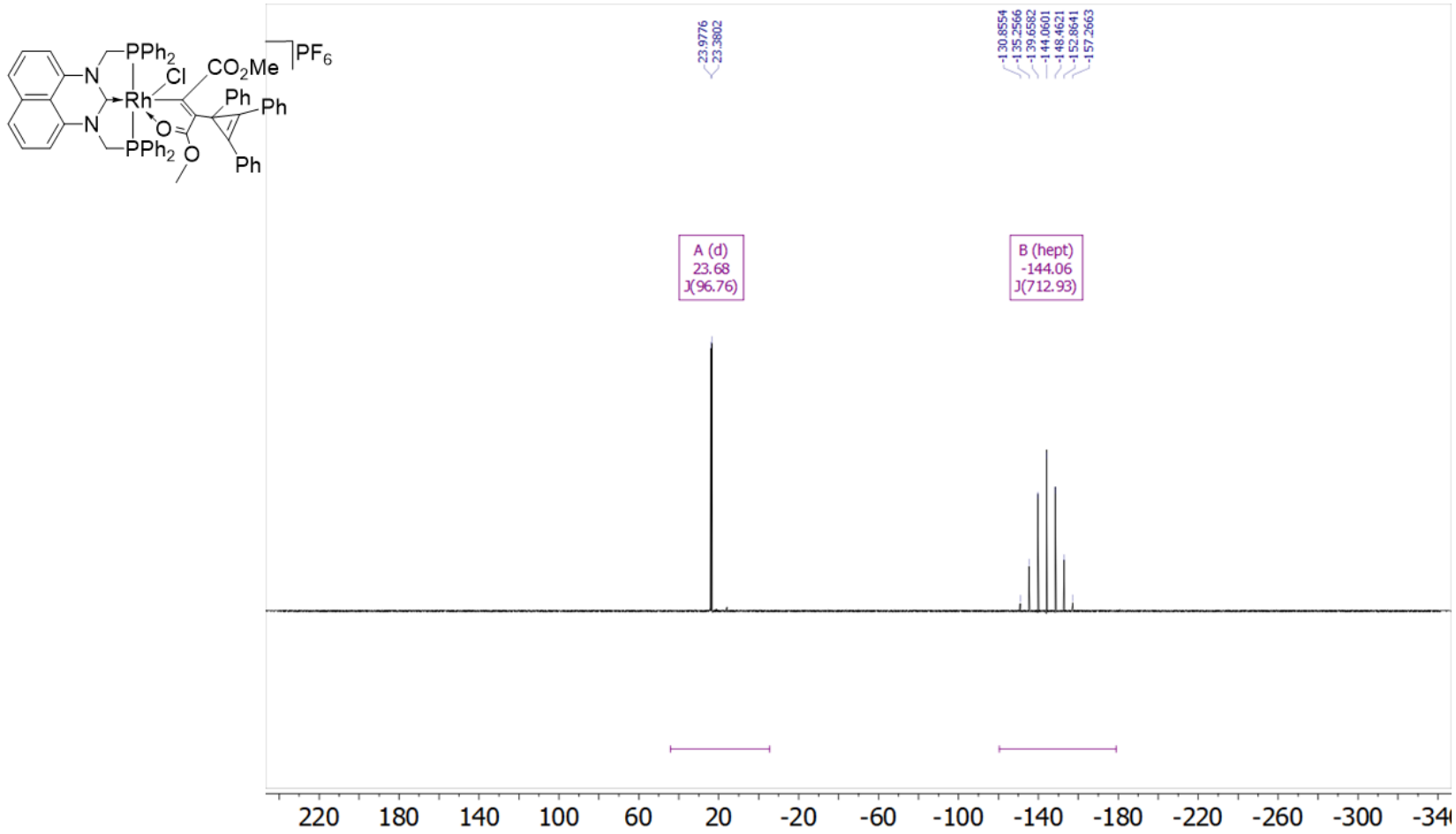

Figure S43. $^{31}P\{^{1}H\}$ NMR Spectrum (283 MHz, $CDCl_3$, 298 K) for $[RhCl\{\kappa^2\text{-}C(CO_2Me)C(CO_2Me)(C_3Ph_3)\}(PhPm)]PF_6$ (**5a**)

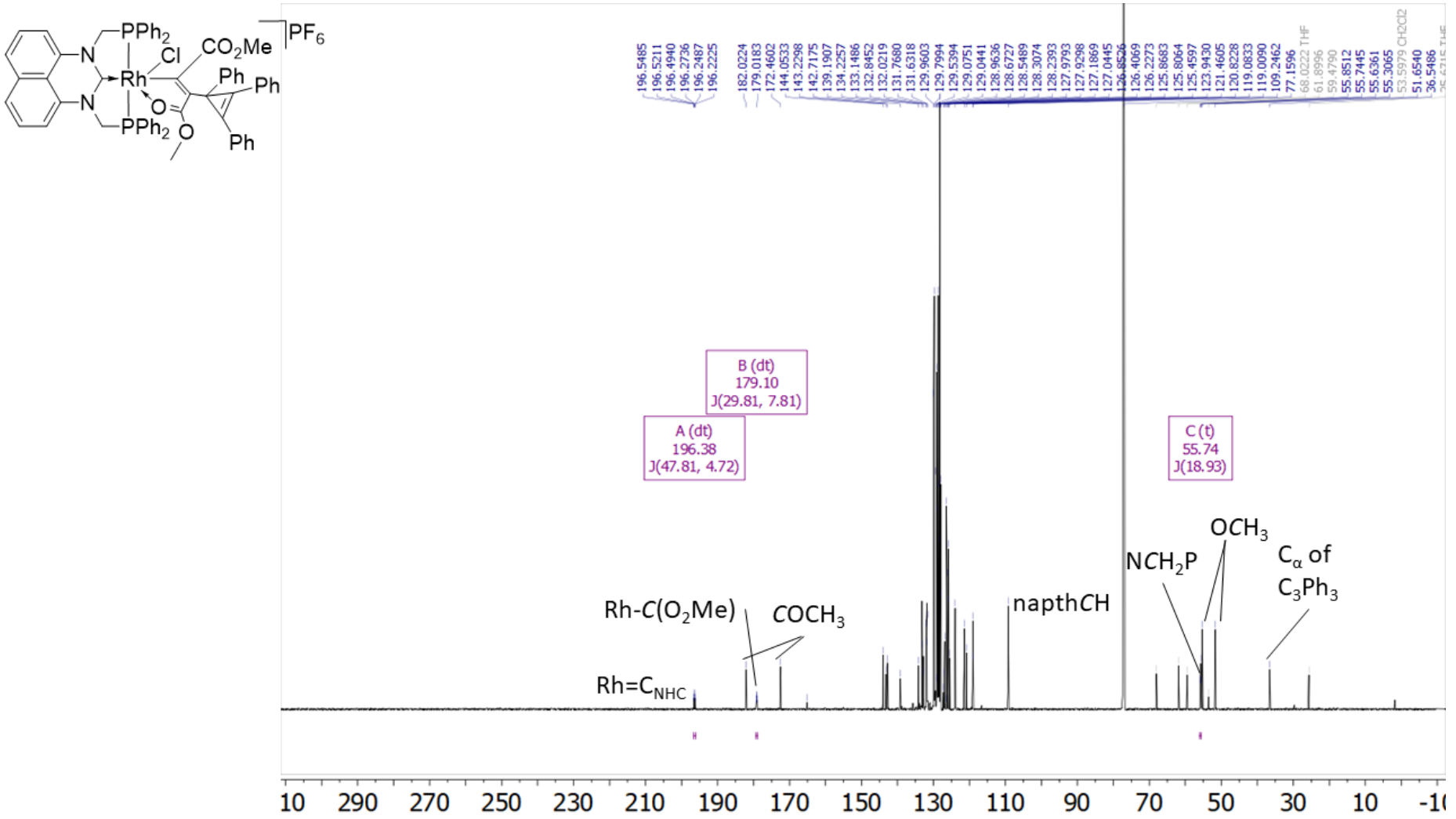

Figure S44. $^{13}C\{^{1}H\}$ NMR Spectrum (176 MHz, $CDCl_3$, 298 K) for $[RhCl\{\kappa^2\text{-}C(CO_2Me)C(CO_2Me)(C_3Ph_3)\}(PhPm)]PF_6$ (**5a**)

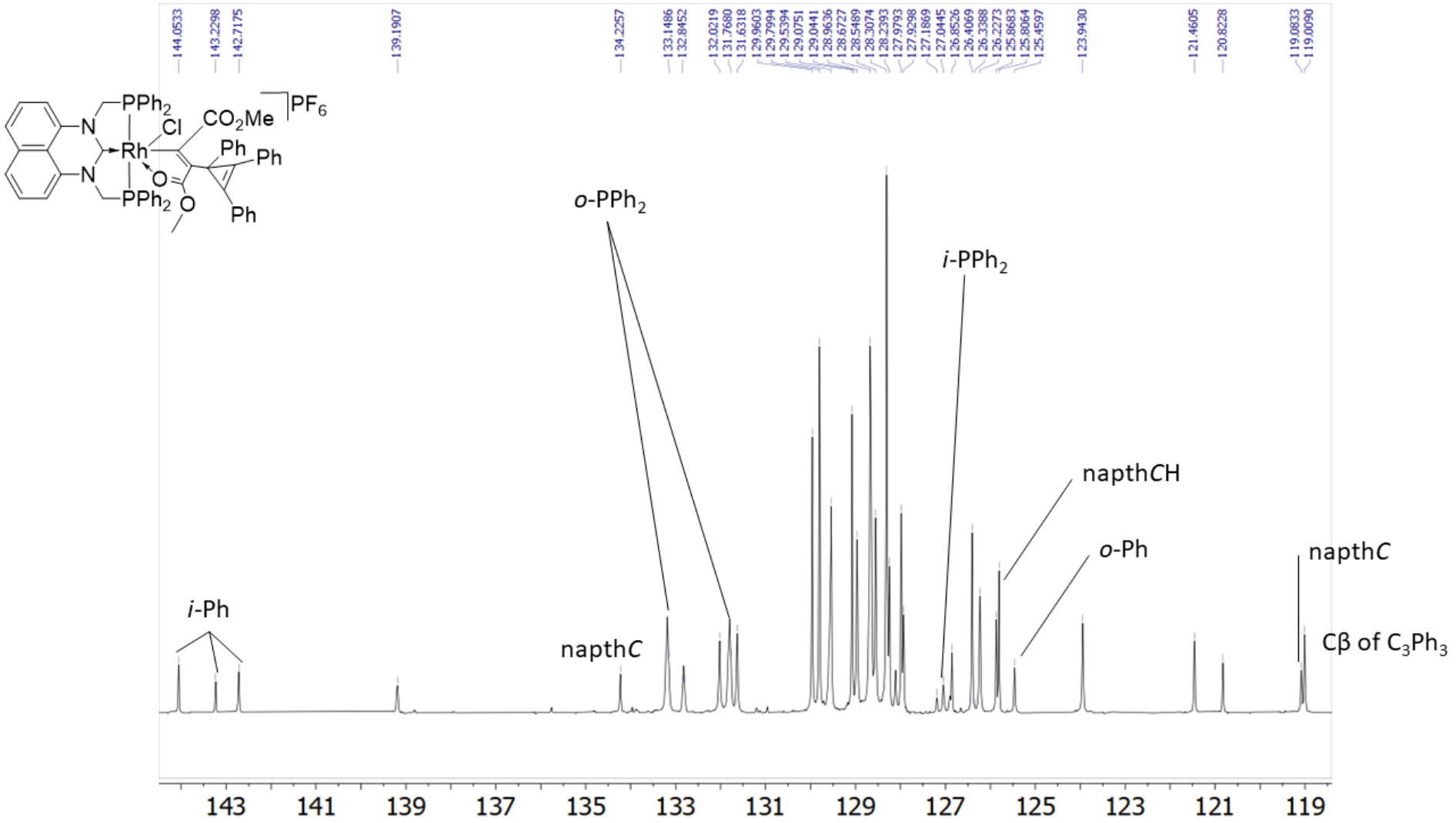

Figure S44 (Continued). Inset of $^{13}C\{^{1}H\}$ NMR Spectrum (176 MHz, $CDCl_3$, 298 K) for $[RhCl\{\kappa^2\text{-}C(CO_2Me)C(CO_2Me)(C_3Ph_3)\}(PhPm)]PF_6$ (**5a**)

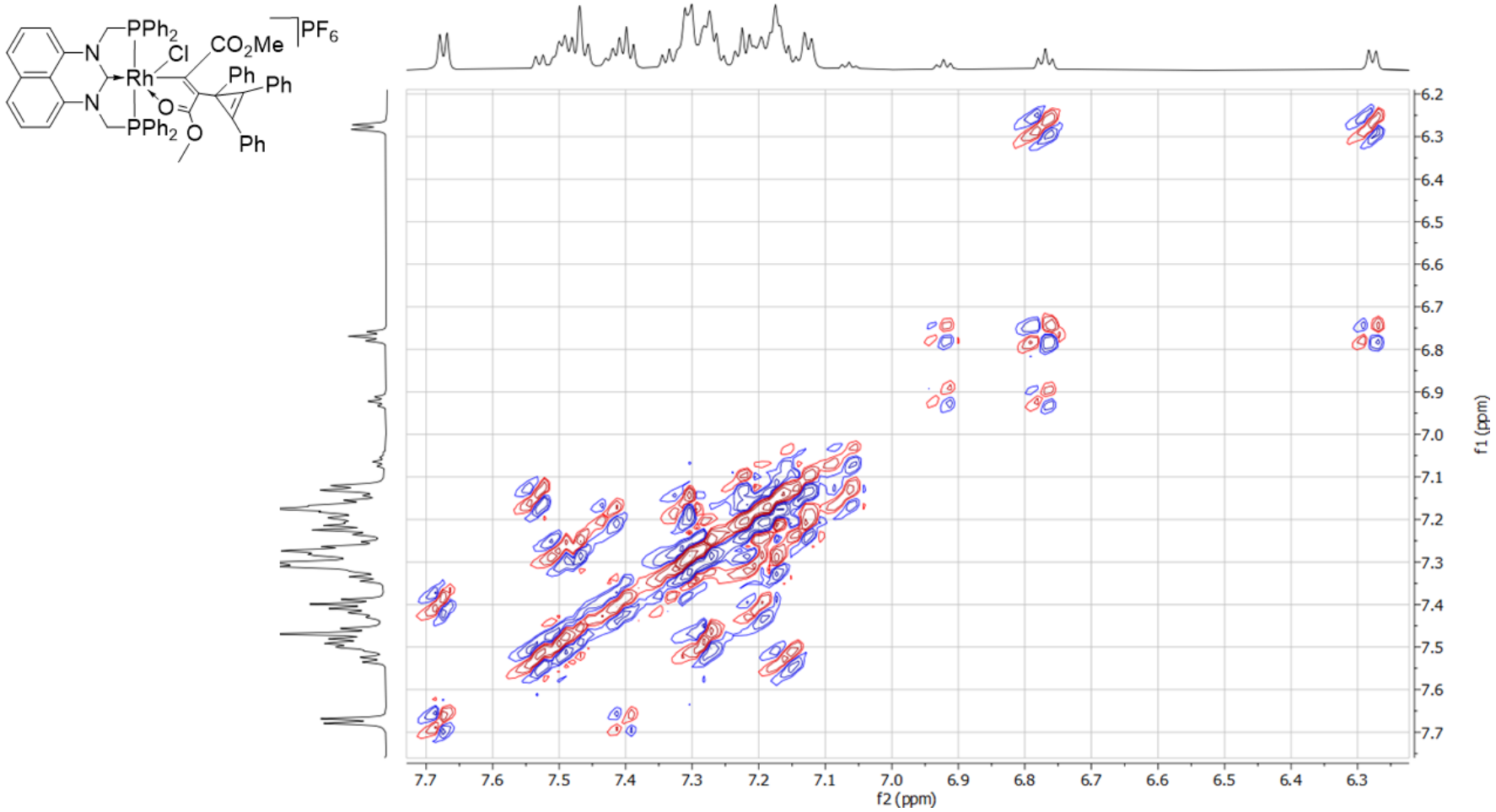

Figure S45. COSY NMR Spectrum ($CDCl_3$, 298 K) for $[RhCl\{\kappa^2\text{-}C(CO_2Me)C(CO_2Me)(C_3Ph_3)\}(PhPm)]PF_6$ (**5a**)

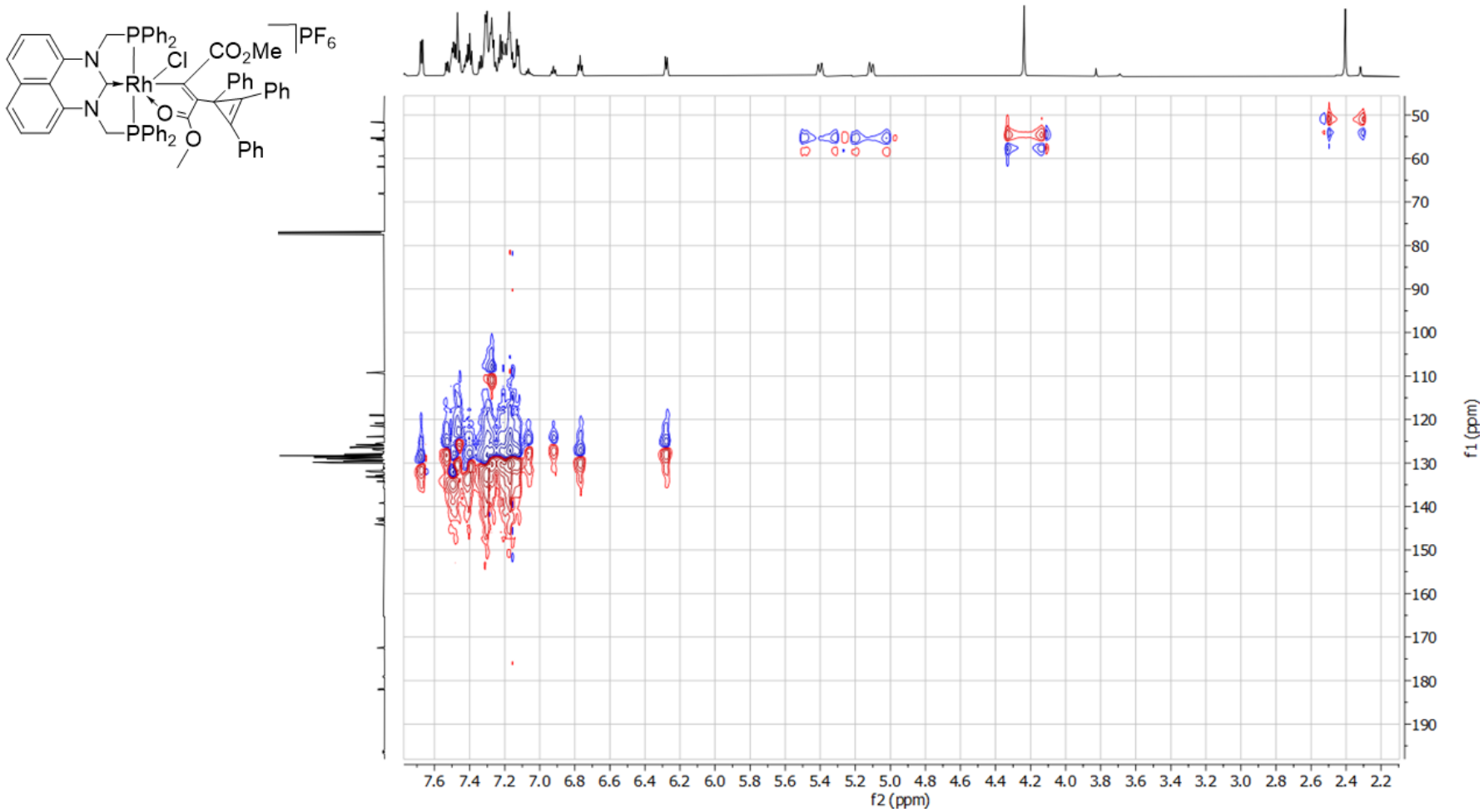

Figure S46. ^{13}C-^{1}H HSQC NMR Spectrum ($CDCl_3$, 298 K) for [RhCl{κ²-C(CO_2Me)C(CO_2Me)(C_3Ph_3)}(PhPm)]PF_6 (**5a**)

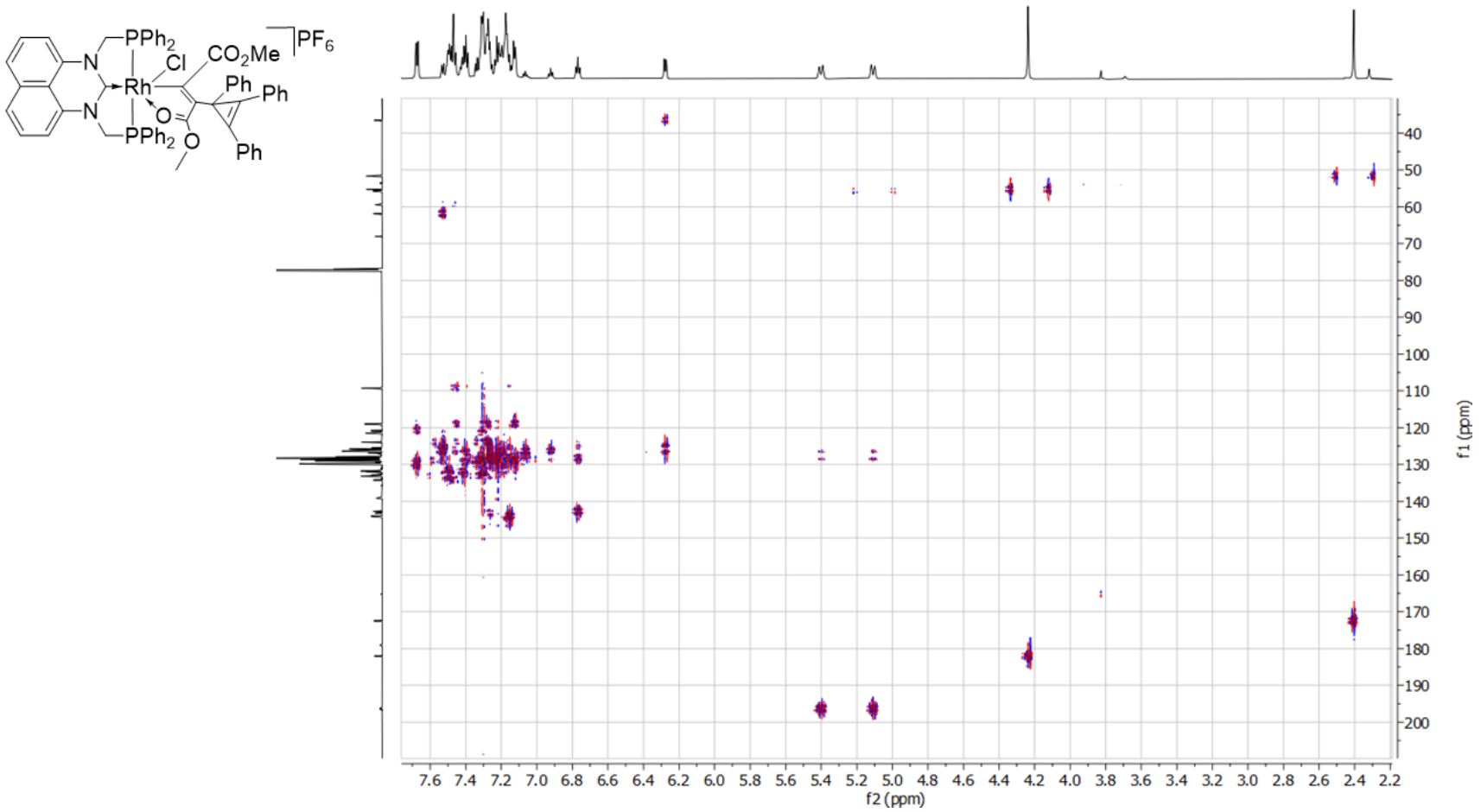

Figure S47. ^{13}C-^{1}H HMBC NMR Spectrum ($CDCl_3$, 298 K) for [RhCl{κ²-C(CO_2Me)C(CO_2Me)(C_3Ph_3)}(PhPm)]PF_6 (**5a**)

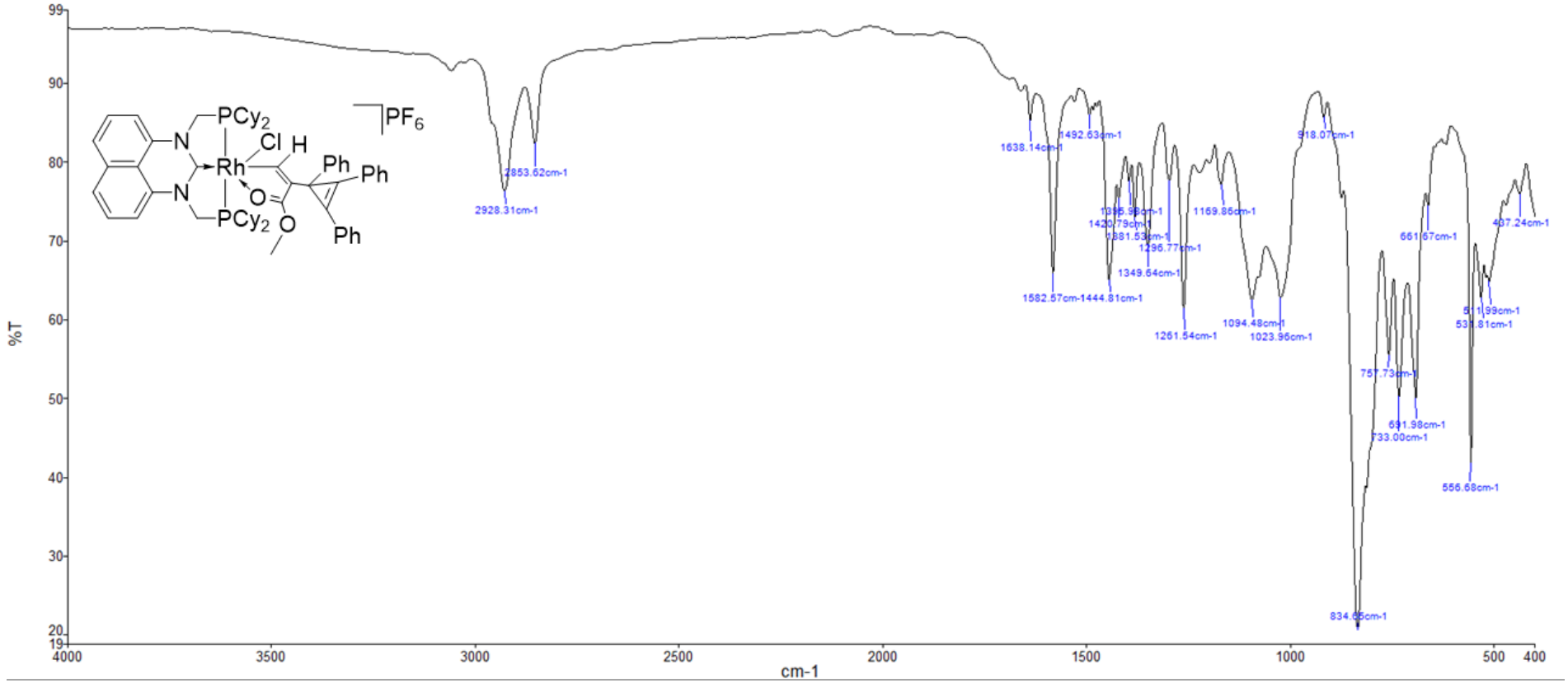

Figure S48. IR spectrum (ATR, cm^{-1}) for $[Rh(CHC\{CO_2Me\}C_3Ph_3)Cl(CyPm)]PF_6$. (**4b**)

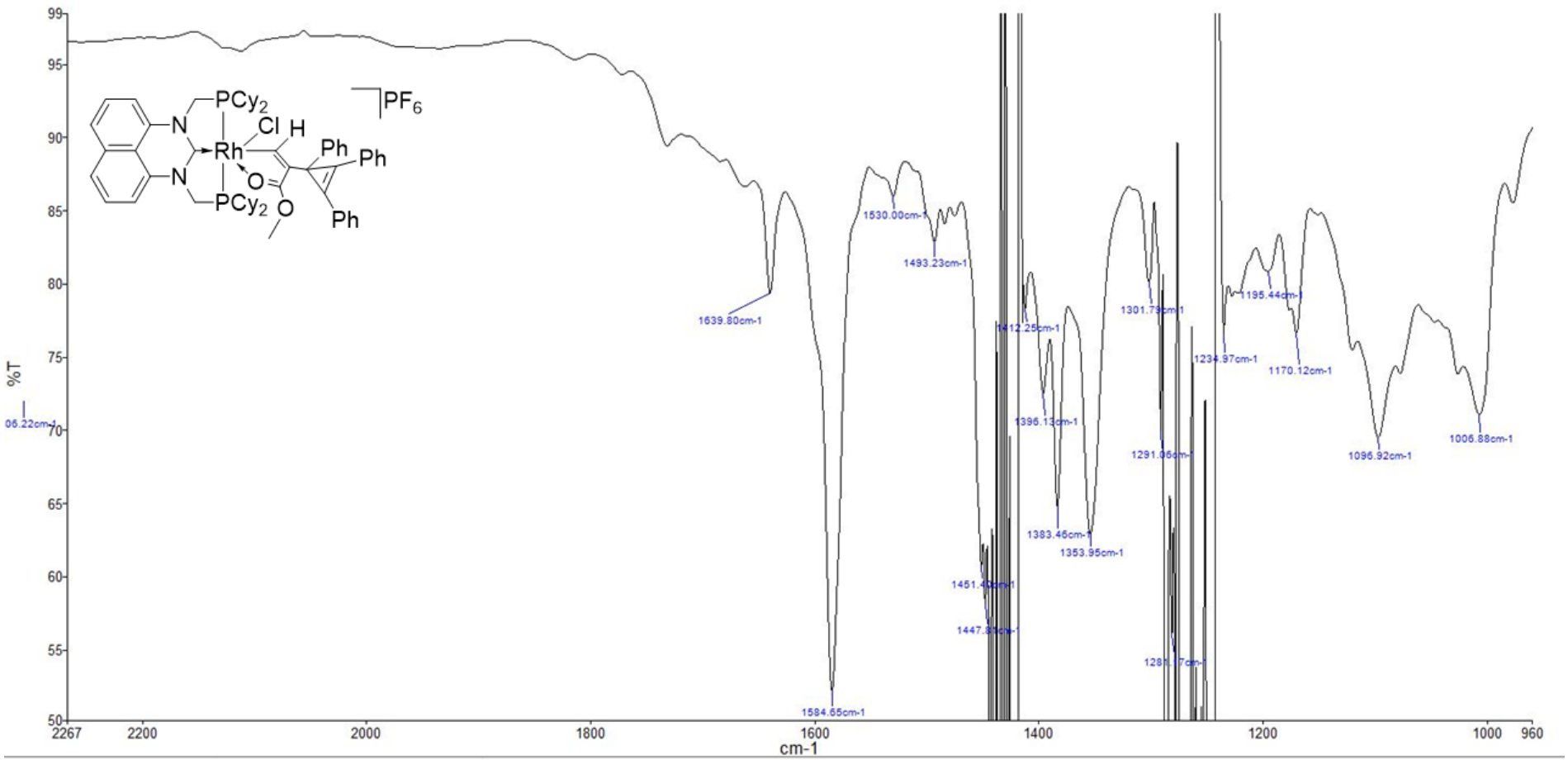

Figure S49. IR spectrum (CH_2Cl_2, cm^{-1}) for [Rh(CHC{CO_2Me}C_3Ph_3)Cl(CyPm)]PF_6. (**4b**)

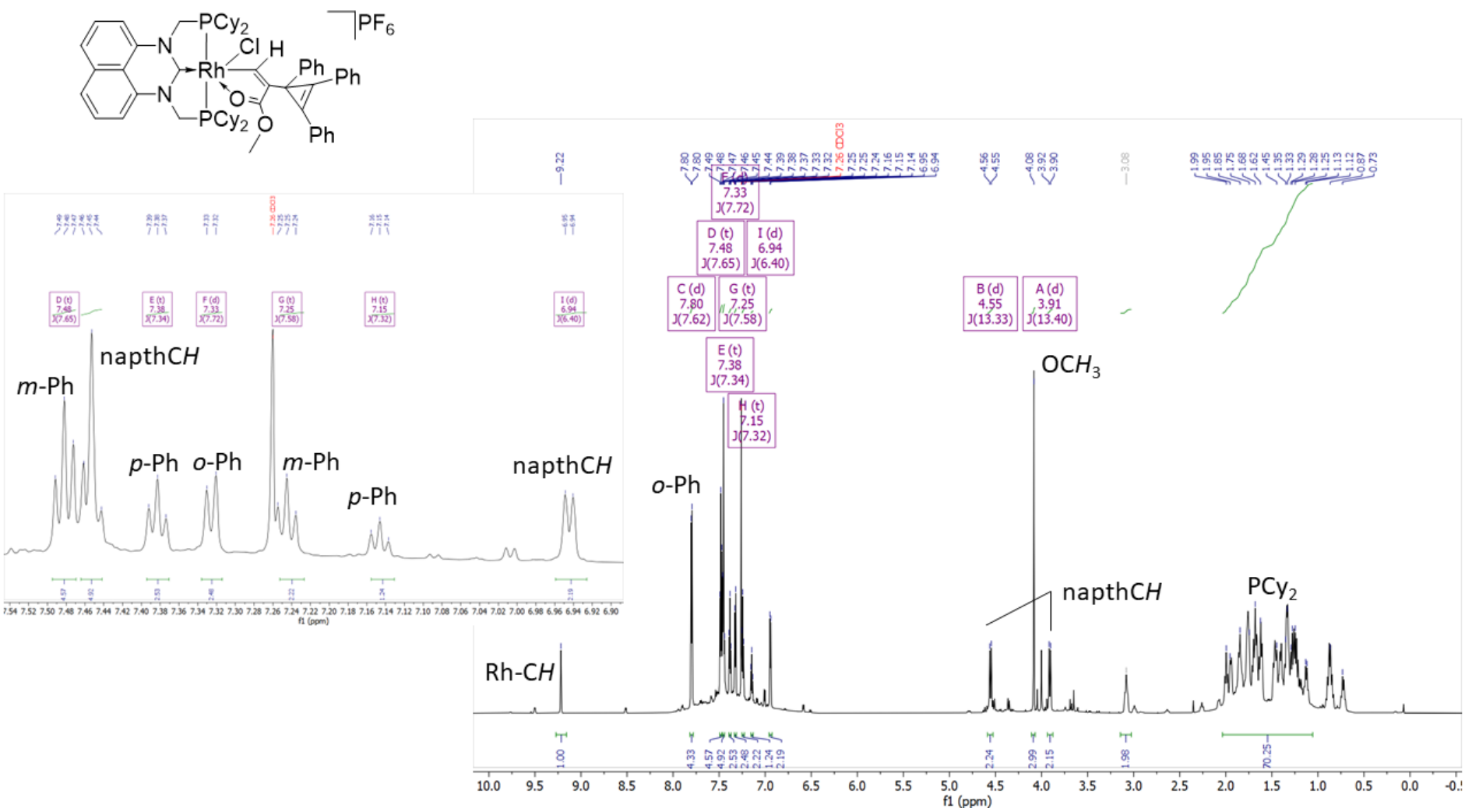

Figure S50. ^{1}H NMR spectrum (800 MHz, $CDCl_3$, 298 K) for $[Rh(CHC\{CO_2Me\}C_3Ph_3)Cl(CyPm)]PF_6$. (**4b**)

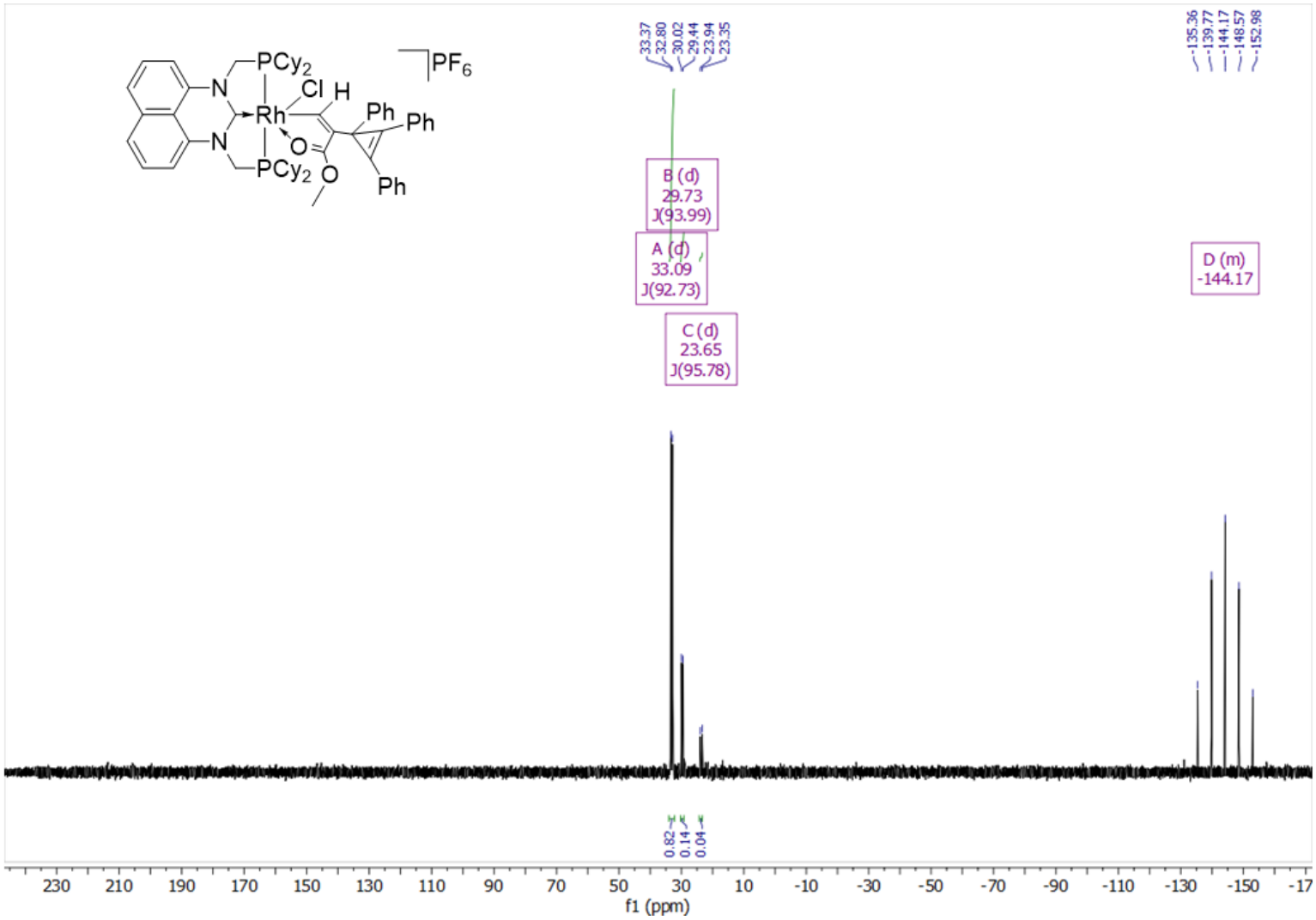

Figure S51. $^{31}P\{^{1}H\}$ NMR spectrum (162 MHz, $CDCl_3$, 298 K) for $[Rh(CHC\{CO_2Me\}C_3Ph_3)Cl(CyPm)]PF_6$. (**4b**)

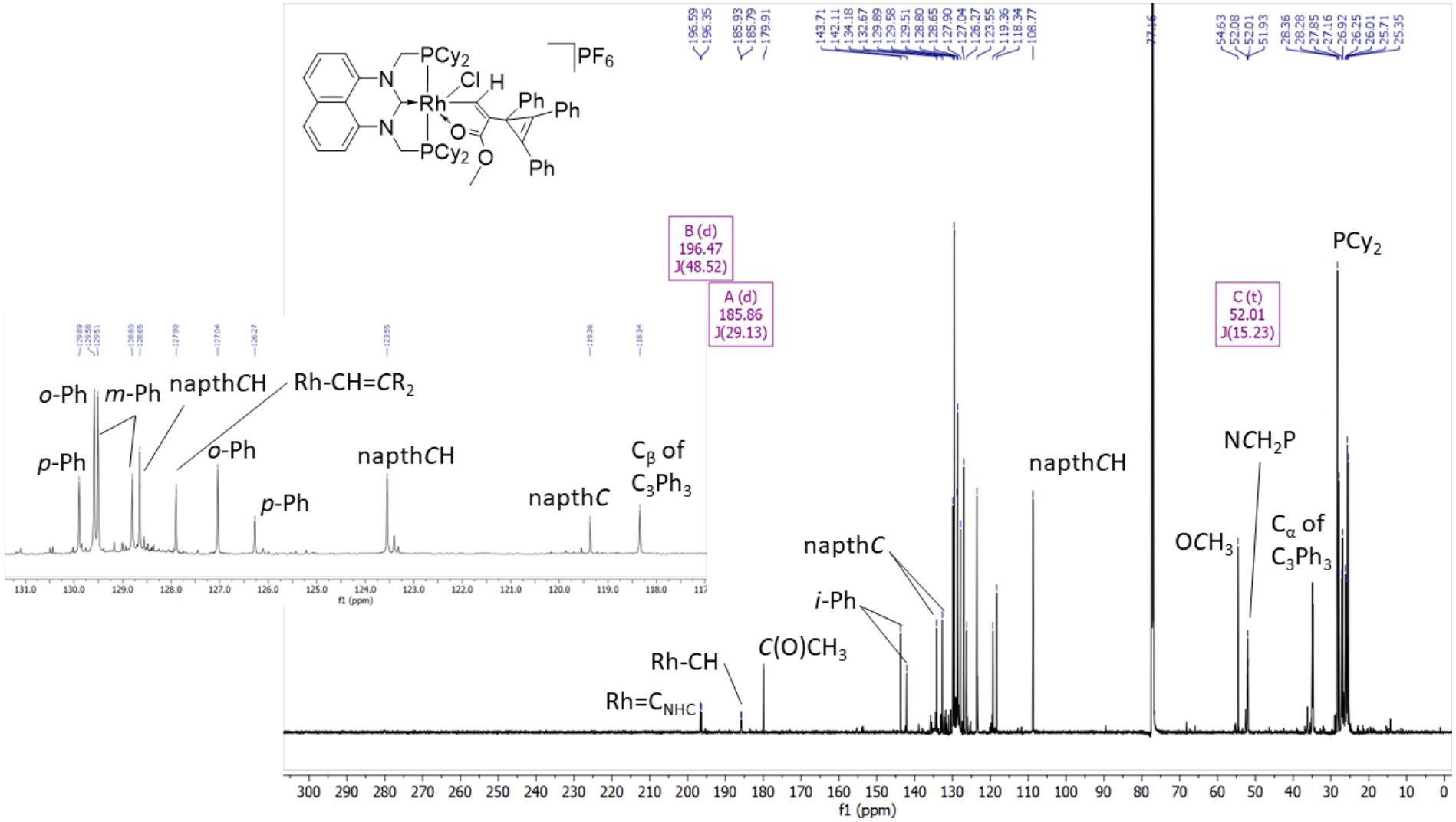

Figure S52. $^{13}C\{^{1}H\}$ NMR spectrum (201 MHz, $CDCl_3$, 298 K) for $[Rh(CHC\{CO_2Me\}C_3Ph_3)Cl(CyPm)]PF_6$. (**4b**)

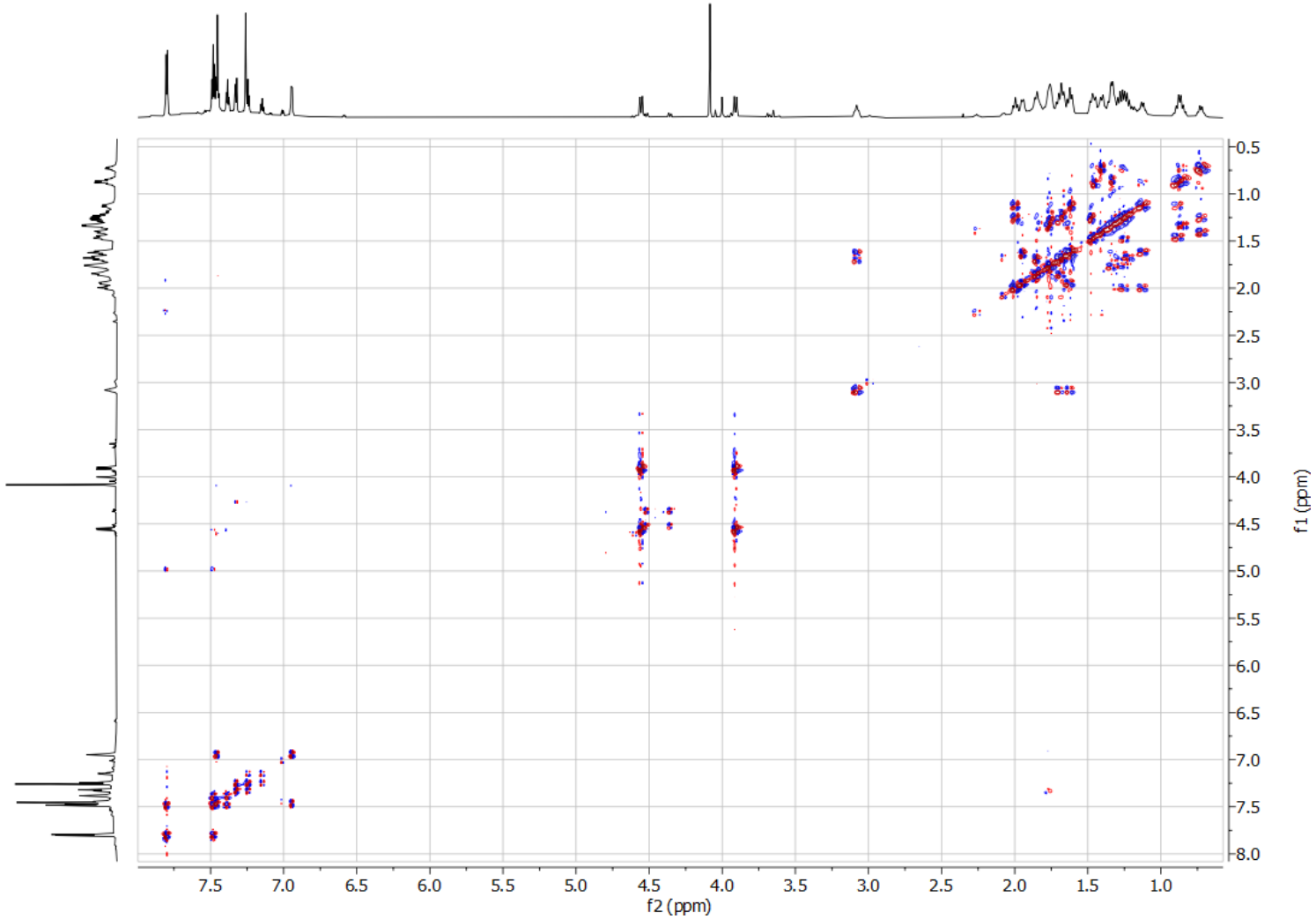

Figure S53. COSY NMR spectrum ($CDCl_3$, 298 K) for $[Rh(CHC\{CO_2Me\}C_3Ph_3)Cl(CyPm)]PF_6$. (**4b**)

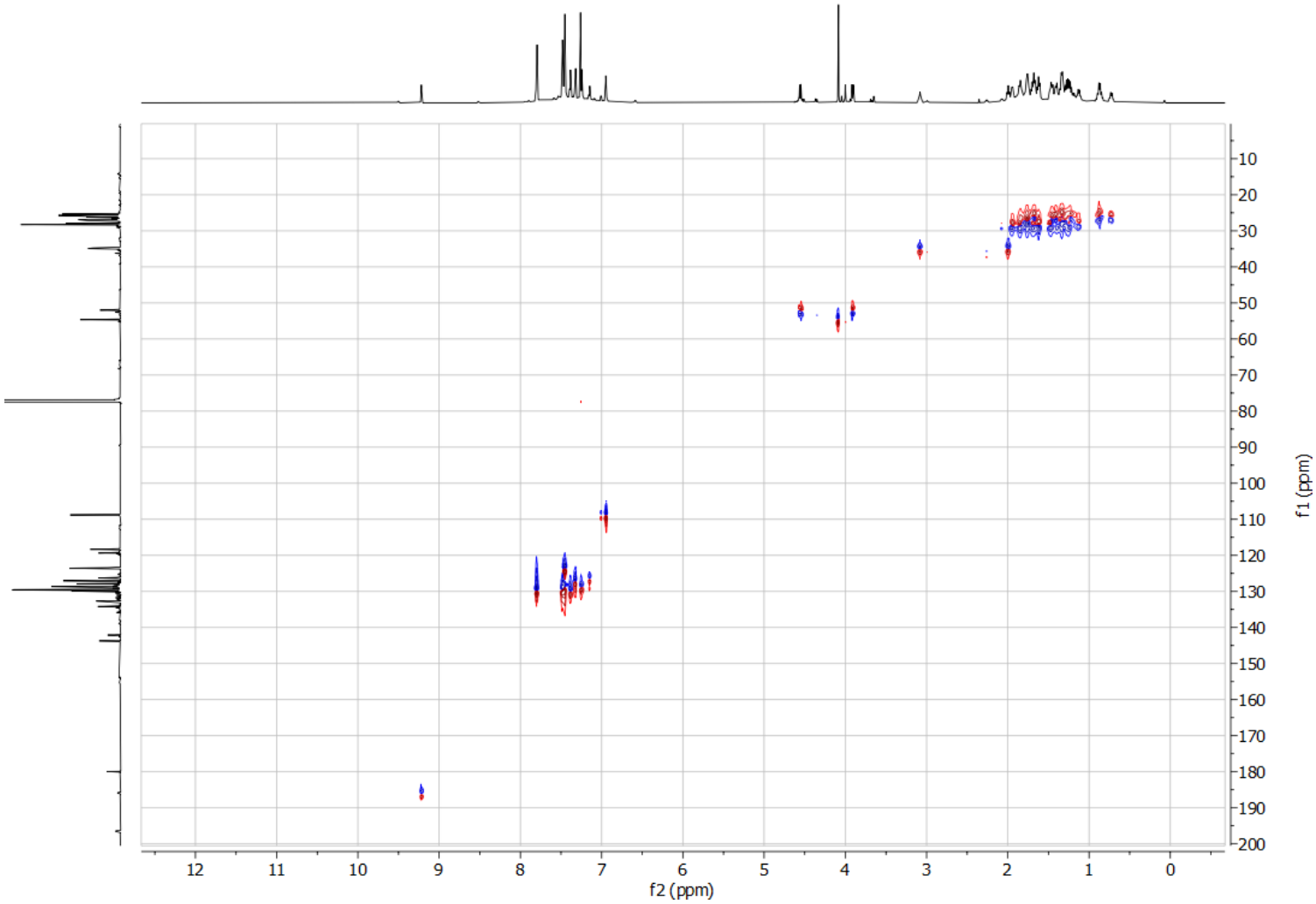

Figure S54. ^{13}C-^{1}H HSQC NMR spectrum ($CDCl_3$, 298 K) for $[Rh(CHC\{CO_2Me\}C_3Ph_3)Cl(CyPm)]PF_6$. (**4b**)

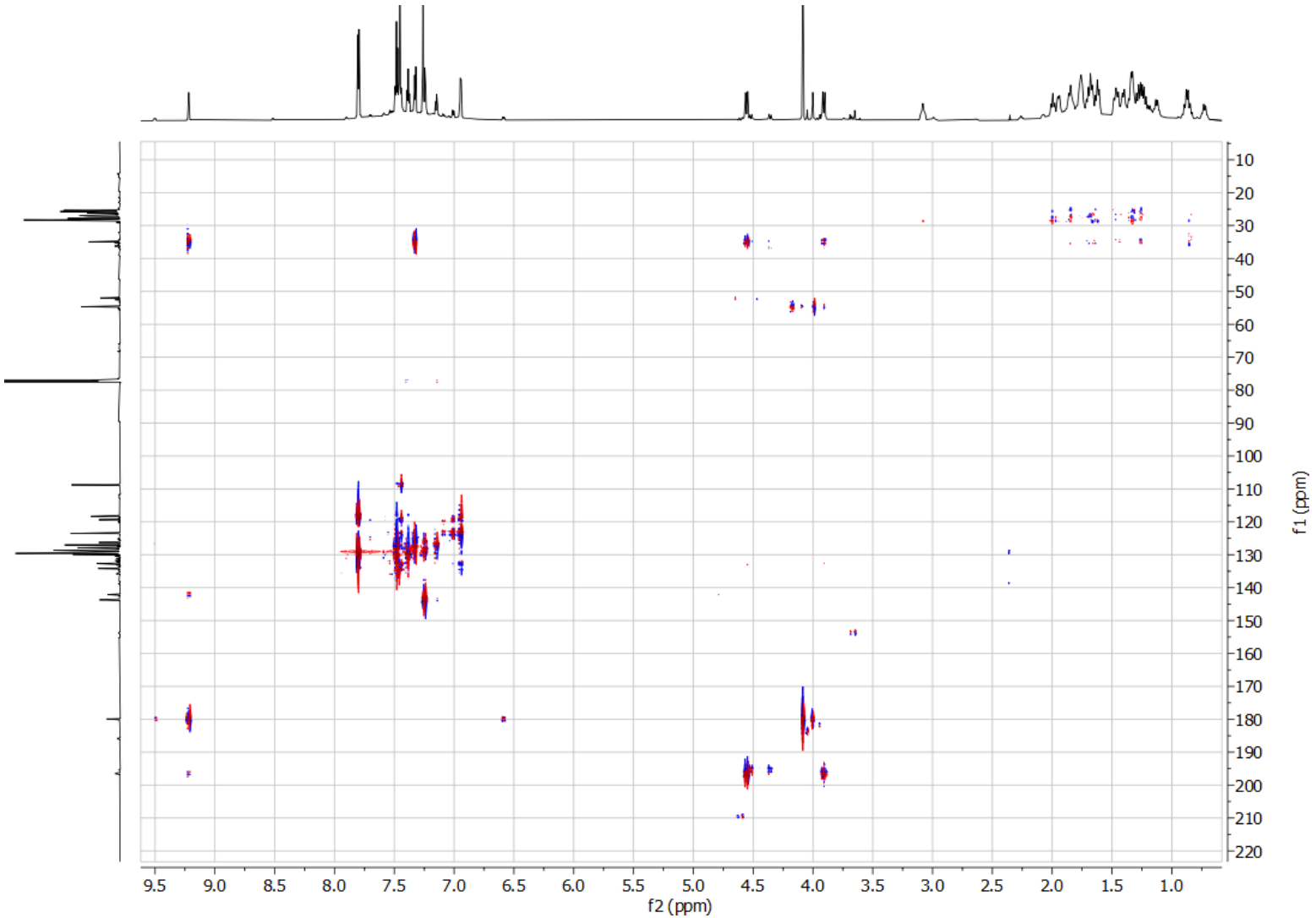

Figure S55. ^{13}C-^{1}H HMBC NMR spectrum ($CDCl_3$, 298 K) for $[Rh(CHC\{CO_2Me\}C_3Ph_3)Cl(CyPm)]PF_6$. (**4b**)

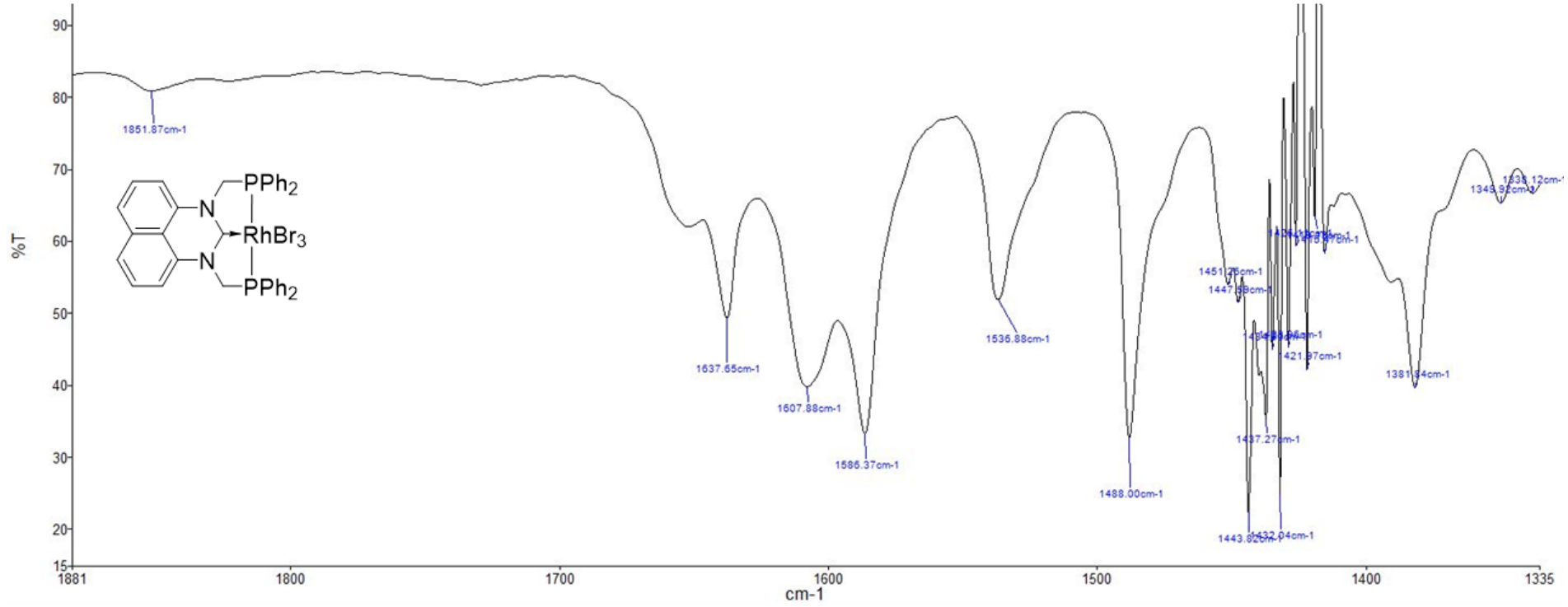

Figure S56. IR spectrum (CH_2Cl_2, cm^{-1}) of [$RhBr_3$(PhPm)] (**2**)

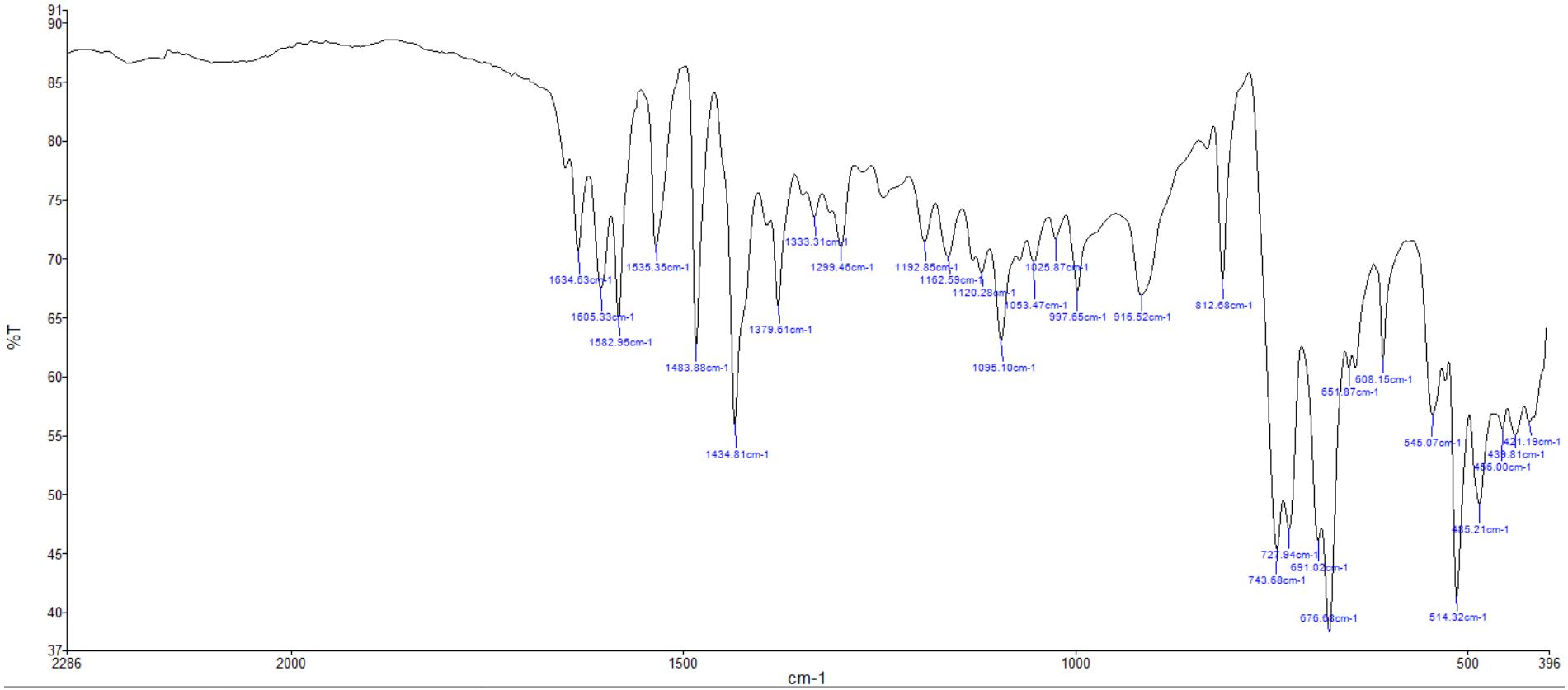

Figure S57. IR spectrum (ATR, cm^{-1}) of [$RhBr_3$(PhPm)] (**2**)

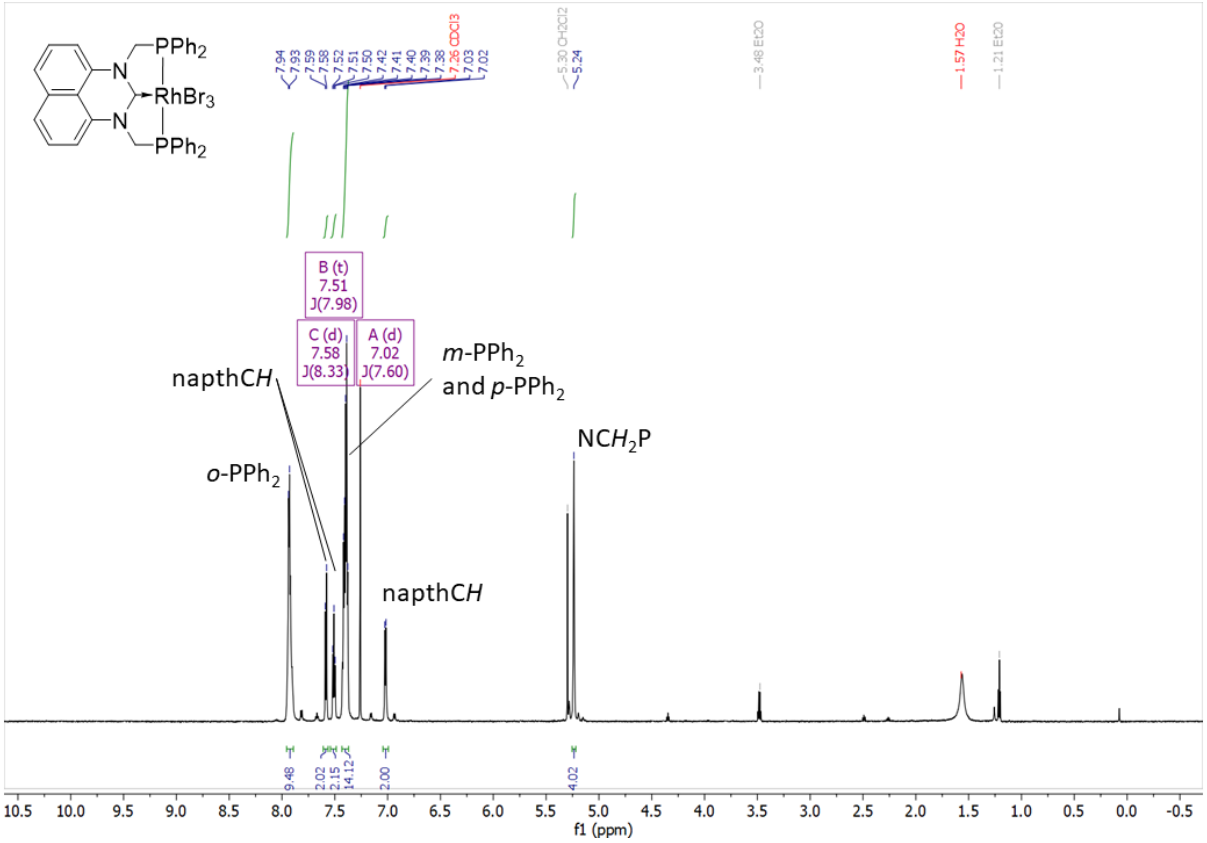

Figure S58. ^{1}H NMR spectrum (700 MHz, $CDCl_3$, 298 K) of [$RhBr_3$(PhPm)] (**2**)

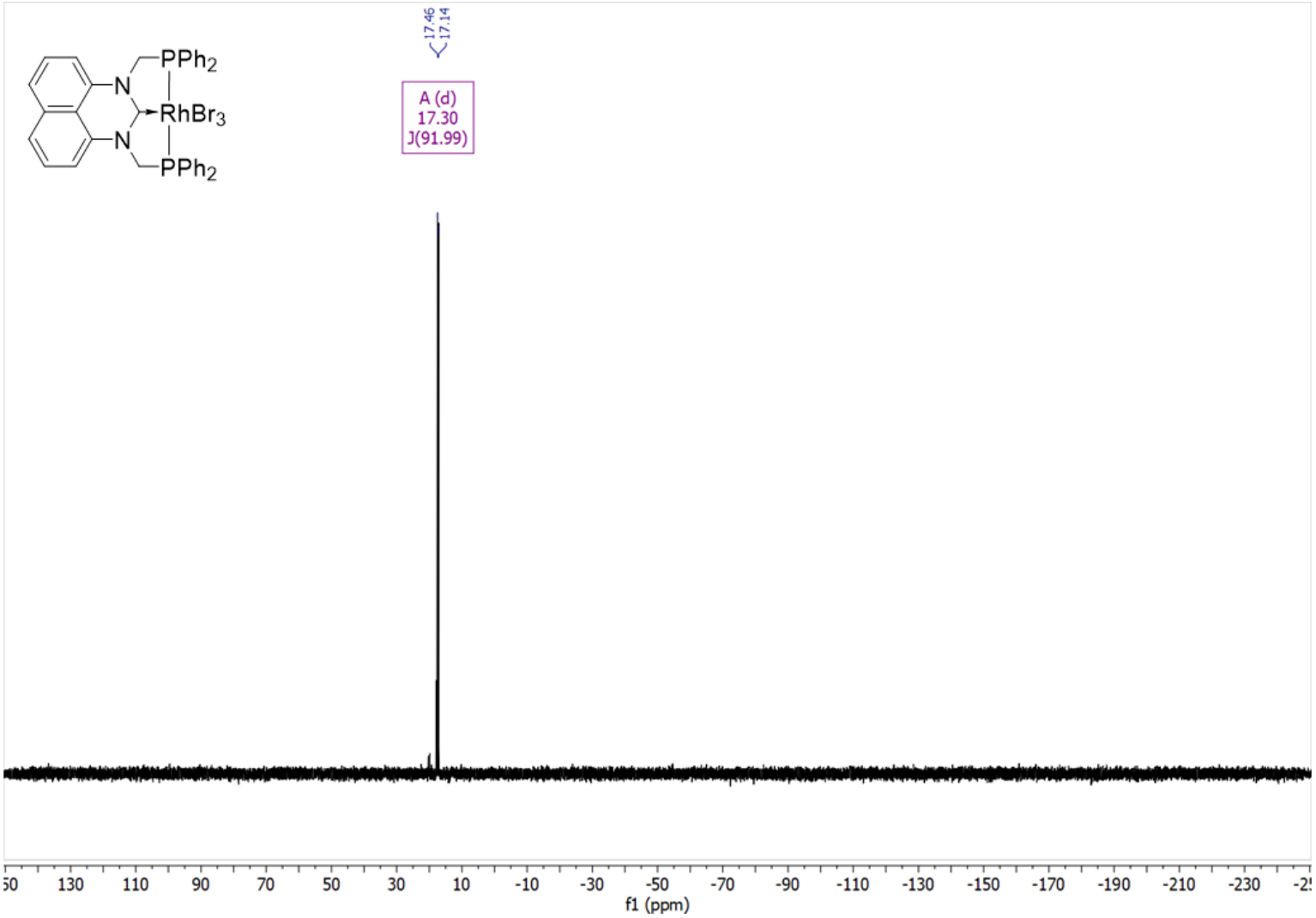

Figure S59. $^{31}P\{^{1}H\}$ NMR spectrum (283 MHz, $CDCl_3$, 298 K) of [$RhBr_3$(PhPm)] (**2**)

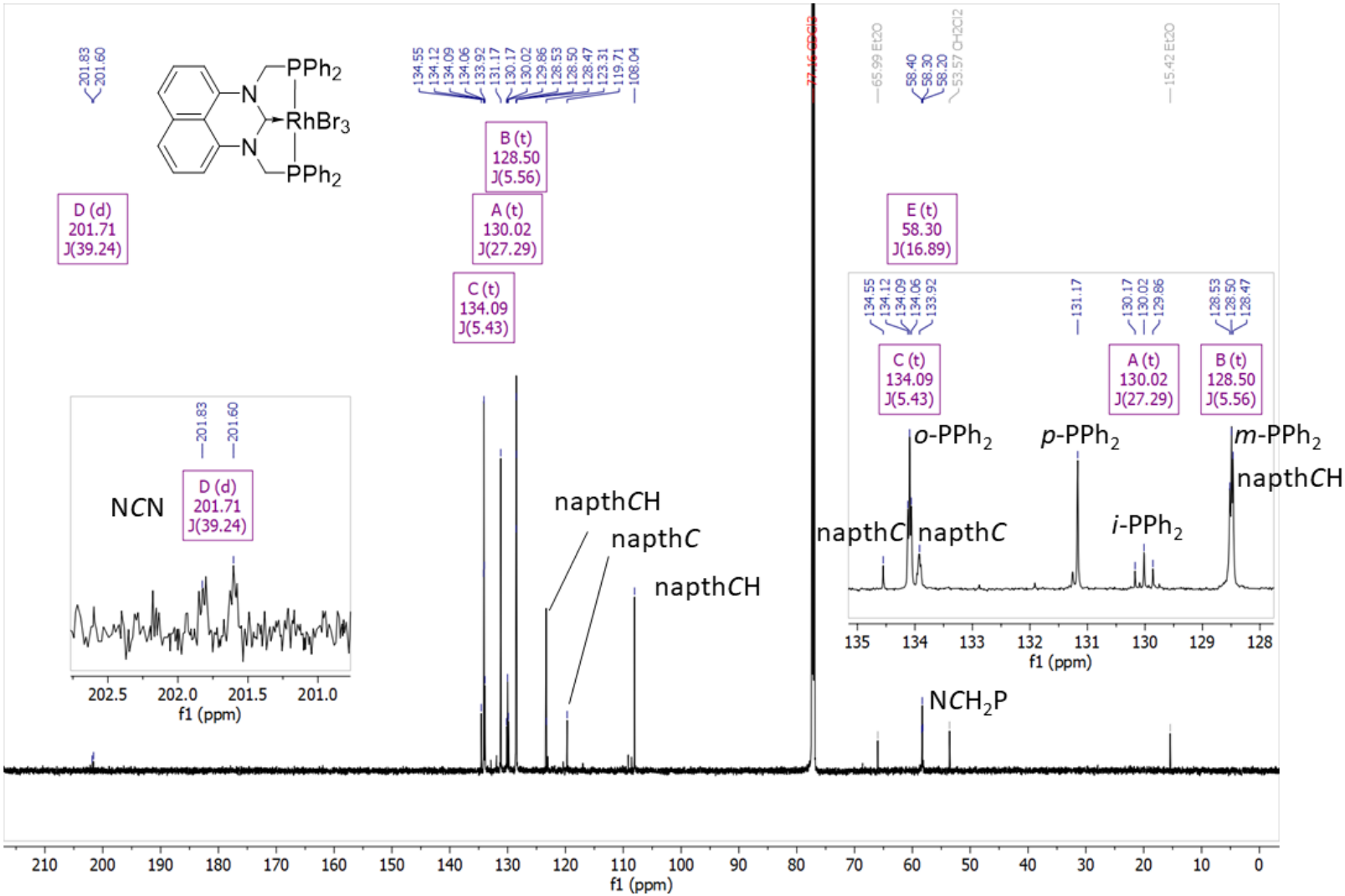

Figure S60. $^{13}C\{^{1}H\}$ NMR spectrum (176 MHz, $CDCl_3$, 298 K) of [$RhBr_3$(PhPm)] (**2**)